Spring 2011

Magnetometer-only attitude determination with application to the M-SAT mission

Jason D. Searcy

Department:

MAGNETOMETER-ONLY ATTITUDE DETERMINATION WITH APPLICATION TO THE M-SAT MISSION

by

JASON DAVID SEARCY

A THESIS

Presented to the Faculty of the Graduate School of the

MISSOURI UNIVERSITY OF SCIENCE AND TECHNOLOGY

In Partial Fulfillment of the Requirements for the Degree

MASTER OF SCIENCE IN AEROSPACE ENGINEERING

2011

Approved by

Henry J. Pernicka, Advisor
S. N. Balakrishnan, Advisor
Robert G. Landers

ABSTRACT

The topic of this thesis focuses on attitude determination for small satellites. The method described uses only a magnetometer to resolve the three-axis attitude of the satellite. The primary challenge is that magnetometers only instantaneously resolve two axes of a satellite's attitude. Typically, magnetometers are used in conjunction with other sensors to resolve all three axes. However, by using a filter over an adequately long orbit arc, the magnetometer data can yield all the information necessary. The magnetic field data are filtered to obtain the magnetic field derivative vector, which are combined with the magnetic field vector to fully resolve the attitude.

Once the magnetic field vector and its derivative are calculated, the filtered measurement and derivative are used as pseudo-measurements for a second filter that estimates the attitude quaternion and the angular rates. This estimate must meet the system requirements that are typically required of the attitude determination and control subsystem for the mission under consideration. In this thesis research, the Missouri University of Science and Technology's M-SAT mission was used as a case study to demonstrate the methods developed.

Finally, the method is tested using varying initial conditions and orbit parameters. The inclination in particular is cautiously observed. The method in which the magnetic field derivative is determined suffers a loss in accuracy for lower inclinations, suggesting that a parametric study with respect to orbit inclination is prudent. Accordingly, such a parametric study was conducted and is presented as part of this thesis.

ACKNOWLEDGMENTS

I would like to thank Dr. Pernicka for being an incredible advisor and friend throughout my undergraduate and graduate studies. The task of teaching complicated orbit dynamics and not scaring students away is a tough one. Not only did he accomplish this with me, he talked me into staying for graduate school.

I would also like to thank Dr. Balakrishnan for his guidance and support through the course of this research. Working with Dr. Balakrishnan has been an honor and a privilege. Dr. Landers was tasked with teaching my first controls class. The groundwork that I learned in that class made this thesis possible. Thank you both for being on my committee.

I would like to thank colleagues Mike Dancer and Dr. Nathan Harl for their help. Mike taught me filters from the ground up and was very helpful for brainstorming along the way. Dr. Harl helped make sure the thesis was written well enough to pass along the development of the method. Completing this research without them would have been much more difficult, and I could not ask for better co-workers and friends.

And last but not least, I would like to thank my parents and grandparents for raising and supporting me, all of my previous teachers and professors for pushing me, and my wife for never doubting in my ability to reach my goals.

TABLE OF CONTENTS

LIST OF ILLUSTRATIONS

1. INTRODUCTION

1.1. M-SAT MISSION OVERVIEW.

The attitude determination and control (ADAC) research that is detailed in this thesis was developed for use on a student-built satellite at the Missouri University of Science and Technology. The design needed to be low in cost and complexity but sufficiently versatile to accomplish the mission tasks. This section highlights the mission objectives as well as the satellite design and specifications.

1.1.1. Mission Objectives. The M-SAT (Missouri University of Science and Technology Satellite) project involved the creation of two satellites named MR SAT (Missouri Rolla Satellite) and MRS SAT (Missouri Rolla Second Satellite). The two satellites will be launched in a docked configuration. Once the satellite pair has powered up, detumbled, and run system diagnostics, the satellites will separate and fly in formation until MR SAT, the chasing satellite, fully consumes its propellant.

MR SAT is the chase satellite, and is therefore equipped with a propulsion system that provides more accurate attitude control (than MRS SAT). The MR SAT propulsion system will be used for orbital corrections as well as attitude corrections. MRS SAT is regarded as the target satellite and, as such, needs no propulsion. Only attitude control is required on MRS SAT to ensure the solar panels receive sufficient exposure to sunlight and to prevent excessive angular velocities from interfering with inter-satellite communications.

The satellite pair was developed under the strict guidelines of the Nanosat 6 competition sponsored by the Air Force Research Laboratory (AFRL) and the Air Force Office of Scientific Research (AFOSR). The competition involved eleven domestic universities and promoted the goal to each participant of fully developing a functional satellite within a two-year timeframe. The satellite project must meet all AFRL requirements, as well as promote new technologies related to spaceflight by performing a useful function requiring a space environment to fully test.

1.1.2. Subsystems and Specifications. The satellite project is organized with eleven technical subsystems that govern the various aspects of the design. Each subsystem directly relevant to the design activities of the ADAC subsystem are described

as a lead into the development of the ADAC subsystem. These subsystems are Propulsion, Communications, Command and Data Handling, Structure, and Power.

1.1.2.1 Propulsion. The Propulsion system on the MR SAT spacecraft provides the actuation necessary to effect three-axis attitude control. This is critical during the formation flight when rapid response time of the propulsion system is needed in order to fire thrusters to provide the control acceleration requested by the control system. The propulsion system is a cold gas system configured with twelve thrusters. The system implements a two-phase cold gas propulsion system, using R-134a refrigerant as the propellant. The R-134a will be stored in a tank as a liquid and expelled as a gas to maximize the amount of propellant that can be carried on-board the spacecraft while maintaining a 100 psi limit on pressure vessels in the satellite (as required by AFRL secondary-payload constraints).

The propulsion system provides three-axis translational and rotational control. The ADAC controller needs to be optimized to minimize propellant consumption to maximize the chances for completing the mission before expending the propellant. The thrusters provide approximately 60 mN thrust with a total ΔV of about two meters per second. The tank and the lines will be equipped with an active thermal control system to manage the phase change of the liquid propellant to gaseous form.

The propulsion system may be used in the future with a hybrid controller that utilizes both thruster-generated torque and torque provided by a magnetic coil. This may conserve propellant consumption, although likely by only a small amount. However, over the life of the mission, the savings may be enough to be significant. A combined attitude and orbit controller is also being considered to take advantage of the coupled nature of the attitude and orbit dynamics. Unfortunately, early trials using this combined controller have shown no benefit. Figure 1.1 shows an open satellite view of the partially constructed propulsion system. Figure 1.2 shows a picture of the partially constructed MR SAT spacecraft. Three panels are visible with the propulsion tank in the middle surrounded by propellant lines and thrusters.

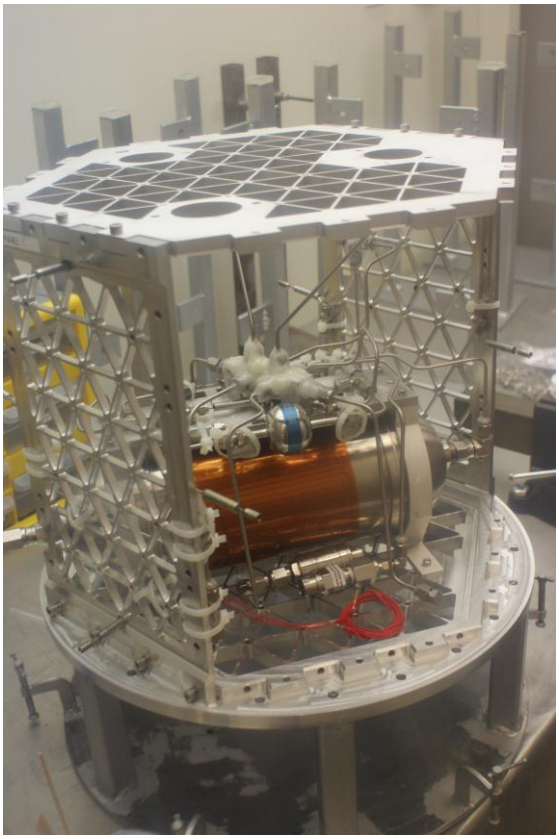

Figure 1.1. MR SAT Propulsion System Integration

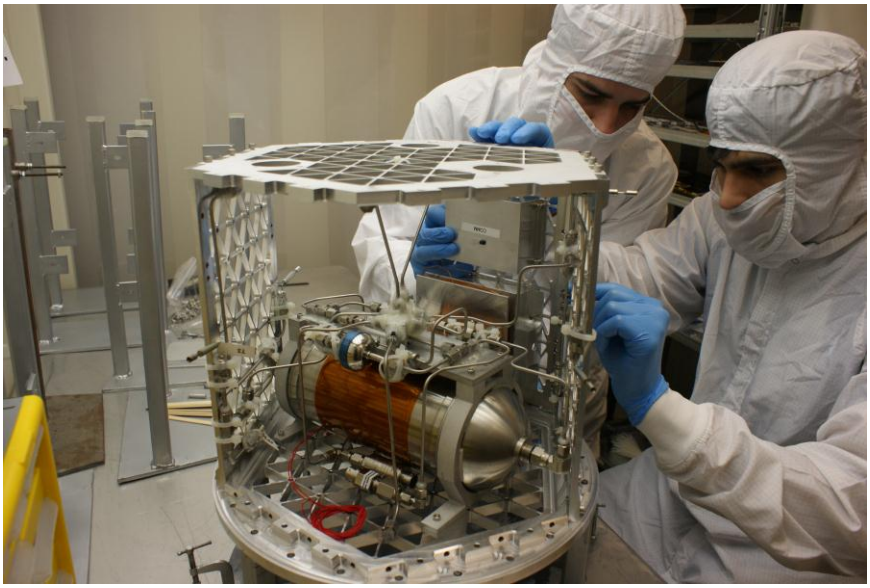

Figure 1.2. MR SAT Propulsion System Integration

1.1.2.2 Command and data handling. The Command and Data Handling (C&DH) subsystem is also vital to the performance of the ADAC subsystem. The C&DH subsystem must execute the attitude determination code, process new measurements, and store data needed for ground analysis. The subsystem is composed of a Gumstix main computer with 8051 microcontrollers with which to interface and control components. Regarding the attitude subsystem, the magnetometer is connected to an 8051 microcontroller that reads the output voltages and converts them to a three-component magnetic field measurement in milliGauss. The attitude determination filter runs on the main computer and the estimated attitude and angular velocity are used by the controller to reorient the satellite to the correct attitude.

1.1.2.3 Structure. The ADAC subsystem must be integrated into the structure of the satellite. There are several concerns to the integration of the system into the structure, as the number of sensors required and the needed placement of the sensors are very important. A magnetometer needs to be placed inside the satellite and located as far as possible and isolated from residual magnetic fields inside the satellite. If another sensor is required, the integration of that sensor will be important as well. Sun sensors, which would likely be used if the magnetometer-only system did not work, would need to be placed on the outside of the structure so that the devices could "sense" the Sun. This would displace a number of solar cells, potentially affecting the Power subsystem. Figure 1.3 shows the MR SAT structure. The integration of the structure will be more complex if the magnetometer-only system is found to be ineffective requiring the use of additional sensors.

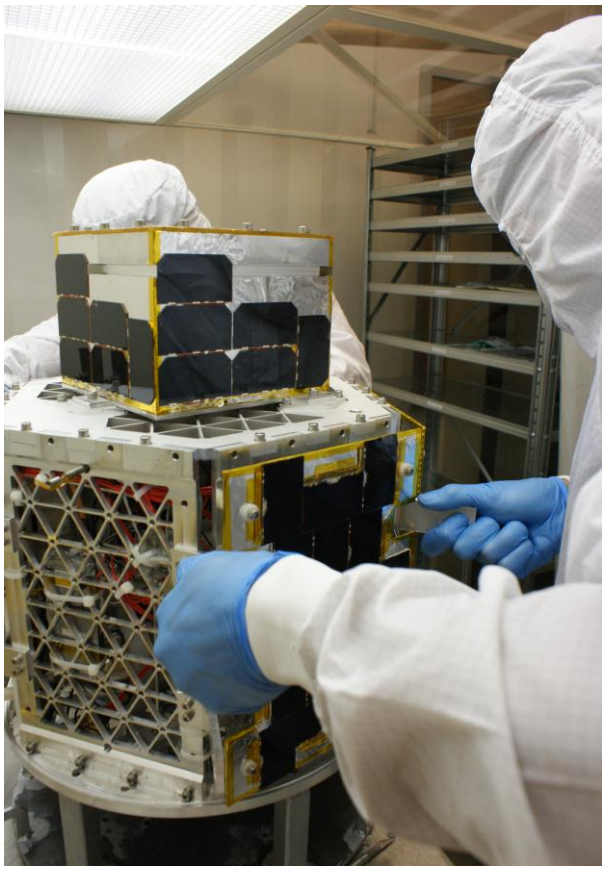

Figure 1.3. MR SAT Structure

1.1.2.4 Power. The Power subsystem imposes requirements that the ADAC subsystem must meet. The ADAC hardware power consumption must stay within the budgeted power available. This is especially important during the detumble phase when the magnetic coils will be powered up for an extended period of time. The Power subsystem will depend on the ADAC subsystem to rotate the satellite into orientations that support the maximum charging of the batteries. The solar panel surface area oriented toward the Sun must be maximized at all times. This requirement is secondary to the goal of pointing the spacecraft-to-ground antenna along the nadir direction. As long as the communications link is maintained with the ground station, orientation of the satellite will depend largely on ensuring the top and bottom panels (panels that do not have solar panels) point away from the Sun.

1.2. ADAC REQUIREMENTS.

The ADAC subsystem is constrained by the mission objectives of the M-SAT mission and must allow all of the mission objectives to be achieved. The requirements placed on the ADAC system are based around meeting the mission objectives and goals. The ADAC system must keep the satellite oriented so that the communications antenna points toward the Earth, most critically when the spacecraft passes over the ground station. This requires the satellite to slew 360 degrees per day to keep the antennas pointed in the nadir direction. In order for this base requirement to be met, the spacecraft must be able to determine its attitude to within three degrees, and control the attitude to within six degrees. If this requirement is met, the space-to-ground antenna will not move more than six degrees from nadir, which is within the specifications of the antenna and transceiver (with a conservative factor of safety included).

It is also important to keep the satellite solar panels exposed to as much sunlight as possible. This can be accomplished by keeping the two panels without solar cells oriented away from the Sun. This must be done, though, while maintaining the satellite-to-ground communication link. These requirements drive the desired attitude and the spacecraft must be able to determine its attitude to within three degrees for the mission to be successful. Therefore, the magnetometer-only attitude determination system can only be used if it can be proven through simulation that the system will determine the attitude of the spacecraft to within three degrees.

1.2.1. Attitude Determination Hardware Selection. The considered attitude determination hardware and the chosen hardware are discussed in the following subsections.

1.2.1.1 Horizon sensor. Horizon sensors use the Earth's horizon to determine spacecraft attitude. They consist of an infrared device that detects a temperature contrast between deep space and the Earth's atmosphere. Two common types of horizon sensors exist: horizon crossing sensors and scanning horizon sensors. The horizon crossing sensors scan the horizon by being statically attached to a spinning spacecraft. The scanning horizon sensors are used on non-spinning spacecraft and employ a rotating lens or mirror mechanism to scan the Earth's horizon. The accuracy for horizon sensors increases for higher altitude orbits, and are most often used in GEO rather than LEO. M-

SAT will likely be in LEO, so the horizon sensor would probably be a poor choice for the attitude determination of the satellites.

1.2.1.2 Sun sensor. Sun sensors use the Sun to determine spacecraft attitude and are currently the attitude determination device most commonly used. To properly determine the spacecraft attitude, one sensor must be installed on each side of the satellite. The foremost disadvantage to Sun sensors is the fact that when the satellite enters Earth's penumbra it precludes satellite attitude measurements during that time. However, Sun sensors are small, lightweight, highly accurate, and require a low amount of power. Sun sensors would likely have been chosen if the magnetometer-only algorithm had not worked sufficiently.

1.2.1.3 Global positioning system (GPS) receivers. The heart of the Global Positioning System is a spread-spectrum broadcast communication message that can be exploited using relatively low-cost receivers. GPS receivers use signals from four or more different GPS satellites to simultaneously solve for the three components of the observer's position and time. Taking several readings can give position and velocity data which in turn allow the determination of the orbital elements.

This GPS signal can also be used to solve for the attitude of the vehicle on which the receiver is located. This is accomplished by using multiple GPS antennas which are a known distance apart and which are attached to a rigid element of the vehicle, and using the phase difference between the signals from one GPS satellite arriving at the two antennas. The GPS receiver serves as an interferometer measuring the angle between the line-of-sight to the GPS satellite and the line joining the two antennas.

This method of attitude determination depends on the system of GPS satellites being maintained, but due to the numerous and growing applications of this technology on and around the world, this is guaranteed for the lifetime of the M-SAT mission. A concern for using this method for attitude determination is the potential lack of availability of four GPS satellites for a short period due to geometrical circumstances or the outage of one or more satellites. Accuracy can also be negatively affected by multipath effects of the same GPS signal reflecting off of the spacecraft. Due to the simplicity of the MR SAT spacecraft these effects will be greatly reduced, and the other effects could be mitigated by using error checking filters. Attitude determination using

GPS would require two antennas, one for each end of the satellites, to determine the attitude of both spacecraft individually. This is important because it cannot be assumed that each satellite will be oriented identically.

This method provides very high accuracy relative to the available methods and their costs. GPS signals also provide independent time signals other than the spacecraft computer. One GPS unit can generally handle input from several antennas, making it possible for each satellite to only need one receiver. However, GPS attitude determination will not be used for the M-SAT mission because the minimum baseline for the separation of GPS antennas needs to be approximately seventy centimeters and the MR SAT spacecraft has no length dimension longer than fifty centimeters. In addition, a deployable boom would need to be used and AFRL, the organization that hosts the Nanosat competition, warns against deployable items on the spacecraft.

1.2.1.4 Magnetometers. Magnetometers can determine the attitude measured relative to the Earth's local magnetic field. The uncertainties and variability in the Earth's magnetic field govern the accuracy of this method. In spite of these uncertainties, sensor filters can provide attitude accuracies of 0.5 to 3 degrees. These sensors need to be isolated from electromagnets, either physically or by duty-cycling the magnets. They are not as accurate as star or horizon sensors; however, these lower accuracies are far exceeded by the simplicity, reliability, lightweight, and low-cost of this sensor. The Earth's magnetic field can be continuously monitored, allowing for partial corrections to be made for these variable effects through adjustments in the filters. These variations tend to follow a daily cycle which can be programmed as weights into the filters. Magnetometers are approximately 0.3 to 1.2 kg in mass and consume less than 1 Watt of power.

Magnetometers were selected as the sensors to provide the on-orbit data to the attitude determination method within the autonomous control system running onboard MR SAT. These devices can provide an accurate value for the magnetic field vector at the location of the satellite. Magnetometers have acceptable accuracy, mass, and power consumption given the MR SAT design constraints.

1.2.1.5 Star-trackers (star sensors). Star sensors use observed star formations and compare the measurements to a database of known star formation information to

determine the attitude of a spacecraft. These sensors allow for extremely accurate attitude measurements. The typical accuracy of a star sensor is 0.0003 to 0.012 degrees.

Most star sensors, however, are too slow to determine a spacecraft's attitude directly. To address this slow processing star sensors are normally complemented with gyroscopes for high accuracy and rapid response. Because star sensors will sometimes be blinded by the Sun and Moon, complimentary sensors are necessary. These two sensors work in conjunction to correct for each of their weaknesses. Star sensors also require between 5 to 20 Watts of power which goes beyond the projected power allowance for the attitude determination system. Star sensors are costly by themselves and incur additional cost because they have to be implemented with other sensors.

1.2.1.6 Gyroscopes. Gyroscopes may be used to measure the angular velocity or angle of rotation of a spacecraft without any input from an external, absolute reference. They are inertial sensors that are most useful for precise attitude sensing between inputs from external sensors (i.e. star trackers, Sun sensors). Gyroscopes may also be briefly used for nutation damping or to control attitude during thruster firing. Gyroscopes use various technologies including spinning wheels, ring lasers, hemispherical resonating surfaces, and laser fiber optic bundles. Individual gyroscopes provide one or two axes of information, so multiple gyroscopes are often combined to form the Inertial Reference Unit (or IRU) with three axes of information. IRUs combined with accelerometers are capable of sensing position and velocity. This setup is referred to as an Inertial Measurement Unit (or IMU). Gyroscopes usually have a mass from 1 to 15 kilograms and require 10 to 200 watts of power.

Advances in manufacturing and design allow the production of smaller gyroscopes that use less power. With the advent of MEMS technology (Micro-Electro-Mechanical Systems), manufacturers have been able to make solid state IMUs. Solid state IMUs have no moving parts. The mass and energy consumption of these new units combined with their ability to withstand higher shock/vibration loadings than previous models make them an ideal choice for attitude determination.

Testing of the solid state IMUs for use on this mission has shown a poor resolution to estimate the angular rates of the spacecraft. The IMUs will not be used and the subsystem has selected magnetometer-only attitude determination.

1.2.2. Attitude Determination Hardware Chosen. For the attitude determination of the MR SAT spacecraft, a magnetometer was chosen because of the simplicity and reliability available from the sensor. The choice to use only the magnetometer was finalized when it was realized that the angular rate measurement from IMUs would not yield the resolution that was required. More sensors could be added, but the decision was made to test if the accuracy could be achieved using only a magnetometer. After a literature review, a paper by Natanson was identified demonstrating the feasibility of achieving the needed accuracy during post-processing of magnetometer data.[14] The challenge then became in adapting the post-processing technique for use in a real-time attitude determination application on board the MR SAT spacecraft. This forms the key contribution of this research study. The selected magnetometers were provided by Billingsley Magnetics shown in Figure 1.4.

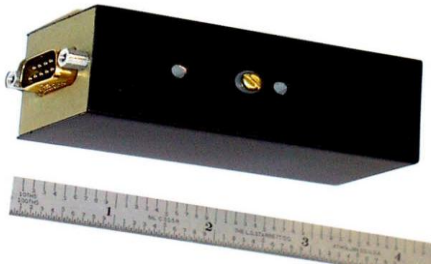

Figure 1.4. Billingsley Magnetics Triaxial Fluxgate Magnetometer

The magnetometers needed to be space-rated and have a reasonably fast sampling rate, as well as provide a high accuracy measurement. The model from Billingsley Magnetics meets all of these qualities with a one second sampling rate and a one degree angular accuracy in the magnetic field reading. These specifications would normally be adequate if the magnetometer was used with other sensors to determine the attitude. The task remained to determine if a magnetometer alone with these specifications could provide the accuracy needed for a successful mission. The remainder of this thesis shows the development of the algorithm that is used onboard the MR SAT spacecraft.

2. LITERATURE SURVEY

Attitude determination is a problem that has been examined in-depth over the last hundred years. Determining the orientation of an object in three-dimensional space has been an interest in dynamics and control since long before Sputnik launched in 1957. The application to spacecraft, of course, began shortly after Sputnik launched. As with any estimation problem, the challenge is to take the available measurements and use them to estimate the spacecraft attitude. The measurements that have historically been used or experimented with are numerous and can be combined in different ways to achieve the necessary attitude estimation accuracy. This section describes a few of the key advances in the field of spacecraft attitude determination.

2.1. ATTITUDE DETERMINATION.

One of the classic early works on spacecraft attitude determination was written by James R. Wertz.[21] Wertz's book on spacecraft attitude determination is still a handbook used by many professionals in the field. Wertz covers many aspects of vector-based attitude determination as well as the basic attitude quaternion derivation that is used in this thesis to reduce the complexity of having a nine element attitude matrix to determine.[21] Other early attitude determination studies have resulted in the TRIAD method, the QUEST method, and additional solutions to Wabha's problem that are discussed later.[9]

Early attitude determination algorithms used least squares methods to obtain estimates. Over the years, those methods have evolved to the more complex Kalman filtering algorithms, and now nonlinear estimation techniques are becoming more common. The evolution could be because of growing estimation accuracy demand, but it is also likely the increase in available computing power has played a large role in the switch to more complex methods. The most common attitude determination techniques today use the Kalman filter or some variant to estimate the spacecraft attitude.[3] The typical sequential filter works well for attitude determination as well. The sequential filter works by taking measurements, one at a time, and updating an estimate at some time-step

interval. The difference in most attitude determination techniques involves the creative use of measurements from different sensors that allow the attitude to be calculated.[6]

There are several deterministic methods for calculating a spacecraft attitude using two inertially defined, independent pointing vectors. If two such vector measurements exist, the attitude can be calculated directly using a method referred to as the TRIAD method.[12] There are also the QUEST and FOAM methods, which can utilize more than two sets of attitude vector measurements.[9] For example, if a rigid body is able to rotate freely in space, knowing one pointing vector will allow for the calculation of the attitude, except the angle around the measurement itself. Regardless of any spacecraft motion (i.e., rotation) about the measurement, the sensor will always read the same value. A second measurement is needed to fully resolve the attitude. This can be seen through Wahba's problem of minimizing a quadratic loss function.[20] Wahba posed the attitude determination problem of minimizing a quadratic loss function where the measurement residual is minimized. Solving Wahba's problem has been a task of great interest over the past forty-five years. Shuster solved the problem using Davenport's q-method.[23] Markley showed that Wahba's problem could be solved using singular value decomposition.[9] Each method has a different level of accuracy and efficiency. It becomes important, even if there are numerous measurements available to resolve the attitude, to find the most efficient way to solve the problem without losing accuracy.

Recently, there has been a significant amount of work in the field of GPS attitude determination. The process requires the use of multiple antennas, which provide multiple position measurements. Filtering of the GPS data can then fix the spacecraft's attitude. There would need to be a minimum of three antennas to lock the attitude, with more being heavily preferred so that there is a better chance of having each antenna in view of several GPS satellites.[1] This method requires a baseline of nearly seventy centimeters between each antenna to provide the best accuracy. This works well for most spacecraft, but for nanosatellites and small satellites, unless deployables are used, the distances between the antennas would not be sufficient to meet the baseline requirements. [1]

Although it is not necessary, a sensor that gives the angular rates of the spacecraft such as a gyroscope can be beneficial to the filter because the filter no longer has to rely on a range of data to sense that the spacecraft is rotating. This can decrease the time that

is needed for the filter to reach steady-state. There has been an abundance of work in the area of attitude determination without a rate sensor because the reliability of gyroscopes is sometimes in question. This thesis study falls in that subset—that of attitude determination without the benefit of rate sensor data.

Work on attitude determination without a rate sensor usually includes the analysis of filters using measurements from magnetometers, Sun sensors, star trackers, horizon sensors, and so forth. A new focus on gyro-less spacecraft attitude determination systems has emerged. These studies show that it is possible to estimate both the attitude and the angular rates from a variety of pointing vector measurements.[2,4,6]

2.2. MAGNETOMETER-ONLY ATTITUDE DETERMINATION.

The idea that the attitude of a spacecraft can be fully determined as long as two independent vectors are known and each expressed in two different coordinate frames (typically an inertial frame and the spacecraft body frame) forms the basis of the TRIAD algorithm. [11,13] From this fact, the use of several combinations of two or more sensors have been attempted to determine spacecraft attitude. Most use a combination of a magnetometer with either a Sun sensor, star tracker, or horizon sensor. The need for low-cost sensors that can provide sufficiently accurate attitude determination led Gebre-Egziabber, et al. to use an accelerometer to provide a measurement of the gravitational field.[2] Santoni and Bolotti showed that the same can be achieved without the second sensor measurement.[4] The study went creatively used the data that was available to the spacecraft, instead of adding a second sensor to obtain the second required pointing vector. It was proposed that the solar panels could be used as Sun sensors, because the direction of the Sun can be found by analyzing the power generation by each panel. This is another example of using fewer, cheaper sensors to provide the same quality attitude determination.

These methods are the basis for the research described in this thesis. However, the second vector measurement used in this research is obtained from manipulating the first measurement. The magnetic field vector provides the first vector measurement and filtering that series of measurements provides the magnetic field vector derivative as the second vector measurement, or in this case pseudo-measurement. The derivative,

however, cannot be expressed relative to an inertial frame without knowledge of the angular velocity of the body frame. Therefore, the typical TRIAD algorithm does not apply in this particular scenario, motivating the development of the attitude filter described in Section 5. Other methods have been completed that use magnetometer-only data for attitude determination, and are detailed in this section.

One of the first attitude determination studies that use magnetometer-only data was completed when a satellite mission, the Earth Radiation Budget Experiment, became the victim of an attitude anomaly and was lost. The data that were able to be downlinked were used to try to determine the causes of the mission failure through post processing. Among the data were data from a magnetometer. The magnetometer data were used with a method that was developed by Natanson, Challa, et al. This method was called DADMOD, or Deterministic Attitude Determination using Magnetometer-Only Data.[14] The method solved for the attitude and angular rates from the magnetometer data by finite differencing the measurements to find the magnetic field derivative. The measurements of the magnetic field and its derivative were then used, along with the fact that the spacecraft angular acceleration is known, to estimate the attitude and angular velocities. The equations became quadratic so that there were multiple solutions, and DADMOD selected which of the two solutions was most likely to be the correct attitude.[14] The method worked well for post processing, but as this research discovered, using noisy, real-time measurements prevents an accurate solution.

Another magnetometer-only attitude determination solution was created by Psiaki. The error magnitudes achieved by Psiaki's Kalman filtering method showed errors of around two-three degrees after about 100 seconds with low initial filter offset.[19] By using two nested Kalman filters, the method presented in this thesis is able to achieve better accuracy than previous Kalman filter based magnetometer-only methods.

There have been many attempts to avoid using high power consuming, expensive, and fragile gyroscopes. MEMS devices have been created that allowed for the creation of solid-state IMUs, but most consider them to be too inaccurate and with inadequate resolution to give the results desired. In 1995, Lizarralde and Wen developed a controller without the need for angular velocity feedback. The controller made use of the passivity of the system, eliminating the need for a filter to directly determine the angular

velocities.[7] The advantage to such a system resides in the processing requirements from the Command and Data Handling system. The disadvantage of the method is that there is no knowledge of the angular velocity of the spacecraft. The controller can stabilize the attitude, but the spacecraft does not know its angular velocity, which is typically unacceptable for autonomous systems. One of the most recent attempts at magnetometer-only attitude determination was completed by Ma and Jiang. The authors used an Unscented Kalman Filter (UKF) with magnetometer measurements to estimate the attitude of a spacecraft and to calibrate the magnetometers.[5] The importance of this method is that it included the ability to account for additional error beyond the specifications of the magnetometer. This calibration could be done on the ground, although the difficulty persists that some residual magnetic fields created by the spacecraft could pollute the measurements creating more noise. The UKF is much less computationally efficient than the EKF which presents an important drawback.[18] The method presented in this thesis study, using the two-step EKF, provides the same magnitude errors and is quite robust, without the need to propagate several state vectors, or sigma points. EMI/EMC analysis can provide calibration of the magnetometer on the ground before the spacecraft is launched. The use of a Kalman filter with a calibrated sensor can thus provide computational efficiency over the UKF method.

At this time there have been several attempts at magnetometer-only attitude determination. Such a capability is a valuable asset for a spacecraft in case of a sensor failure or anomaly, or in the case of the M-SAT project, to reduce and implementation complexity by using only magnetometers by design. The first methods, shown using the SAMPEX mission, were executed during post processing, and failed when they were applied in real time. Earth's magnetic field is very nonlinear, changes with time and position in space, and has different characteristics depending on the spacecraft's orbit. The sensor that reads the field, however, is relatively inexpensive, easy to implement, accurate, and reliable. If the proper steps are taken to mitigate minor complications with the magnetic field model, the outcome is a cheap and viable alternative to expensive and complex sensors.

Natanson and Challa originally proposed, during post-processing, that finite differencing could be used to find the derivative of the magnetic field vector to provide a

second vector measurement. In real-time this is not feasible because of the nonlinearity of the magnetic field. Slight fluctuations with a sample time of one second cause drastic errors in the derivative calculation. This work proposes a pre-filter to filter the magnetic field data and yield the magnetic field derivative vector. This process works well as seen in Section 4. At most orbital inclinations, the filter provides a derivative estimation that has better accuracy than a Sun sensor would provide. Once the two vectors were available, it was assumed that the DADMOD method would be used to combine them and achieve an estimate of the spacecraft's attitude, following the rest of Natanson and Challa's work closely.

When the noisy magnetic field vector and derivative vectors were used in the DADMOD algorithm, though, the attitude estimates were off by sixty to seventy degrees in most cases. When the truth model magnetic field vector and derivative were used (i.e., the noise-free case), attitude was successfully determined. It was determined that the DADMOD algorithm was overly sensitive to noise and inaccurate for real-time implementation. The difficulty is caused by the fact that the derivative vector in the body coordinate frame is not referenced relative to an inertial frame. Without accounting for the angular velocity of the frame, which is unknown, the TRIAD and QUEST methods cannot be used.

The solution proposed in this study was conceived while exploring an analytical solution to the problem shown in Section 4. When the work was being completed, an algorithm was developed that calculates the magnetic field vector and its derivative *relative to the (rotating) body frame* from the magnetic field vector and its derivative *relative to the inertial frame* (the spacecraft attitude and its angular rates). By using a pre-filter to provide the magnetic field vector and its derivative (pseudo-measurements) and knowing the inertially-referenced vectors from the model, the only unknowns were the attitude and angular rates. Making the attitude and angular rates the state vector for a Kalman filter, the equations can be differentiated to find the measurement matrix. Although the complex equations may someday yield an analytical solution, the Kalman filter, once tuned properly, yields results that match and even surpass the magnetometer-only algorithms that have been found during the literature review and summarized previously in this section. The next three sections describe the new method in detail.

3. MAGNETIC FIELD AND ITS BEHAVIOR

The attitude determination system using magnetometer-only data is dependent on an accurate magnetic field model for the filtering method to successfully converge to an accurate solution. This section describes the process of modeling the Earth's magnetic field and its implications on this research. The World Magnetic Model is used, and the derivative of the magnetic field with respect to time must be found in order to complete the attitude determination system.

3.1. WORLD MAGNETIC MODEL.

The model used by the attitude determination system is the World Magnetic Model. [29] The World Magnetic Model uses spherical harmonics to quantify the Earth's magnetic field vector at any point in space over time. The model requires the current time and the position of the spacecraft to return the magnetic field vector.

A magnetometer measures the direction and magnitude of the Earth's magnetic field in space. The magnetic field changes in direction and magnitude depending on the position in space around Earth. Using the field as a measurement, and by knowing the spacecraft's location, a filter can determine the satellite's attitude. The measurements relate to the state-space through nonlinear spherical harmonics. The following sections describe the magnetic field model that relates the magnetic field to the Cartesian spacecraft position.

The Earth's magnetic field vector can be calculated at any point given the position in spherical coordinates. The magnetic field model used in this work takes the form[29]

$$\mathbf{B}(\lambda,\varphi,r,t) = -\nabla V(\lambda,\varphi,r,t) \tag{1}$$

where

$$V(\lambda,\varphi,r,t) = a\left\{\sum_{n=1}^{N}\sum_{m=0}^{n}\left(g_n^m(t)\cos(m\lambda)+h_n^m(t)\sin(m\lambda)\right)\left(\frac{a}{r}\right)^{n+1}\breve{P}_n^m(\sin\varphi)\right\} \tag{2}$$

The spherical coordinates λ, φ, and r are the longitude, latitude, and radial distance to the center of the Earth respectively. The Schmidt semi-normalized associated Legendre polynomials are calculated using

$$\begin{aligned} \breve{P}_n^m(\nu) &= \sqrt{2\frac{(n-m)!}{(n+m)!}}P_{n,m}(\nu) \quad if \;\; m>0 \\ \breve{P}_n^m(\nu) &= \qquad\qquad P_{n,m}(\nu) \;\; if \;\; m=0 \end{aligned} \tag{3}$$

The parameters g and h in Equation (2) are determined empirically and are available in a tabular format in the World Magnetic Model. The parameter a is the geomagnetic reference radius. The longitude, latitude and radius for spherical coordinates can be easily found from Cartesian coordinates (with appropriate quadrant checks) using

$$r = \sqrt{x^2 + y^2 + z^2} \tag{4}$$

$$\lambda = \tan^{-1}\left(\frac{y}{x}\right) \tag{5}$$

$$\varphi = \tan^{-1}\left(\frac{z}{\sqrt{x^2 + y^2}}\right) \tag{6}$$

The magnetic field vector, expressed in Cartesian coordinates, is then found by taking the gradient of the potential function, using the chain rule, and substituting in for latitude, longitude, and radius as

$$\mathbf{B}(x,y,z,t) = -J(x,y,z,t)^{\mathrm{T}}\nabla\mathbf{V}(\lambda,\varphi,r,t) \tag{7}$$

where

$$\nabla V(\lambda,\varphi,r,t)=\begin{bmatrix}\frac{\partial V}{\partial\lambda}\\ \frac{\partial V}{\partial\varphi}\\ \frac{\partial V}{\partial r}\end{bmatrix}=\begin{bmatrix} a\left\{\sum_{n=1}^{N}\sum_{m=0}^{n}\left(\frac{a}{r}\right)^{n+1} m\breve{P}_n^m[\sin\varphi]\left(h_n^m(t)\cos(m\lambda)-g_n^m(t)\sin(m\lambda)\right)\right\}\\ a\left\{\sum_{n=1}^{N}\sum_{m=0}^{n}\frac{d}{d\varphi}\left(\breve{P}_n^m[\sin\varphi]\right)\left(g_n^m(t)\cos(m\lambda)+h_n^m(t)\sin(m\lambda)\right)\right\}\\ -\left\{\sum_{n=1}^{N}\sum_{m=0}^{n}\left(h_n^m(t)\cos(m\lambda)-g_n^m(t)\sin(m\lambda)\right)(n+1)\left(\frac{a}{r}\right)^{n+2} m\breve{P}_n^m[\sin\varphi]\right\}\end{bmatrix} \tag{8}$$

$$\frac{d}{d\varphi}\breve{P}_n^m[\sin\varphi]=\sqrt{2\frac{(n-m)!}{(n+m)!}}\left(P_{n,m+1}\left[\sin(\varphi)\right]-m\tan(\varphi)P_{n,m}\left[\sin(\varphi)\right]\right) \tag{9}$$

and

$$J=\begin{bmatrix}\frac{-zx(x^2+y^2)^{-\frac{1}{2}}}{(x^2+y^2+z^2)} & \frac{-zy(x^2+y^2)^{-\frac{1}{2}}}{(x^2+y^2+z^2)} & \frac{\sqrt{x^2+y^2}}{(x^2+y^2+z^2)}\\ \frac{-y}{x^2+y^2} & \frac{1}{x+\frac{y^2}{x}} & 0\\ \frac{x}{\sqrt{x^2+y^2+z^2}} & \frac{y}{\sqrt{x^2+y^2+z^2}} & \frac{z}{\sqrt{x^2+y^2+z^2}}\end{bmatrix} \tag{10}$$

The above equations allow one to calculate the magnetic field vector in units of nanoTesla, nT. The conversion to milliGauss, mG, is accomplished using the simple relationship

$$1\,mG=100\,nT \tag{11}$$

The conversion is needed because the magnetometer used in this study measures in units of mG. The coefficients $g_n^m(t)$ and $h_n^m(t)$ are calculated as

$$g_n^m(t) = g_n^m(t_0) + (t - t_0)\dot{g}_n^m(t_0)$$
$$h_n^m(t) = h_n^m(t_0) + (t - t_0)\dot{h}_n^m(t_0) \quad (12)$$

where t is in years and t_0 = 2010.0. The coefficients $g_n^m(t_0)$, $h_n^m(t_0)$ and their derivatives were taken from the World Magnetic Model database.

Using the equations above, the magnetic field vector can be calculated at any point in space and time. This model is used to simulate the magnetic field measurements, as well as provide the truth model for this research. The accuracy of this model does not reflect the overall accuracy of the final attitude filter because the truth model of the spacecraft's attitude is what ultimately determines the accuracy achieved. However, because the method depends on the magnetic field derivative, that must also be modeled. Because an attempt to obtain the derivative analytically did not provide useful results, the magnetic field derivative model is found by finite differencing of the magnetic field model as detailed in the next section.

3.2. CALCULATING THE MAGNETIC FIELD DERIVATIVE.

When determining the magnetic field derivative (with respect to time), measurement noise must be considered. The Billingsley magnetometer has a 3σ directional error of three degrees when sensing a magnetic field vector. When attempting to determine the magnetic field derivative vector by finite differencing, as suggested in Reference 14, a noise level of three degrees can result in significant error. This error is mitigated by using a Kalman filter. The filter removes some of the effects of the noise in the measurements, producing a magnetic field vector estimate with less than one degree error, and finding derivative estimates of the magnetic field vector to within seven degrees, which is sufficient for the M-SAT mission. The entire attitude determination process is briefly described below.

3.2.1. Magnetic Field Derivative. In order to use the magnetic field measurements to determine the satellite's attitude, the actual magnetic field vector must be known. Additionally, the Earth's magnetic field is a highly complex, dynamic system, so the magnetic field varies with both location and time. Though highly nonlinear, the

magnetic field can be modeled using spherical harmonics as shown in Section 3.1. Using the orbital position vector obtained from the orbit determination process, the magnetic field vector is thereby known as a function of time and spacecraft position.

Time derivatives of the magnetic field must also be calculated for use later in the attitude determination algorithm. Finite differencing of the magnetic field model is used to calculate the needed magnetic field derivatives. The finite differencing technique used for this thesis study was central differencing. The magnetic field derivative can be calculated from the chain rule as

$$\frac{d}{dt}B(x,y,z,t)=\begin{bmatrix}\frac{\partial B_x}{\partial x}\frac{dx}{dt}+\frac{\partial B_x}{\partial y}\frac{dy}{dt}+\frac{\partial B_x}{\partial z}\frac{dz}{dt}+\frac{\partial B_x}{\partial t}\\ \frac{\partial B_y}{\partial x}\frac{dx}{dt}+\frac{\partial B_y}{\partial y}\frac{dy}{dt}+\frac{\partial B_y}{\partial z}\frac{dz}{dt}+\frac{\partial B_y}{\partial t}\\ \frac{\partial B_z}{\partial x}\frac{dx}{dt}+\frac{\partial B_z}{\partial y}\frac{dy}{dt}+\frac{\partial B_z}{\partial z}\frac{dz}{dt}+\frac{\partial B_z}{\partial t}\end{bmatrix} \tag{13}$$

The equation can be rearranged such that

$$\frac{d}{dt}B(x,y,z,t)=\begin{bmatrix}\frac{\partial B_x}{\partial x} & \frac{\partial B_x}{\partial y} & \frac{\partial B_x}{\partial z}\\ \frac{\partial B_y}{\partial x} & \frac{\partial B_y}{\partial y} & \frac{\partial B_y}{\partial z}\\ \frac{\partial B_z}{\partial x} & \frac{\partial B_z}{\partial y} & \frac{\partial B_z}{\partial z}\end{bmatrix}\begin{bmatrix}\frac{dx}{dt}\\ \frac{dy}{dt}\\ \frac{dz}{dt}\end{bmatrix}+\begin{bmatrix}\frac{\partial B_x}{\partial t}\\ \frac{\partial B_y}{\partial t}\\ \frac{\partial B_z}{\partial t}\end{bmatrix} \tag{14}$$

The gradient of the magnetic field vector is given by

$$\nabla \mathbf{B} = \begin{bmatrix} \frac{\partial B_x}{\partial x} & \frac{\partial B_x}{\partial y} & \frac{\partial B_x}{\partial z} \\ \frac{\partial B_y}{\partial x} & \frac{\partial B_y}{\partial y} & \frac{\partial B_y}{\partial z} \\ \frac{\partial B_z}{\partial x} & \frac{\partial B_z}{\partial y} & \frac{\partial B_z}{\partial z} \end{bmatrix} \tag{15}$$

And the spacecraft velocity vector, **V**, is

$$\mathbf{V} = \begin{bmatrix} \frac{dx}{dt} \\ \frac{dy}{dt} \\ \frac{dz}{dt} \end{bmatrix} \tag{16}$$

The columns of the gradient matrix in Equation (17) are given by

$$\begin{aligned} \frac{\partial \mathbf{B}}{\partial x} &= \frac{\mathbf{B}(x+\Delta x, y, z, t) - \mathbf{B}(x-\Delta x, y, z, t)}{2\Delta x} \\ \frac{\partial \mathbf{B}}{\partial y} &= \frac{\mathbf{B}(x, y+\Delta y, z, t) - \mathbf{B}(x, y-\Delta y, z, t)}{2\Delta y} \\ \frac{\partial \mathbf{B}}{\partial z} &= \frac{\mathbf{B}(x, y, z+\Delta z, t) - \mathbf{B}(x, y, z-\Delta z, t)}{2\Delta z} \end{aligned} \tag{17}$$

Substituting the gradient of the magnetic field and the spacecraft velocity into Equation (14) yields

$$\dot{\mathbf{B}} = \nabla \mathbf{B}\mathbf{V} + \frac{\partial \mathbf{B}}{\partial t} \tag{18}$$

where

$$\frac{\partial \mathbf{B}}{\partial t} = \frac{\mathbf{B}(x, y, z, t + \Delta t) - \mathbf{B}(x, y, z, t - \Delta t)}{2\Delta t} \tag{19}$$

is also obtained through central finite differencing.

Equation (18) quantifies the magnetic field derivative, where **V** is the spacecraft velocity vector in Cartesian coordinates. An analytical solution of the magnetic field derivative would be more computationally efficient, however, attempts to derive the second derivative of the spherical harmonics potential function failed to produce useful results. For future work, identifying an analytic derivative would make the method more efficient.

3.2.2. Magnetometer Measurement Filter. After the actual magnetic field vector and its derivative (finite differencing) are calculated with respect to the inertial frame (see Section 3.1-3.2.1), a Kalman filter is used to estimate the local magnetic field vector and its derivative using the magnetometer measurements, which are expressed in terms of and relative to the satellite body frame. The Kalman filter details are given in Section 5.1. The estimates of the magnetic field are then used as pseudo-measurements in a second filter to estimate the attitude quaternion and angular rates of the spacecraft.

3.3. MAGNETIC FIELD BEHAVIOR AND EXPECTATIONS.

Using the Earth's magnetic field vector as the only measurement can create difficulties if the magnetic field vector behaves in certain ways. The magnetic field needs to vary significantly throughout the orbit or the magnetic field derivative estimate obtained from the magnetometer measurement filter will not have sufficient accuracy. In an equatorial orbit, the magnetic field vector does not vary as much as in a polar orbit. To study the effects of the type of orbit on the accuracy of the magnetic field derivative estimate, simulations were performed for both a polar and an equatorial orbit. The simulations reflect the baseline case, presented in Section 6, with varying inclination. The results from the magnetometer measurement filter (derived in Section 5.1) for the polar orbit scenario are summarized below in Figures 3.1 and 3.2.

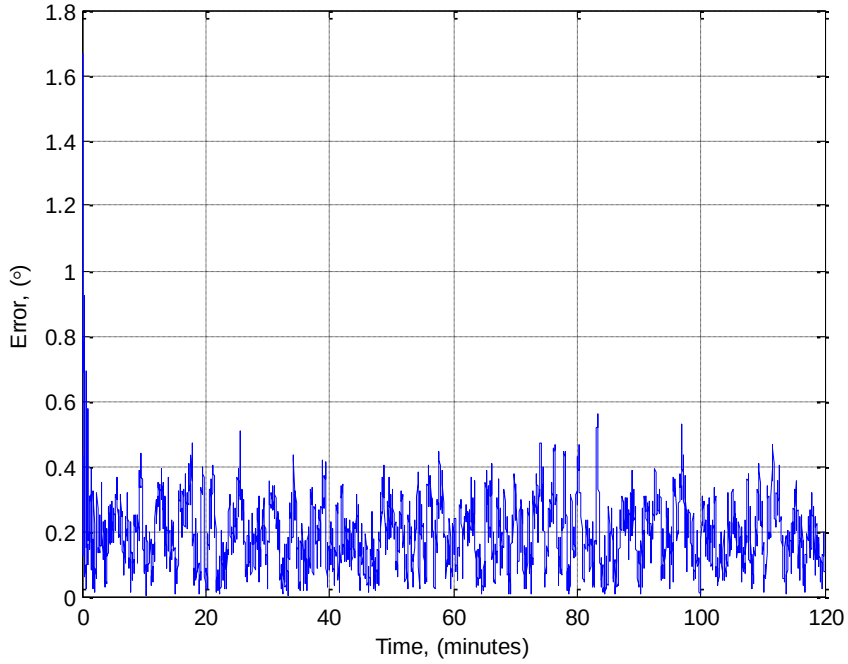

Figure 3.1. Magnetic Field Vector Angular Error for Polar Orbit

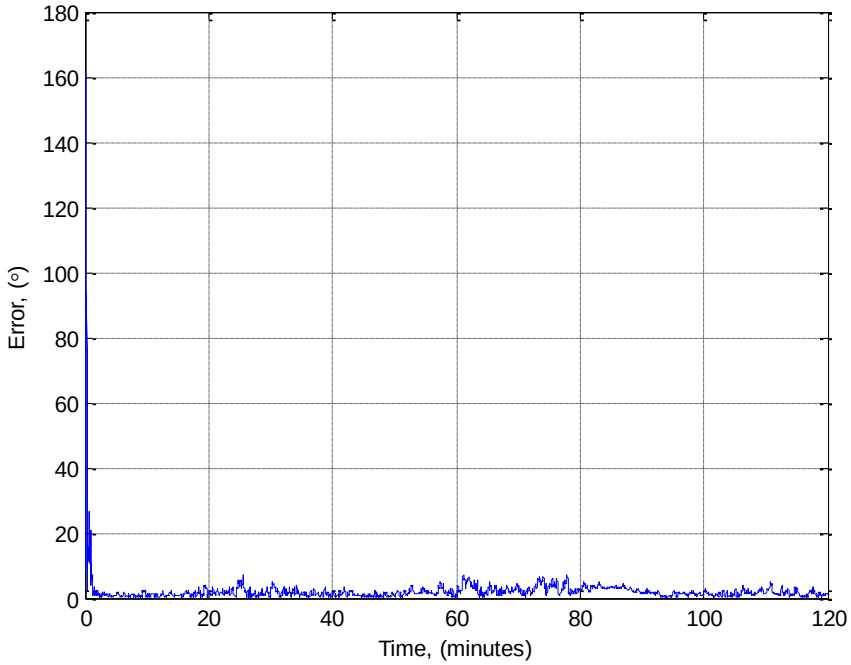

Figure 3.2. Magnetic Field Derivative Vector Angular Error for Polar Orbit

It can be observed from the above figures that in a polar orbit the magnetic field vector is estimated with an angular error of less than 0.5 degrees. The magnetic field derivative vector is estimated to within seven degrees. Comparable attitude determination systems typically use the magnetic field vector and a second pointing vector from another sensor, such as a Sun sensor. Sun sensors typically have around ten degrees accuracy in their measurements. The Kalman filtering in this study yields two pointing vectors with accuracies higher than that of adding an additional sensor, with the difficulty being that the magnetic field vector derivative is dependent on the spacecraft angular velocity, which is unknown (and a solution to this difficulty is shown in Section 5).

Because the polar orbit case shows a reasonable estimation of the magnetic field derivative, the equatorial orbit is now tested, as shown in Figures 3.3 and 3.4.

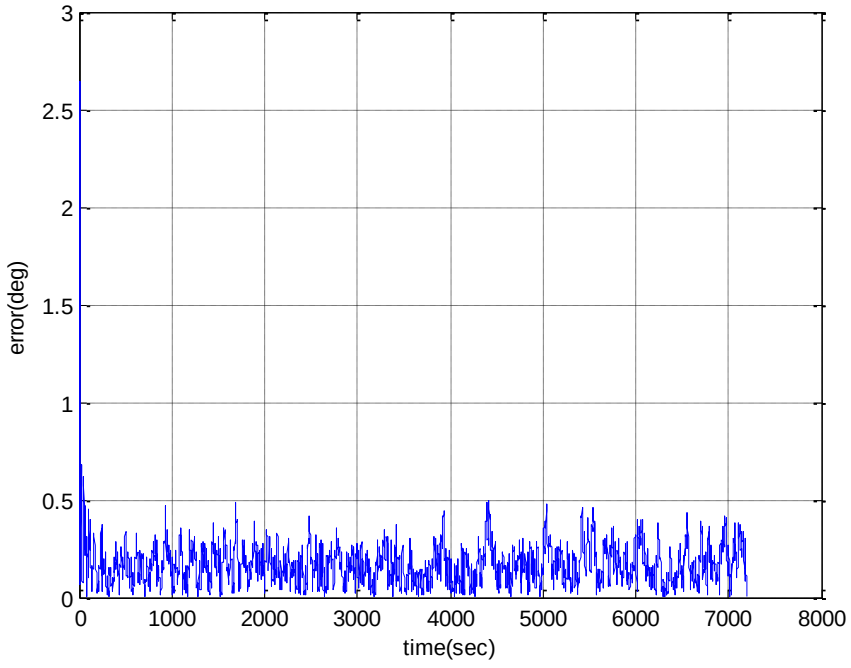

Figure 3.3. Magnetic Field Vector Angular Error for Equatorial Orbit

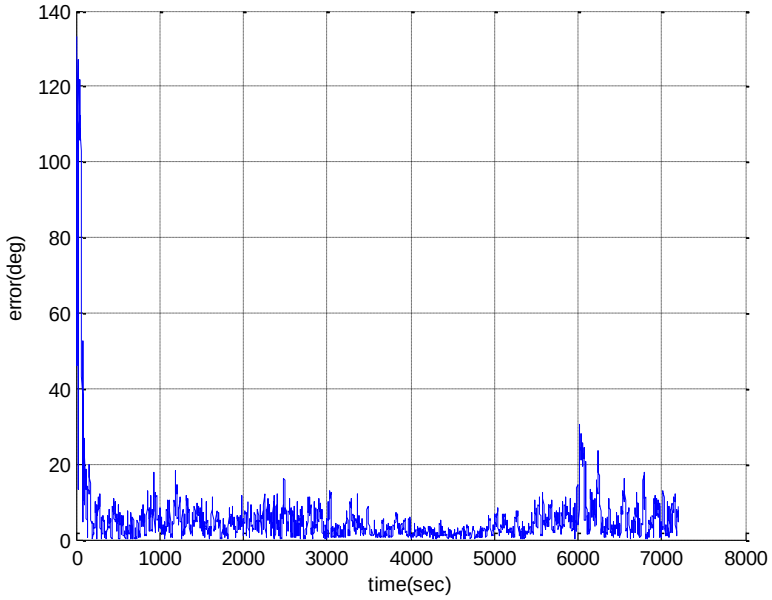

Figure 3.4. Magnetic Field Derivative Vector Angular Error for Equatorial Orbit

The simulations show that the ability of the filter to estimate the magnetic field derivative vector is much less when the spacecraft is in an equatorial orbit in comparison to the polar orbit. The initial spike at $t = 0$ remains, and the filter takes longer to converge than in the polar case. The average error in the magnetic field derivative vector estimate is around ten degrees with spikes above twenty degrees for the equatorial orbit. The ability of the attitude filter to handle uncertainty in the pseudo-measurements from the magnetometer measurement filter is further analyzed in the Parametric Analysis section of this thesis.

4. ATTITUDE DYNAMICS

4.1. RIGID BODY ATTITUDE DYNAMICS.

This section provides an overview of the attitude dynamics used as a background for this thesis. The attitude determination technique incorporates quaternions, so the basic attitude quaternion is developed and the relationship to Euler's equations is given. The section concludes with the presentation of a semi-analytic solution to the magnetometer-only attitude determination problem.

4.1.1. Euler's Equations. The basic rigid body attitude dynamics problem can be modeled using Euler's equations. Euler's equations show that a rigid body's attitude dynamics are dependent on the object's moment of inertia and its angular velocity. The Euler equations that describe the angular velocity of a spacecraft are

$$\begin{aligned}\dot{\omega}_x &= \frac{\tau_x - \left(I_{zz} - I_{yy}\right)\omega_y\omega_z}{I_{xx}} \\ \dot{\omega}_y &= \frac{\tau_y - \left(I_{xx} - I_{zz}\right)\omega_x\omega_z}{I_{yy}} \\ \dot{\omega}_z &= \frac{\tau_z - \left(I_{yy} - I_{xx}\right)\omega_x\omega_y}{I_{zz}}\end{aligned} \tag{20}$$

where I_{xx}, I_{yy}, and I_{zz} are the principal axes moments of inertia of the spacecraft and $\tau_{x\text{-}z}$ are the external torques applied to the satellite.[28]

4.1.2. Attitude Representation. The attitude of a spacecraft is often represented using a direction cosine matrix. This matrix represents a rotational transformation from one reference frame to another.

The spacecraft attitude matrix is used to relate the inertial frame to the body frame through

$$\mathbf{V}_I = A\mathbf{V}_b \tag{21}$$

where $\mathbf{V}_I$ is any vector expressed in terms of the inertial frame and $\mathbf{V}_b$ is the same vector, expressed in terms of the body frame. The goal of attitude determination is to find this relationship (i.e., determine the *A* matrix). The attitude matrix, *A*, has nine elements and is orthonormal. The problem cannot be solved by knowing one vector in each frame, because, as can be seen from Equation (21), there are nine unknowns and only three scalar equations.

4.2. QUATERNIONS.

Quaternions are four-dimensional vectors that can be used to express the attitude of an object. They are manipulated similarly to imaginary numbers. The benefit of using quaternions for this research is the ability to represent the spacecraft attitude using four elements instead of the nine elements of the typical attitude matrix. Quaternions also avoid the singularity issue that is commonly a problem when using Euler's equations.[28]

4.2.1. Quaternion Introduction. Quaternions can be used for many applications. As mentioned previously, a quaternion is a four-dimensional vector that is treated similarly to an imaginary number. In fact, Hamilton coined the term "quaternion" to refer to hyper-complex numbers of rank four.[26] The fundamental rule for quaternions is

$$i^2 = j^2 = k^2 = ijk = -1 \tag{22}$$

The above rule applies to the so-called vector part of the quaternion. The quaternion is typically broken up into a scalar and a vector part as

$$q = \left\langle q_o, \mathbf{v}_q \right\rangle \tag{23}$$

The components of $\mathbf{v}_q$ are usually denoted by q_1, q_2, and q_3. The next step is to define the operations necessary to utilize quaternions. Addition is performed by simply adding components, analogous to adding two four-dimensional vectors. Quaternions are multiplied using the relationship

$$pq = \left\langle p_0 q_0 - p \cdot q, p_0 \mathbf{v}_q + q_0 \mathbf{v}_p + \mathbf{v}_p \times \mathbf{v}_q \right\rangle \tag{24}$$

where p and q are quaternions whose scalar components are represented by p_0 and q_0 respectively, and vector components are $\mathbf{v}_p$ and $\mathbf{q}_p$ respectively. These relationships are important for using quaternions for attitude representation. Another useful property defines the complex conjugate of the quaternion as

$$q^c = \left\langle q_0, -\mathbf{v}_q \right\rangle \tag{25}$$

The conjugate is the same as the inverse for the unit magnitude quaternion. The next section shows how the quaternion and its properties can be used for representing attitude dynamics.

4.2.2. Attitude Representation with Quaternions. Quaternions can be used to describe a rotation in much the same way as the attitude matrix or direction cosine matrix. The attitude quaternion has unit magnitude so the rotation does not affect the magnitude of the vector being rotated. The inverse of the quaternion is the complex conjugate, similar to the transpose of the attitude matrix being equal to the inverse of the attitude matrix.

Let q be the attitude quaternion representing the attitude of a spacecraft, and let the spacecraft have angular velocity ω. The attitude matrix A in Equation (21) can be expressed in terms of the attitude quaternion q as

$$A = \begin{bmatrix} 1-2q_3^2-2q_4^2 & 2(q_2q_3-q_1q_4) & 2(q_2q_4-q_1q_3) \\ 2(q_2q_3-q_1q_4) & 1-2q_2^2-2q_4^2 & 2(q_3q_4-q_1q_2) \\ 2(q_2q_4-q_1q_3) & 2(q_3q_4-q_1q_2) & 1-2q_2^2-2q_3^2 \end{bmatrix} \tag{26}$$

where q_0, q_1, q_2, and q_3 are the elements of the attitude quaternion; the latter three make up the vector v_q. Note that by using quaternions, the attitude matrix in Equation (26) is a function of only four unknowns instead of nine as before. Only three

The quaternion can be used to propagate the attitude through the dynamic equation

$$\dot{q} = \frac{1}{2} q\boldsymbol{\omega}^* \tag{27}$$

where $\boldsymbol{\omega}^*$ is the quaternion representation of the spacecraft angular velocity, $\langle 0, \boldsymbol{\omega} \rangle$.[26]

4.3. ATTITUDE CALCULATION FROM MAGNETIC FIELD DERIVATIVE.

The attitude quaternion can be determined from a (somewhat complicated) quadratic equation shown in this section. Several attempts were made to find the solution to this equation before the final solution of using a Kalman filter to estimate the attitude quaternion was arrived upon. Test cases were completed that showed the algorithm could calculate the attitude when an optimization routine was used to find the attitude and angular rates that satisfy the equations. The algorithm only found the correct solution for cases in which the spacecraft had no angular velocity. When angular velocity was added to the simulation, the optimization routine would not converge.

4.3.1. Attitude Derivation with Matrices. The basic attitude rotation matrix *A* relates the magnetic field vector when expressed in inertial and body frames through

$$\mathbf{B}_I = A\mathbf{B}_b \tag{28}$$

The attitude matrix *A* is a three-by-three matrix with nine separate elements. All elements must be determined to truly know the attitude of the spacecraft. The known quantities in Equation (24) are the magnetic field vector in both frames. The term $\mathbf{B}_\mathrm{I}$ is known from the magnetic field model after inputting the spacecraft position as provided from the orbit determination system. The $\mathbf{B}_\mathrm{b}$ term is the magnetic field measurement obtained directly from the magnetometer. The matrix equation can be broken down from one matrix equation to three scalar equations with nine unknowns. There are more equations relating the different elements of the attitude matrix to each other, which decrease the number of unknowns, but these equations are accounted for later.

Differentiating Equation (24) with respect to time gives

$$\dot{\mathbf{B}}_I = \dot{A}\mathbf{B}_b + A\dot{\mathbf{B}}_b \tag{29}$$

It should be noted that by taking the derivative, more unknowns are introduced. However, by using the magnetometer measurement filter, the magnetic field derivative with respect to the body frame can be treated as known. Also, by finite differencing the magnetic field model, the magnetic field derivative with respect to the inertial frame can be considered known. With these two equations, there are now six scalar equations and eighteen unknowns. Although the gap between the number of equations and unknowns has grown, by differentiating one more time the second derivative of the attitude matrix appears. With an attitude model to determine the angular acceleration on the spacecraft due to perturbations, and knowing the control torques, the attitude second derivative can be considered to be known. Also, the second derivatives of the magnetic field vector in each frame would need to be calculated. If these are found, the system has nine equations and eighteen unknowns. Using the fact that the attitude matrix must not affect the magnitude of the vector it is transforming, nine more equations are gained, and the attitude can be determined.[28] However, the quaternion method, as described in the next section, shows that an analogous approach can be used with quaternion representation that does not require the second derivatives to determine the attitude.

4.3.2. Attitude Derivation with Quaternions. The quaternion approach uses the same basic steps detailed in the above subsection, with quaternion transformations used instead of the direction cosine matrix. It is shown here that the number of equations required to solve for the attitude, with the given position and magnetic field measurement, is significantly reduced.

First, start with a basic equation representing the magnetic field vector calculated from the measurement as

$$\langle 0, \mathbf{B}_b \rangle = q^c \langle 0, \mathbf{B}_I \rangle q \tag{30}$$

where q is the spacecraft attitude quaternion, and q_c is the attitude quaternion conjugate, defined in Equation (25).

When broken down, Equation (30) yields three scalar equations and four unknowns (the elements of the attitude quaternion). Using the same approach as the previous section, the time derivative is taken of the magnetic field equation resulting in

$$\left\langle 0,\dot{\mathbf{B}}_b \right\rangle = \dot{q}^c \left\langle 0,\mathbf{B}_I \right\rangle q + q^c \left\langle 0,\dot{\mathbf{B}}_I \right\rangle q + q^c \left\langle 0,\mathbf{B}_I \right\rangle \dot{q} \tag{31}$$

Equation (31) represents six scalar equations and eight unknowns. By using the fact that the attitude quaternion has unit magnitude, the constraint equations[26]

$$q_0^2 + \mathbf{v}_q \cdot \mathbf{v}_q = 1 \tag{32}$$

$$2q_0\dot{q}_0 + 2q_1\dot{q}_1 + 2q_2\dot{q}_2 + 2q_3\dot{q}_3 = 0 \tag{33}$$

can be obtained.

These equations show that enough information can be gathered when using quaternions to fully determine the attitude without the need for finding the second derivative of the magnetic field vector. Due to the quaternion's lack of "gimbal lock" issues and the ability to resolve the attitude with fewer equations, the use of quaternions was selected over direction cosine matrices (and other options). Because both of these systems are quadratic, however, multiple attitude and attitude rate combinations solve the given system, requiring a method by which to resolve the correct attitude solution

The first attempt to address this issue was to solve the equations with an optimization routine. As long as the initial guess is "close enough" the correct solution should be found. When implemented, however, the estimate was often not sufficiently close, causing the optimization routine to diverge. The solution to this problem, presented in the next section, is to use Equations (30, 31, 32, and 33) as the measurement equations for a Kalman filter. The equations relate the measurements $\mathbf{B}_b$ and their derivatives to the system states, q, and its derivative. The filter uses the time history of the measurements to determine which attitude solution is the correct solution.

5. FILTER DESIGN

This section describes the method by which the magnetometer measurement is used to obtain an estimate of the spacecraft attitude. The algorithm uses two Kalman filters: one to estimate the measurement derivatives needed to make the system observable, and a second filter to estimate the attitude quaternion and rates. This section describes the process in detail.

The first step is to realize that the attitude of a spacecraft cannot be determined from a single magnetometer measurement alone. A measurement taken from one attitude (orientation) is the exact same as a measurement that would result after rotating the satellite (i.e., the magnetometer) about the local magnetic field line. In typical spacecraft bus designs additional sensors provide sufficient information so that a particular set of measurements can only lead to one attitude without ambiguity. In order to perform magnetometer-only attitude determination, the time history of measurements must be used in some manner to allow the estimator to resolve the attitude about the local magnetic field line. The approach used in this study involved the development of a pre-filter. This pre-filter uses a Markov model to estimate the derivatives of the magnetic field vector.

5.1. EXTENDED KALMAN FILTER.

The Extended Kalman Filter (EKF) is used for both the pre-filter and the attitude filter. The Kalman filter provides a way to account for inaccuracies in the dynamic model of a system by combining sensor measurements with knowledge of the system dynamics. A dynamic model is used that describes the system, and measurements are used that can be related to the states of the system, the quantities that are being estimated. With knowledge of how accurate the system model is, as well as knowledge of how accurate the sensor measurement is, an estimate of the system states is obtained. The Kalman filter propagates the state dynamics and error covariance forward in time.[25]

The EKF calculates the estimate covariance, propagates it, and then uses it to update the states. Consider the system

$$\dot{x} = f\left(x\right) + w \tag{34}$$

$$y = h(x) + v \tag{35}$$

where y is the measurement, w is the process noise and v is the measurement or sensor noise with a mean of zero, and a variance of Q and R, respectively. A set of partial derivative matrices is next defined as

$$\begin{aligned} F &= \frac{\partial}{\partial x} f(x) \\ H &= \frac{\partial}{\partial x} h(x) \end{aligned} \tag{36}$$

The F and H matrices in Equation (36) are the Jacobian matrices of the plant and measurement, respectively. The system is numerically integrated including the states and the estimate covariance.

The system dynamics in Equation (34) are used to propagate the states forward in time. The *f(x)* function describes the system itself. The model can be very accurate or inaccurate, with the process noise, *w*, used to account for any inaccuracies. The covariance propagation equation for the EKF takes the form

$$\dot{P} = PF + F^T P + Q \tag{37}$$

where P is the estimate covariance, F is the Jacobian of the system dynamics, and Q is the process noise covariance. The results of the integration are known as the *a priori* state estimate and the covariance, and they are designated by a "bar" above the variable. *Posteriori* estimates are designated with a "caret" above them. The estimate and covariance are then updated using the equations

$$
\begin{aligned}
K_k &= \bar{P}_k H_k{}^T (H_k \bar{P}_k H_k{}^T + R_k)^{-1} \\
\hat{x}_k &= \bar{x}_k + K_k (y_k - h_k(\bar{x}_k, t_k)) \\
\hat{P}_k &= (I - K_k H_k)\bar{P}_k
\end{aligned}
\tag{38}
$$

Results obtained from a Kalman filter are optimal for linear systems, and the Extended Kalman Filter is very accurate and robust in most cases. Another benefit to the Extended Kalman filter is that it is very computationally efficient. If the results in this thesis study were not sufficiently accurate to meet the mission requirements of the M-SAT mission, a nonlinear filtering technique such as the Unscented Kalman Filter (UKF) or particle filter would be attempted. Currently, the EKF provides acceptable accuracy while minimizing the impact on the Command and Data Handling subsystem.

5.2. MARKOV MODEL AND PRE-FILTER.

This section describes how the magnetic field vector is used as a measurement to the pre-filter in order to estimate the magnetic field derivative. The Kalman filter uses a third-order Markov process to model the magnetic field. The model is given by

$$
\frac{\mathrm{d}^3}{\mathrm{d}t^3}\mathbf{B} = w \tag{39}
$$

where **B** is the magnetic field vector and *w* is white Gaussian process noise. The filter is initialized by using finite differencing on the first three magnetometer measurements. The use of a third-order Markov process allows the filter to estimate the first and second derivatives of the magnetic field vector as well as the field vector itself. The third-order Markov model used to estimate the magnetic field derivative is given by

$$
\begin{aligned}
\frac{\mathrm{d}}{\mathrm{d}t}\mathbf{B} &= \dot{\mathbf{B}} \\
\frac{\mathrm{d}}{\mathrm{d}t}\dot{\mathbf{B}} &= \ddot{\mathbf{B}} \\
\frac{\mathrm{d}}{\mathrm{d}t}\ddot{\mathbf{B}} &= \mathbf{0}
\end{aligned}
\tag{40}
$$

The model in Equation (40) represents the dynamics of the pre-filter. The measurement is represented by

$$y = \begin{bmatrix} B_x \\ B_y \\ B_z \end{bmatrix} \tag{41}$$

The state dynamics can be represented as

$$\dot{x} = \frac{d}{dt}\begin{bmatrix} B_x \\ B_y \\ B_z \\ \dot{B}_x \\ \dot{B}_y \\ \dot{B}_z \\ \ddot{B}_x \\ \ddot{B}_y \\ \ddot{B}_z \end{bmatrix} = \begin{bmatrix} \dot{B}_x \\ \dot{B}_y \\ \dot{B}_z \\ \ddot{B}_x \\ \ddot{B}_y \\ \ddot{B}_z \\ 0 \\ 0 \\ 0 \end{bmatrix} \tag{42}$$

The F matrix and measurement matrix, H, for the Kalman filter are given by

$$F = \begin{bmatrix} 0 & 0 & 0 & 1 & 0 & 0 & 0 & 0 & 0 \\ 0 & 0 & 0 & 0 & 1 & 0 & 0 & 0 & 0 \\ 0 & 0 & 0 & 0 & 0 & 1 & 0 & 0 & 0 \\ 0 & 0 & 0 & 0 & 0 & 0 & 1 & 0 & 0 \\ 0 & 0 & 0 & 0 & 0 & 0 & 0 & 1 & 0 \\ 0 & 0 & 0 & 0 & 0 & 0 & 0 & 0 & 1 \\ 0 & 0 & 0 & 0 & 0 & 0 & 0 & 0 & 0 \\ 0 & 0 & 0 & 0 & 0 & 0 & 0 & 0 & 0 \\ 0 & 0 & 0 & 0 & 0 & 0 & 0 & 0 & 0 \end{bmatrix} \tag{43}$$

$$H = \begin{bmatrix} 1 & 0 & 0 & 0 & 0 & 0 & 0 & 0 & 0 \\ 0 & 1 & 0 & 0 & 0 & 0 & 0 & 0 & 0 \\ 0 & 0 & 1 & 0 & 0 & 0 & 0 & 0 & 0 \end{bmatrix} \tag{44}$$

The Kalman Filter used for the pre-filter calculates the *a priori* state estimate as

$$\bar{x}_k = f(\hat{x}_{k-1}, dt) \tag{45}$$

The *a priori* estimate is calculated using the dynamic model. The covariance is propagated using

$$\dot{P} = FP + PF^T + Q \tag{46}$$

The update stage of the Kalman filter proceeds as

$$\begin{aligned} K_k &= \bar{P}_k H_k{}^T (H_k \bar{P}_k H_k{}^T + R_k)^{-1} \\ \hat{x}_k &= \bar{x}_k + K_k (y_k - h_k(\bar{x}_k, t_k)) \\ \hat{P}_k &= (I - K_k H_k)\bar{P}_k \end{aligned} \tag{47}$$

where K is the filter gain, R is the measurement noise covariance, and the caret represents *a posteriori* information. The new estimate is represented by $\hat{x}$.

The pre-filter results, shown below in Figures 5.1 and 5.2, show the estimates of the magnetic field vector and derivative for a simulation running 1000 seconds. The pre-filter is evaluated for the baseline case discussed in Section 6.1, which is an orbit with a 400 km altitude, forty degrees inclination, and an initial spacecraft angular velocity of [2, 5, 3] degrees per second. The simulation shows that the magnetic field derivative can be accurately estimated even without knowledge of the satellite rotation in the model. The estimates track very closely to the actual data. The error in the magnetic field vector and derivative estimates is shown in Figures 5.3 and 5.4.

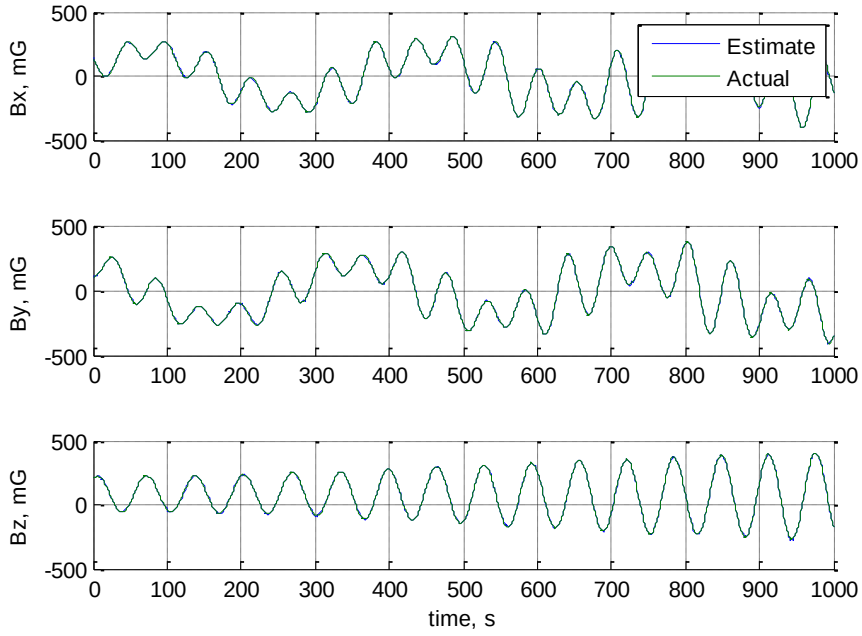

Figure 5.1. Estimated and Actual Magnetic Field Components

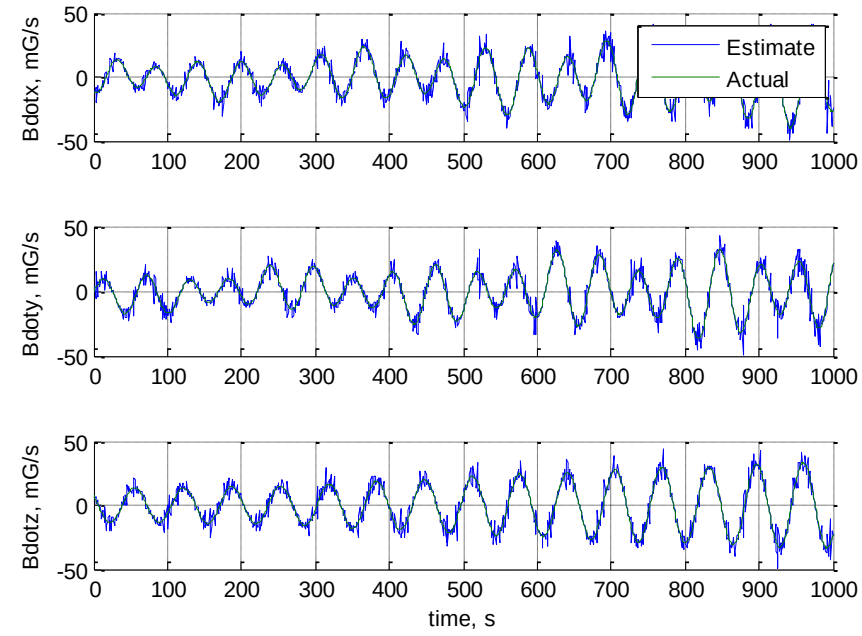

Figure 5.2. Estimated and Actual Magnetic Field Derivative Components

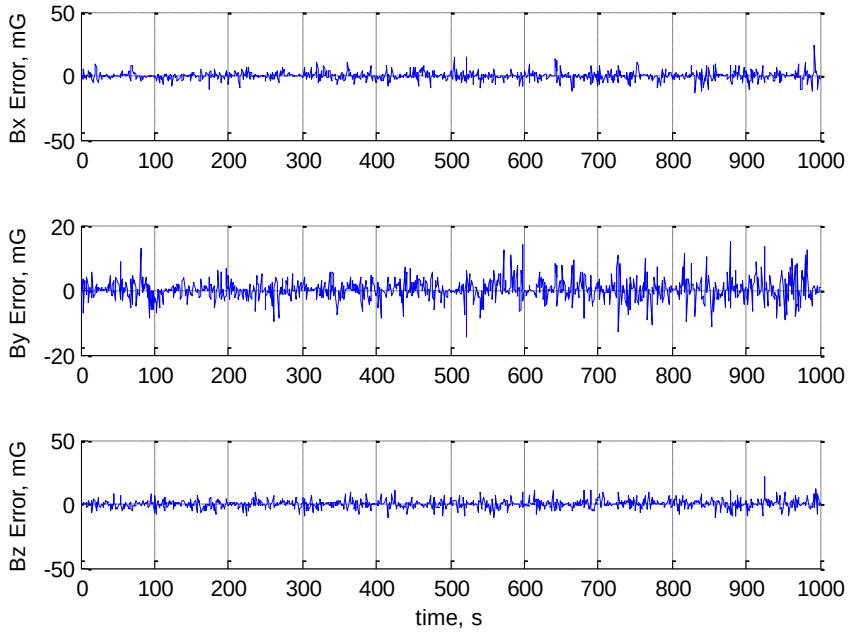

Figure 5.3. Magnetic Field Vector Component Estimation Error

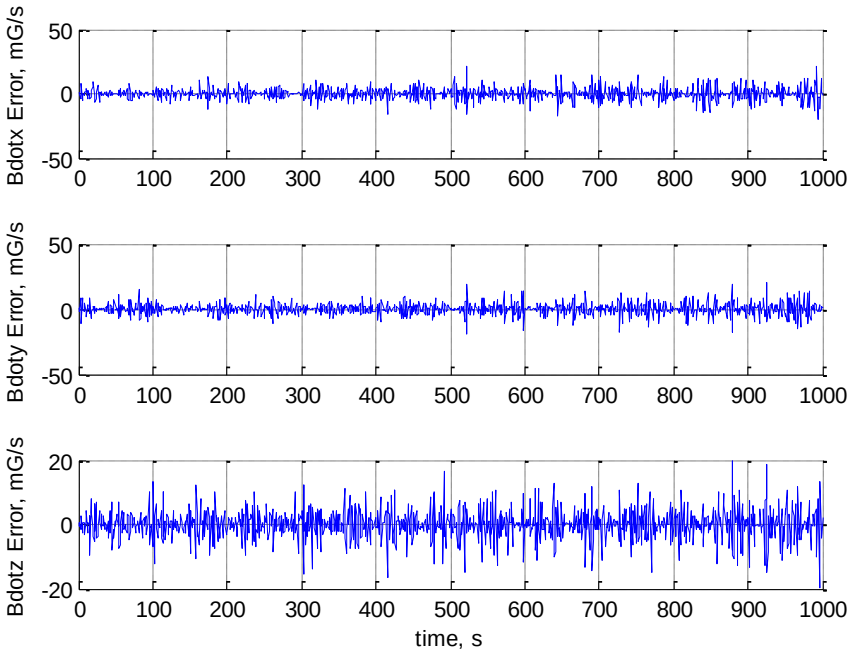

Figure 5.4. Magnetic Field Derivative Vector Component Estimation Error

The pre-filter estimates the magnetic field derivative with sufficient accuracy to calculate the spacecraft attitude. The filter can be tuned to obtain improved results depending on the situation, but the current initial error covariance and process noise covariance provide more consistent results regardless of the simulation conditions considered. The filter parameters are discussed in Section 6.1.

5.3. PSEUDO-MEASUREMENTS AND ATTITUDE FILTER.

Adding the first derivative of the magnetic field measurement to the attitude filter gives two vectors each expressed in terms of two different frames, which from past well-known attitude determination studies suggests that the TRIAD method may be a good choice to calculate the spacecraft attitude.[14] The TRIAD method is used to determine the attitude rotation that results from having two different vectors expressed in two different coordinate frames, but if one vector is a derivative, the rotation of the body frame must be accounted for in the applicable kinematic equations. However, the magnetic field derivative depends not only on fluctuations in the Earth's magnetic field, but also on the satellite's angular velocity, due to the magnetic field derivative being expressed in the rotating body frame. The TRIAD algorithm requires all four vectors, two in each frame, to be inertially referenced. This leads to a complication for this study, because the attitude rate is needed and there are no onboard sensors to provide the attitude rate. This section shows the adjustment used to make the magnetometer-only system viable.

The governing equations for the spacecraft attitude quaternion with respect to the magnetic field vector and derivative are now used to setup the filter. Equations (30, 31, 32, and 33) are used to relate the states, attitude quaternion and spacecraft angular rates to the pseudo-measurements, the magnetic field vector and its derivative. These attitude equations provide a system with eight equations and eight unknowns, and this system could theoretically be solved. However, the quadratic nature of the equations leads to multiple solutions, and the equations are difficult to solve. Another approach uses the system in a filter that uses a sequence of estimates and measurements to find the best estimate without needing to choose between two solutions. So the next step is to construct an Extended Kalman Filter using the magnetic field vector and its derivative as measurements and estimate the attitude quaternion and rates.

The attitude determination filter is configured to accept the magnetic field and its derivative as measurements with the states for the filter as the attitude quaternion and the spacecraft angular rates. The states are related to the measurement through the *H* matrix which is contains the derivatives of the quaternion equations derived in Section 4. Finite differencing is used to calculate the measurement matrix needed for the EKF filter used in the attitude determination code.

The measurements for the attitude filter are

$$y = \begin{bmatrix} B_{b_x} \\ B_{b_y} \\ B_{b_z} \\ \dot{B}_{b_x} \\ \dot{B}_{b_y} \\ \dot{B}_{b_z} \end{bmatrix} \tag{48}$$

By substituting Equations (27, 30, and 31) into Equation (48), the measurements can be related to the states as

$$y = \begin{bmatrix} q^c \langle 0, B_I \rangle q \\ \dot{q}^c \langle 0, B_I \rangle q + q^c \langle 0, \dot{B}_I \rangle q + q^c \langle 0, B_I \rangle \dot{q} \end{bmatrix} = \begin{bmatrix} q^c \langle 0, B_I \rangle q \\ \frac{1}{2} q^c \omega \langle 0, B_I \rangle q + q^c \langle 0, \dot{B}_I \rangle q + q^c \langle 0, B_I \rangle \frac{1}{2} q\omega \end{bmatrix} \tag{49}$$

Note that in the above equation, the multiplications are quaternion multiplications and the brackets around the magnetic field values add a zero as the first element so that the vector becomes a four element vector that can be multiplied with quaternions. It is also assumed that the first element (which is always zero) of each resultant four-element vector is removed after the multiplications (in order to preserve the dimension of *y* having six elements instead of eight).

The system dynamics are represented using quaternion dynamics and Euler's equations as

$$\frac{\mathrm{d}}{\mathrm{d}t}\begin{bmatrix} q_0 \\ q_1 \\ q_2 \\ q_3 \\ \omega_x \\ \omega_y \\ \omega_z \end{bmatrix} = \begin{bmatrix} \frac{1}{2} q\omega \\ \frac{M_x - (I_z - I_y)\omega_y\omega_z}{I_x} \\ \frac{M_y - (I_x - I_z)\omega_x\omega_z}{I_y} \\ \frac{M_z - (I_y - I_x)\omega_x\omega_y}{I_z} \end{bmatrix} \tag{50}$$

The filter matrices become

$$F = \begin{bmatrix} 0 & -\frac{1}{2}\omega_x & -\frac{1}{2}\omega_y & -\frac{1}{2}\omega_z & -\frac{1}{2}q_1 & -\frac{1}{2}q_2 & -\frac{1}{2}q_3 \\ \frac{1}{2}\omega_x & 0 & \frac{1}{2}\omega_z & -\frac{1}{2}\omega_y & \frac{1}{2}q_0 & -\frac{1}{2}q_3 & \frac{1}{2}q_2 \\ \frac{1}{2}\omega_y & -\frac{1}{2}\omega_z & 0 & \frac{1}{2}\omega_x & \frac{1}{2}q_3 & -\frac{1}{2}q_0 & -\frac{1}{2}q_1 \\ \frac{1}{2}\omega_z & \frac{1}{2}\omega_y & -\frac{1}{2}\omega_x & 0 & -\frac{1}{2}q_2 & \frac{1}{2}q_1 & \frac{1}{2}q_0 \\ 0 & 0 & 0 & 0 & 0 & \frac{-(I_z - I_y)\omega_z}{I_x} & \frac{-(I_z - I_y)\omega_y}{I_x} \\ 0 & 0 & 0 & 0 & \frac{-(I_x - I_z)\omega_z}{I_y} & 0 & \frac{-(I_x - I_z)\omega_x}{I_y} \\ 0 & 0 & 0 & 0 & \frac{-(I_y - I_x)\omega_y}{I_z} & \frac{-(I_y - I_x)\omega_x}{I_z} & 0 \end{bmatrix} \tag{51}$$

The *H* matrix for the EKF filter is calculated using finite differencing on the equations that represent the measurements in terms of the states as shown in Equation (49).

To analyze the filter's performance, a simulation was performed using an orbit with a 400 km altitude, zero eccentricity, and a 40 degrees inclination. This baseline case is described in more detail in Section 6.1. Figure 5.5 shows the attitude angular estimation error for the simulation. The requirement for the ADAC subsystem is that the attitude be determined within three degrees with a goal of determination within one degree. Figure 5.5 shows that the requirement for this case would be met, and the goal is very close to being met as well. The error drops to about one degree within about 800 seconds which corresponds to about one sixth of an orbit.

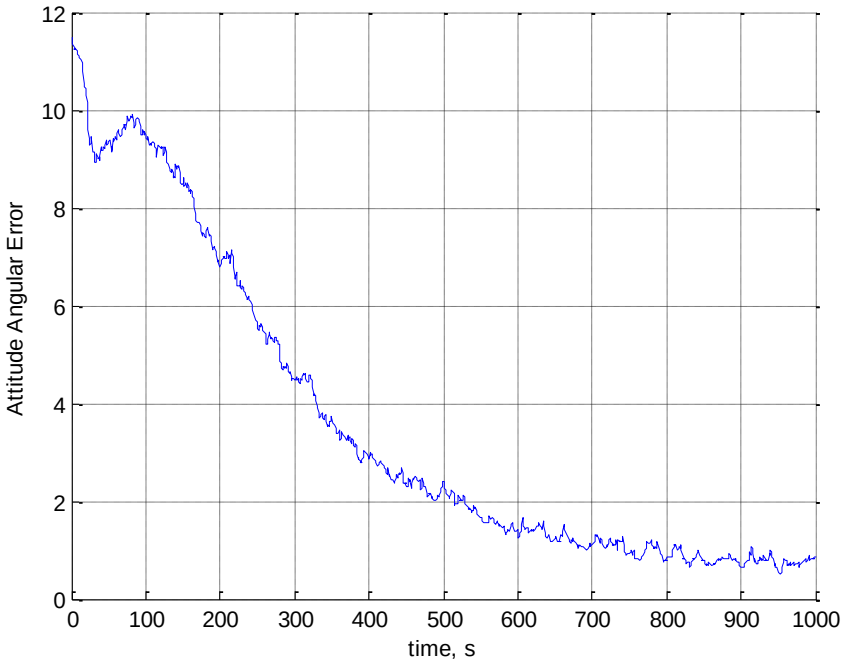

Figure 5.5. Attitude Angular Estimation Error, in Degrees

The error in the filter states, the attitude quaternion and the angular velocity, are shown in Figures 5.6 and 5.7. The seven states composed of the four elements of the attitude quaternion and the three angular rates are both estimated accurately. The components of the attitude quaternion are estimated to within about 0.01, and the angular velocity components to within 0.03 degrees per second. This helps understand why the error covariance matrix needs to be small. When simulating this scenario for the first time, the initial error covariance was set relatively high. An initial spike in the state error was exacerbated by a high initial error covariance matrix, and in response the matrix diagonals were reduced until the spike was diminished.

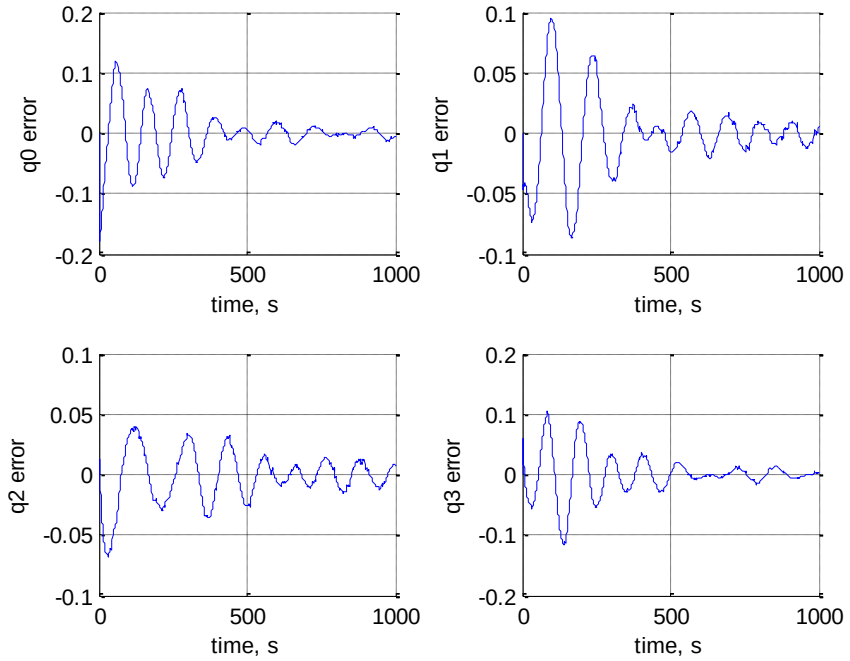

Figure 5.6. Attitude Quaternion Estimation Error

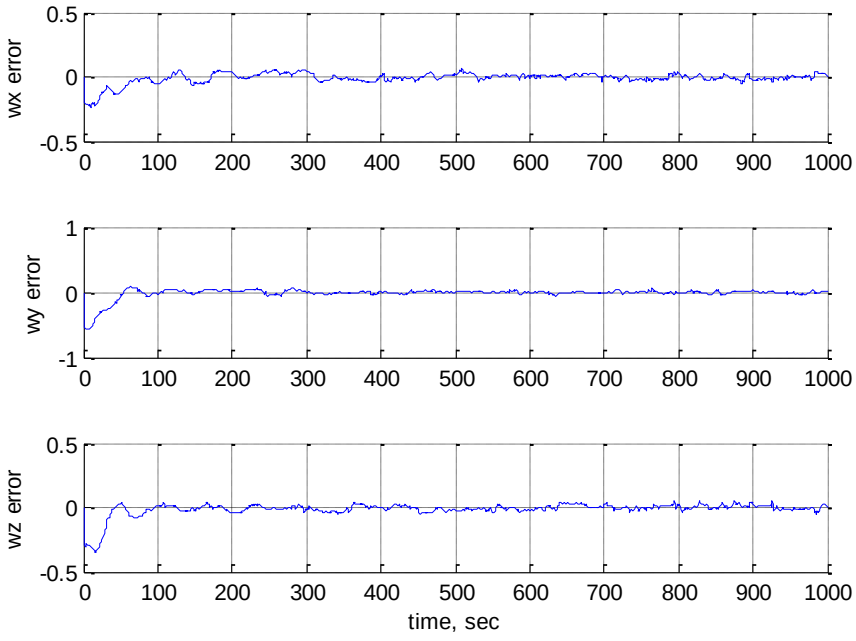

Figure 5.7. Angular Rate Estimation Error in Degrees/Second

The histories of the diagonal elements of the error covariance matrix are shown in Figure 5.8. The diagonals start small, and remain small. The elements corresponding to the quaternion show an oscillatory behavior similar to the magnetic field vector estimates. Typically, when using the EKF filter, the diagonal elements of the covariance matrix start high, then fall to a fairly constant steady state value. For this simulation, although the behavior is not typical, the matrix diagonal elements stay small and bounded, without any signs of divergence.

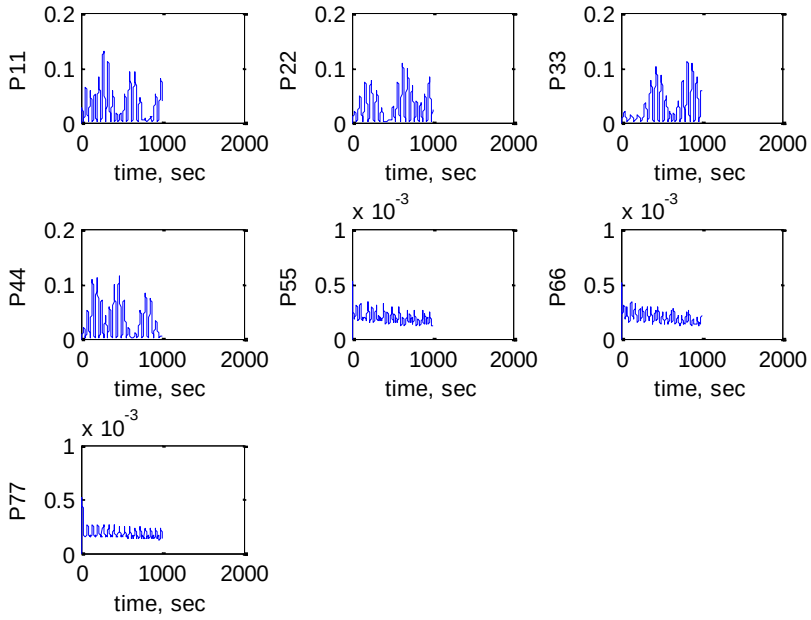

Figure 5.8. *A Posteriori* State Estimate Covariance Diagonals

The baseline simulation shows very promising results. These results are dependent on the spacecraft orbit parameters, the mass properties, the spacecraft angular velocity, and the filter tuning parameters. With so many variables, a parametric study is needed to evaluate the performance under many different conditions. Section 6 summarizes a number of simulations subjecting the filter to a more rigorous test under varying conditions.

5.4. TUNING AND COVARIANCE.

The first consideration with tuning addressed the pre-filter. The estimates for the magnetic field derivative must be accurate in order for the method in this study to converge to a suitable solution. Using a Markov model as the model for the filter creates some errors. The Markov model assumes the derivative of one state is the next state, and chains the states together until some higher order derivative is assumed to be zero. Some higher-order derivative must be modeled to zero (in this case, the third derivative of the magnetic field was set to zero, so the method uses a third order Markov model).

The method of using a pre-filter to calculate pseudo measurements raises some issues regarding how to address the pseudo-measurement noise covariance. The first attempts at creating a working, magnetometer-only attitude algorithm were done by using the error covariance of the pre filter to feed directly in as the measurement covariance of the attitude filter. This was unsuccessful, because the propagated error covariance for the states of the pre-filter are simply estimates of the true error covariance. The second attempt used the actual error from the pre-filter (note this will not be available in a real-time on-orbit scenario!) to determine the magnitude of the actual error covariance. The error for the state being used as a pseudo-measurement was then used; however, the attitude filter still did not work (no relevant data could be obtained from the estimate). A large oscillation showed spikes of up to 40 degrees error in the attitude estimate at the beginning of the simulation, and estimates diverged because the error spike was overly excessive from the onset. To mitigate the effects of the initial spike, the initial error covariance matrix was manipulated so that each element had a lower magnitude. After some trial-and-error, it was determined that the initial covariance for this simulation needed to be very small relative to most applications. When the initial covariance was lowered, the attitude error was bounded, usually to around ten to fifteen degrees of error in the attitude. Further tuning showed that in order to obtain the accuracy needed from the algorithm; the filter must “believe” that the pseudo-measurement is not as good as the pre-filter error plots show. By raising the measurement covariance corresponding to the pseudo-measurement, the estimation errors in the attitude filter dropped to very acceptable levels.

6. SIMULATION RESULTS

6.1. BASELINE INITIAL CONDITIONS AND RESULTS.

In order to properly perform a parametric analysis, a baseline set of conditions must be set and the performance analyzed for comparison. A baseline case was defined using a circular, 400 km altitude orbit. The orbital inclination is set to forty degrees because that is the minimum inclination MR SAT can be placed in and still communicate with the Missouri S&T ground station, and it falls conveniently near the middle of the range between polar and equatorial. The right ascension is arbitrarily set to ten degrees. Because of the time dependence of the magnetic field, a simulation start date must be given. The simulations in this thesis assume the epoch time is March 28, 2011. The initial conditions for the attitude quaternion and angular rates are arbitrarily selected as

$$q = \begin{bmatrix} 0.1031 \\ 0.5157 \\ 0.2063 \\ 0.8251 \end{bmatrix} \tag{52}$$

$$\omega = \begin{bmatrix} 2 \\ 5 \\ 3 \end{bmatrix} \text{deg/sec} \tag{53}$$

The model is propagated for 1000 seconds. The attitude rates change slowly over time due to the asymmetries in the spacecraft resulting in unequal principle moments of inertia. The principle moments of inertia for the MR SAT spacecraft are

$$\begin{aligned} I_{xx} &= 0.8918222 \text{kg} \cdot \text{m}^2 \\ I_{yy} &= 0.8753646 \text{kg} \cdot \text{m}^2 \\ I_{zz} &= 0.6176641 \text{kg} \cdot \text{m}^2 \end{aligned} \tag{54}$$

The measurements, which consist of the Earth's magnetic field vector components, are generated by adding Gaussian noise to the magnetic field truth model. The noise is assumed to be white noise with a norm of zero and a mean of three degrees. The noise is added in an angular manner because the magnetometer specifications state a one degree error in the magnetic field measurement. The measurement is assumed to be random within a three degree cone of the true vector. With the simulation of the truth model, described in Section 4, complete, the next step is to initialize the filter and run the attitude determination algorithm. The pre-filter is initialized exactly as it was for the results in Section 5. The pre-filter does not need to be adjusted for each individual simulation, and is not for the results presented in this thesis. There is the possibility, however, that in certain orbits, adjusting the weights on the Markov model or the measurements could improve the results because the pre-filter could be subject to sensitivities in the magnetic field fluctuations. In this research, it is assumed that the pre-filter is a standalone add-on to the attitude filter that does not need to be adjusted.

The filter states are the attitude quaternion and the angular rates. The initial estimates for each of the simulations in the parametric analysis (unless otherwise noted) are assumed as

$$\hat{q} = \begin{bmatrix} 0.28222 \\ 0.56443 \\ 0.18814 \\ 0.75258 \end{bmatrix} \tag{55}$$

$$\hat{\omega} = \begin{bmatrix} 2.2 \\ 5.5 \\ 3.3 \end{bmatrix} \text{deg/sec} \tag{56}$$

These filter initial conditions reflect an 11.48 degree attitude error and a 10% error in the initial angular velocity estimate. These estimates can be updated by using data available from the launch vehicle provider on expected tip off rates when the spacecraft is ejected onto orbit.

The pre-filter initial error covariance matrix for the simulation is set to

$$P = \begin{bmatrix} 1\times10^{4} I_{3x3} & 0 & 0 \\ 0 & 1\times10^{6} I_{3x3} & 0 \\ 0 & 0 & 1\times10^{6} I_{3x3} \end{bmatrix} \tag{57}$$

The pre-filter measurement noise covariance is

$$R = \left[1\times10^{-9} I_{3x3} \right] \tag{58}$$

The pre filter process noise covariance is

$$Q = \left[1\times10^{-1} I_{9x9} \right] \tag{59}$$

The weights for the magnetic field pre-filter were set by trial and error, but with a logical approach. The tuning process incorporated the fact that the angular velocity of the spacecraft is not present in the model, which means a higher weight on the measurement is preferred when the angular velocity is high. By weighting the measurement more than the process noise, the filter will "trust" the measurements more, and it was clear from simulations that if the process noise covariance was raised, the estimate of the magnetic field vector shifted out of phase from the true direction when the angular velocity is increased.

The attitude filter initial error covariance matrix was required to be set low in order for the filter to function. The error covariance matrix for these simulations is

$$P = \begin{bmatrix} 1\times10^{-3} I_{4x4} & 0 \\ 0 & 1\times10^{-4} I_{3x3} \end{bmatrix} \tag{60}$$

The attitude filter measurement noise covariance matrix, *R*, and process noise covariance matrix, *Q*, were chosen as

$$R = \begin{bmatrix} 80I_{3x3} & 0 \\ 0 & 160I_{3x3} \end{bmatrix} \tag{61}$$

$$Q = \left[1 \times 10^{-5} I_{7x7} \right] \tag{62}$$

The weight selection for the attitude filter was also chosen through trial and error. The error covariance matrix needed to be set very low. If it were too high, the attitude estimate would diverge. The estimation error spiked at the beginning of the simulation, and if the error covariance matrix was not set sufficiently low to lower the spike, the estimate diverged. The first attempts at selecting a measurement noise covariance matrix for the attitude filter involved using the error covariance estimates from the pre-filter in the attitude filter. The results produced were not acceptable. The measurement covariance matrix elements needed to be increased for the filter to work properly.

The pre-filter produces a magnetic field vector and derivative estimate that is adequate to drive the attitude filter. The results (in Figures 6.1 - 6.8) show that the magnetic field vector is tracked very well, and the magnetic field derivative is tracked, but shows much more noise than the magnetic field vector estimate.

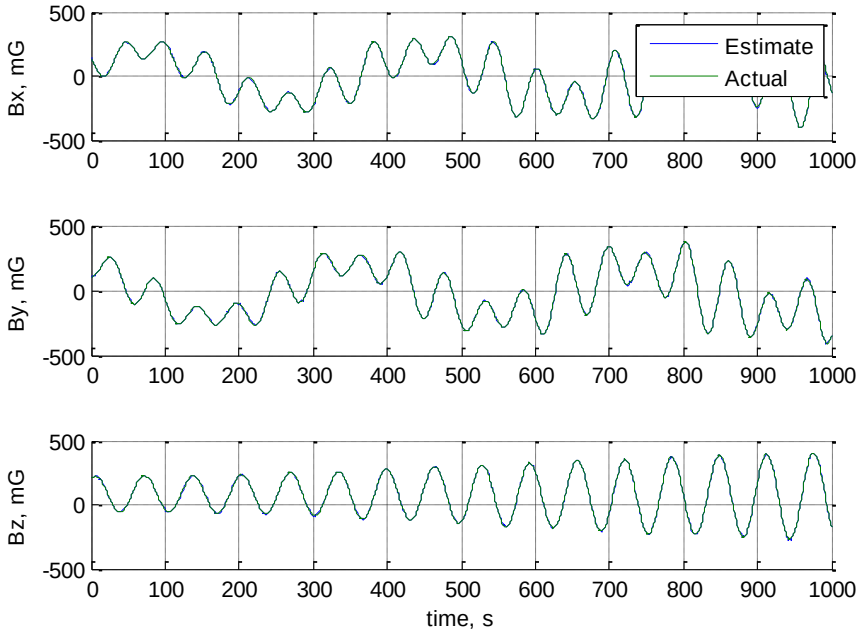

Figure 6.1. Magnetic Field Vector Baseline Estimation

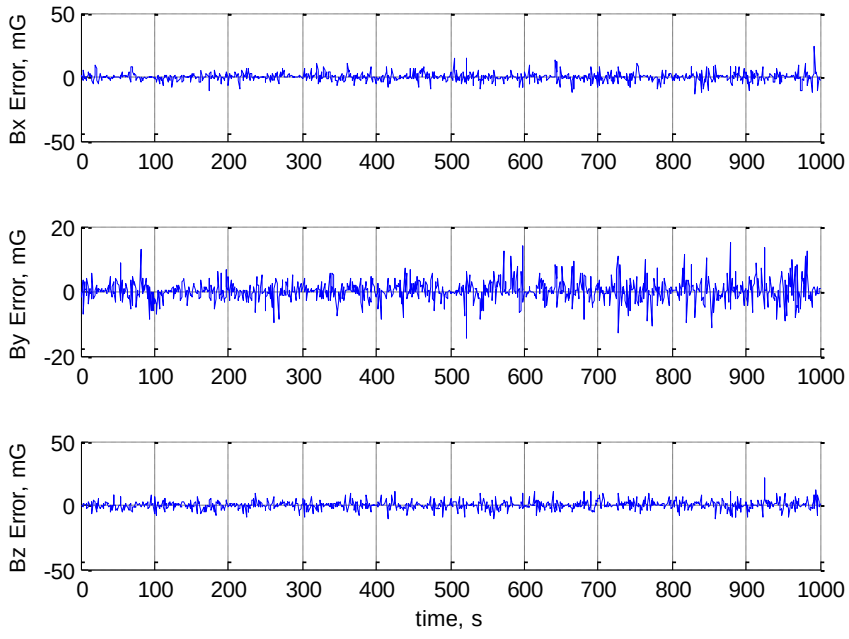

Figure 6.2. Magnetic Field Vector Baseline Estimation Error

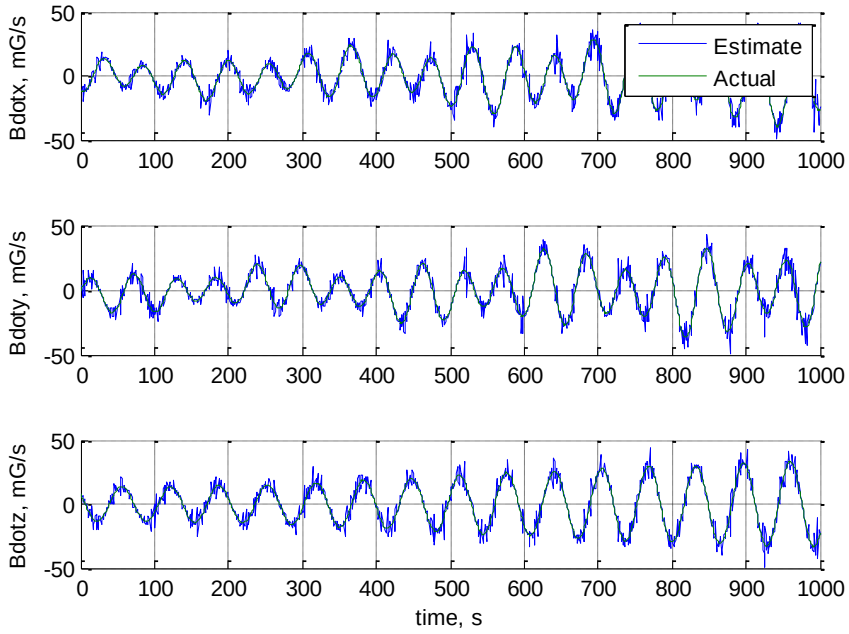

Figure 6.3. Magnetic Field Vector Derivative Baseline Estimation

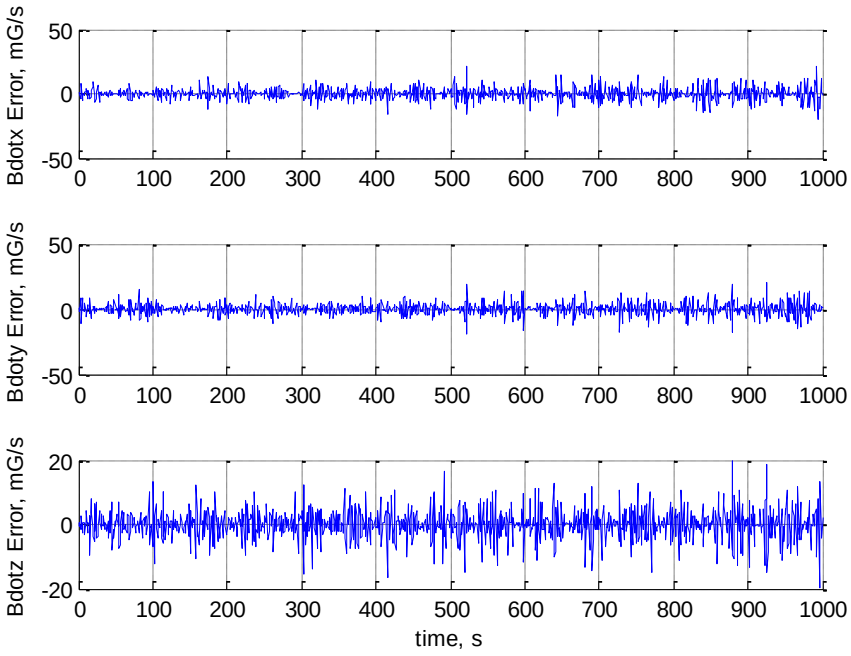

Figure 6.4. Magnetic Field Vector Derivative Baseline Estimation Error

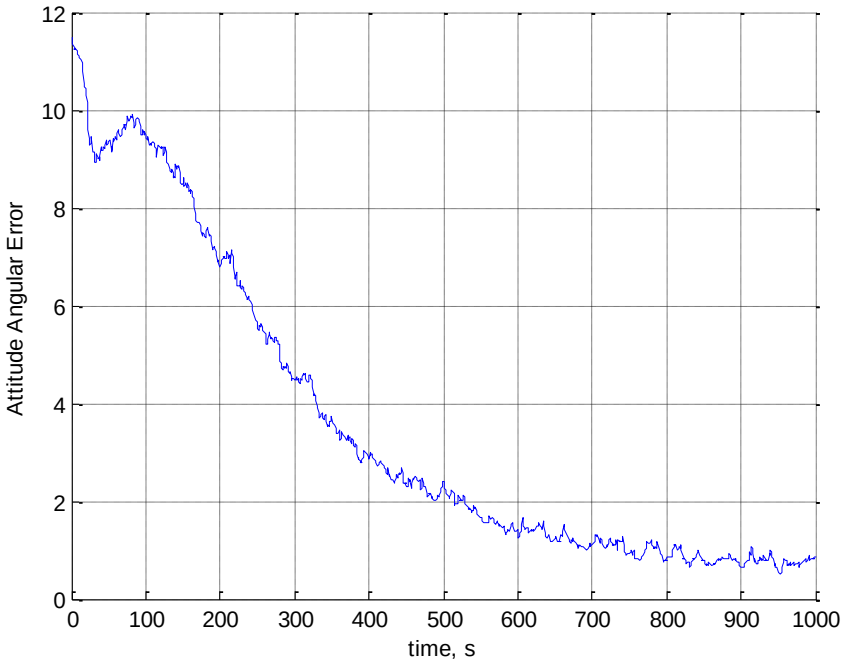

Figure 6.5. Angular Error in Spacecraft Attitude, in Degrees

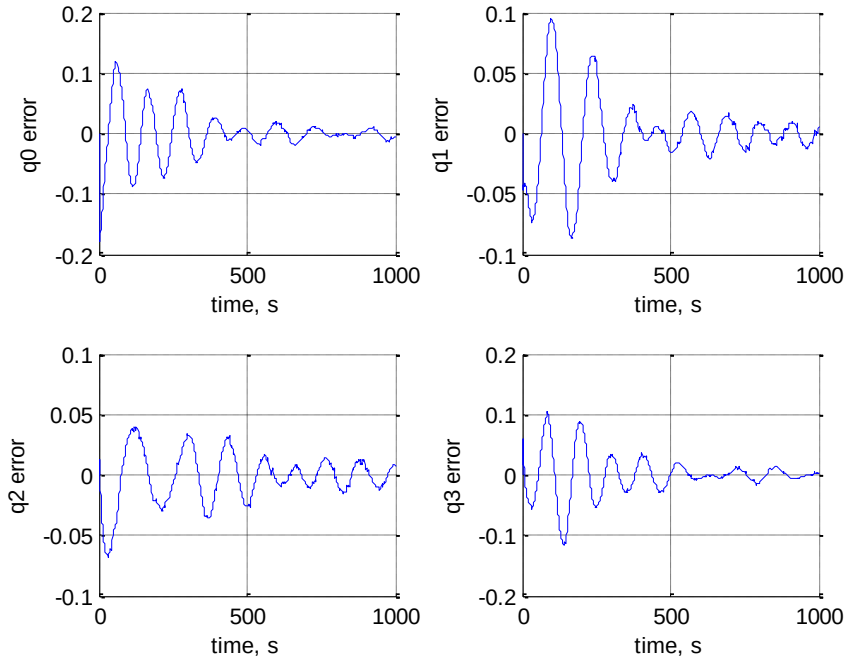

Figure 6.6. Attitude Quaternion Error

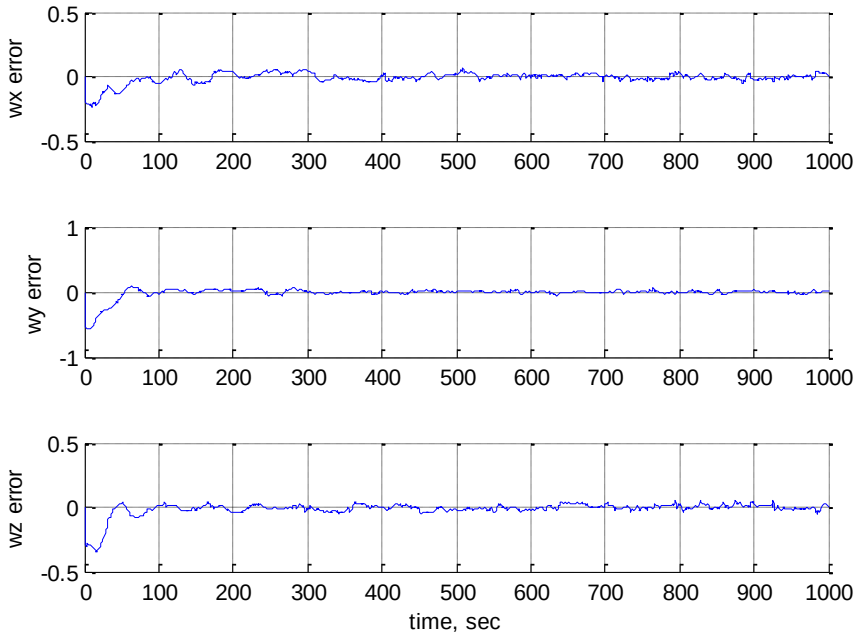

Figure 6.7. Angular Rate Estimation Error in Degrees/Second

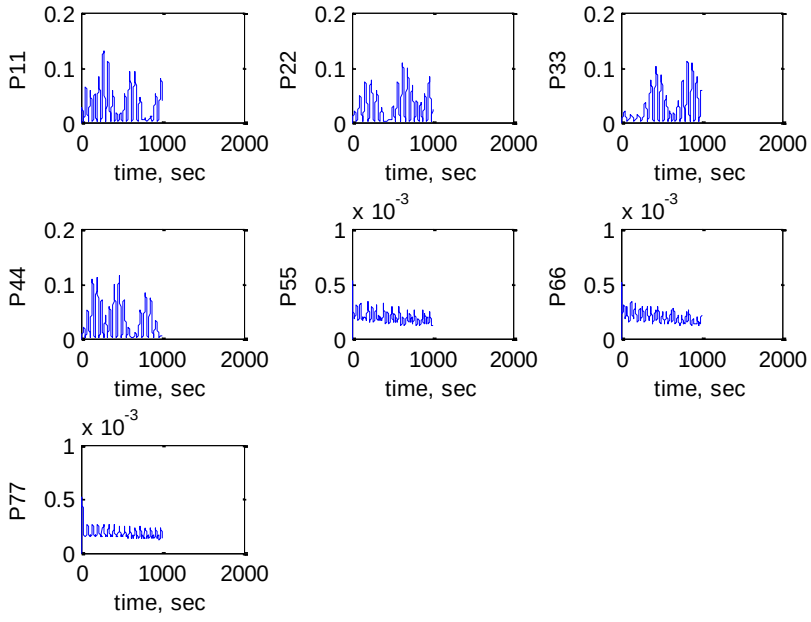

Figure 6.8. Diagonal Elements of *A Posteriori* Covariance Matrix

The plot of the magnetic field vector components show the oscillations in the magnetic field vector are mostly due to the spacecraft rotation. Comparisons between the baseline case and the low and high angular velocity cases show the oscillations increase from very low to very high as the angular velocity increases. The error covariance matrix diagonal elements are initialized very low because of the error spike at the beginning of the simulation. This causes the covariance diagonal elements to actually increase from the initial condition, unlike the typical filter setup. Though the error covariance diagonals, shown in Figure 6.8, remain low and bounded (simulations that have been run over longer time frames show the bounded nature), the noise and nonlinearities cause fluctuations in the value. The next subsection shows how the filter simulation responds to changes in orbit and initial conditions.

6.2. PARAMETRIC ANALYSIS.

With the attitude determination algorithm working for baseline cases, the system must be tested for robustness and reliability by varying mission parameters to identify any ambiguities or singularities, if any. The simulations in this section use the same initial conditions as the baseline case, only varying the parameter of interest to be analyzed.

6.2.1. Altitude. The first parameter varied in the magnetometer-only attitude determination algorithm is the altitude. The spacecraft orbital altitude is important because the magnetic field decreases in intensity as altitude increases. It is important to determine if there is a limit as to how high in orbital altitude the algorithm will perform adequately. Common sense suggests that the algorithm should work better at lower altitudes because of the higher magnitudes of the magnetic field vector and because the derivative is likely changing more rapidly.

The first simulation is performed with an altitude of 3,000 km. The baseline altitude of 400 km is sufficiently low to define the minimum altitude considered. The only change in the simulation of the baseline case and the results shown below is the altitude increase. The new altitude of 3000 km was chosen because it was the next lowest altitude considered that showed a significant change in the results. The results in Figures 6.9-6.16 show an increase in accuracy as the altitude increases.

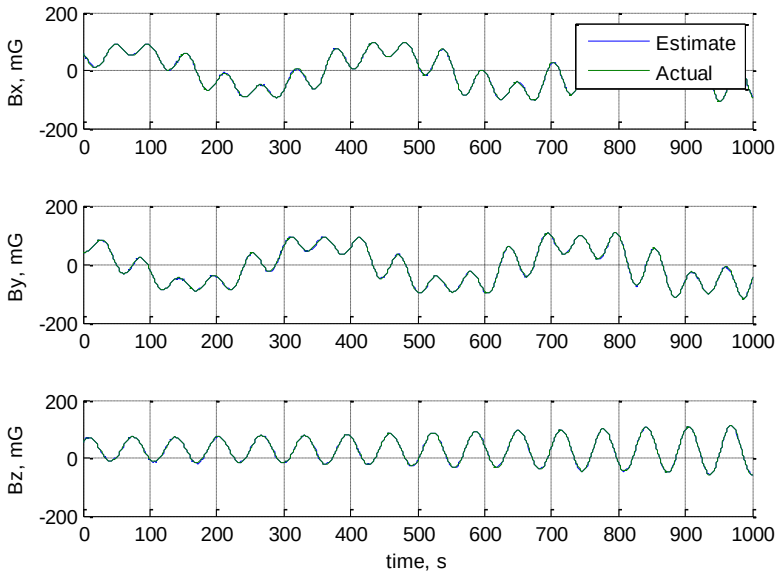

Figure 6.9. Magnetic Field Vector Estimation for 3,000 km Altitude

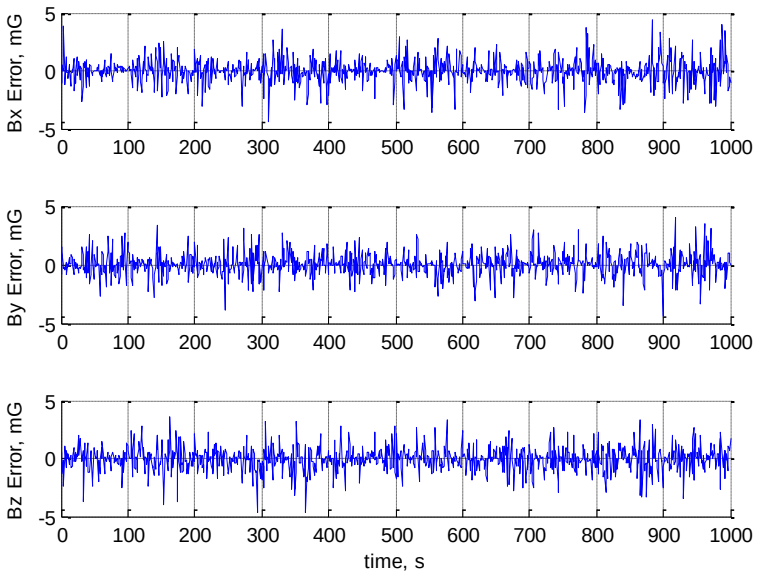

Figure 6.10. Magnetic Field Vector Estimation Error for 3,000 km Altitude

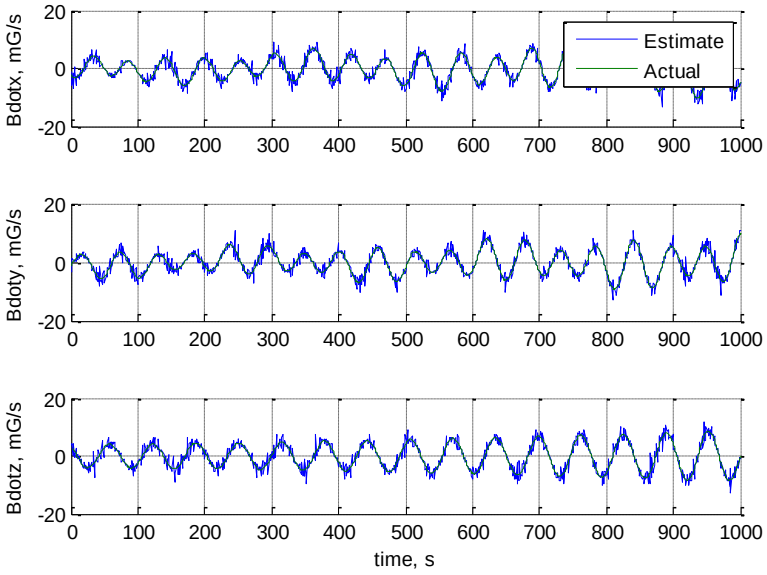

Figure 6.11. Magnetic Field Vector Derivative Estimation for 3,000 km Altitude

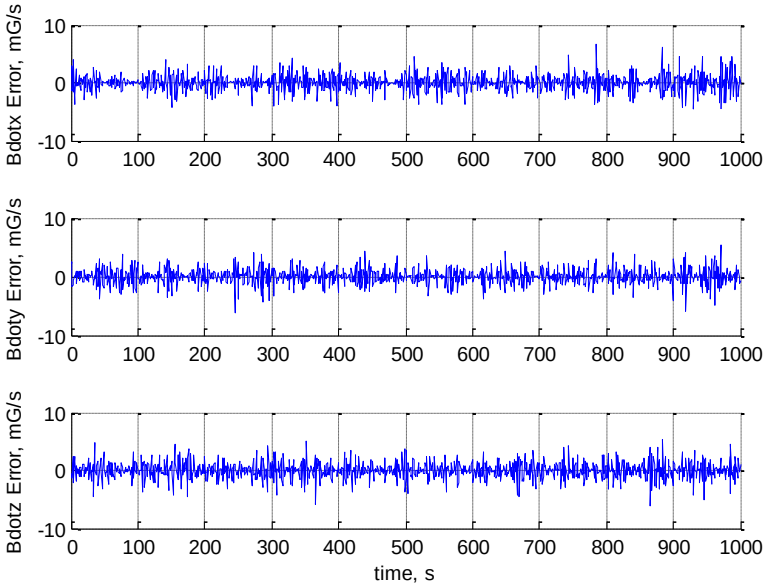

Figure 6.12. Magnetic Field Vector Derivative Estimation Error for 3,000 km Altitude

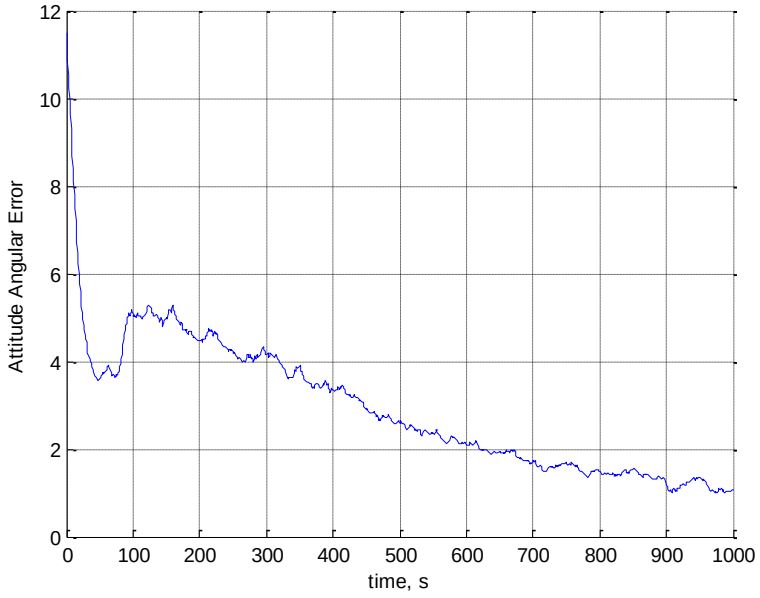

Figure 6.13. Angular Error in Spacecraft Attitude, in Degrees, for 3,000 km Altitude

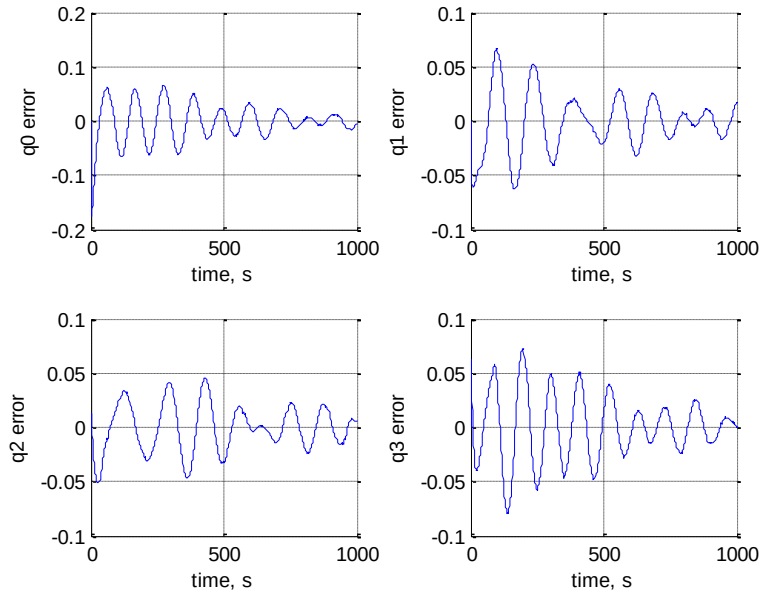

Figure 6.14. Attitude Quaternion Estimation Error for 3,000 km Altitude

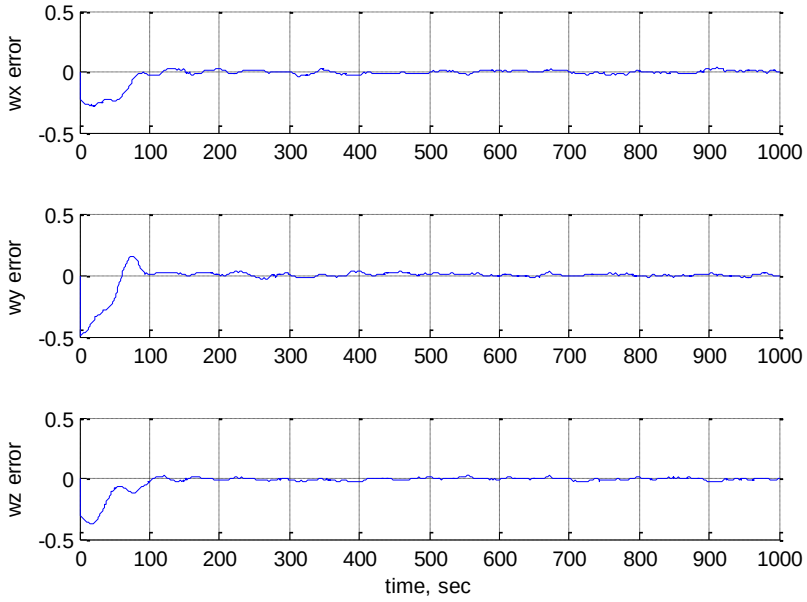

Figure 6.15. Angular Velocity Estimation Error in Degrees/Second for 3,000 km Altitude

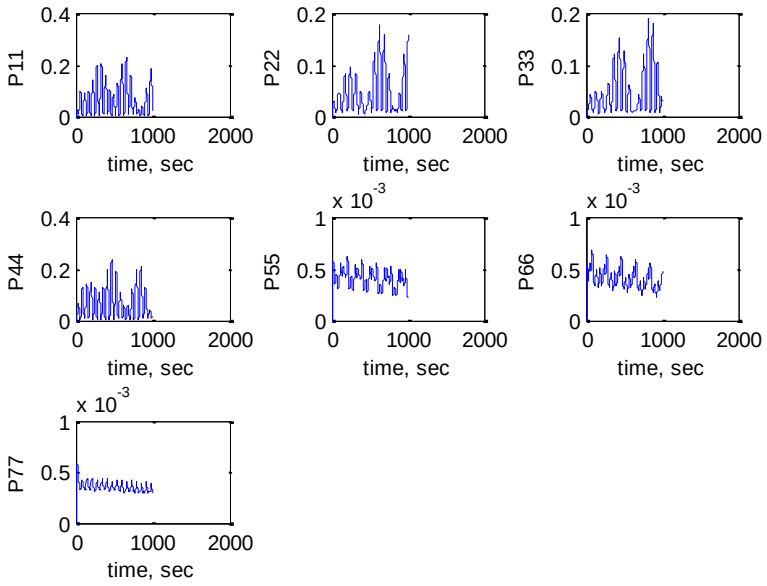

Figure 6.16. *A Posteriori* Error Covariance Estimation for 3,000 km Altitude

The results of the 3,000 km simulation show that the estimation error of the pre-filter is decreased with the large increase in altitude. There is marginal change in the overall attitude error for the simulations. It is important to now examine a simulation at a much higher altitude to determine if the accuracy trend continues. Figures 6.17-6.24 show the results of such a simulation with the altitude increased to 10,000 km.

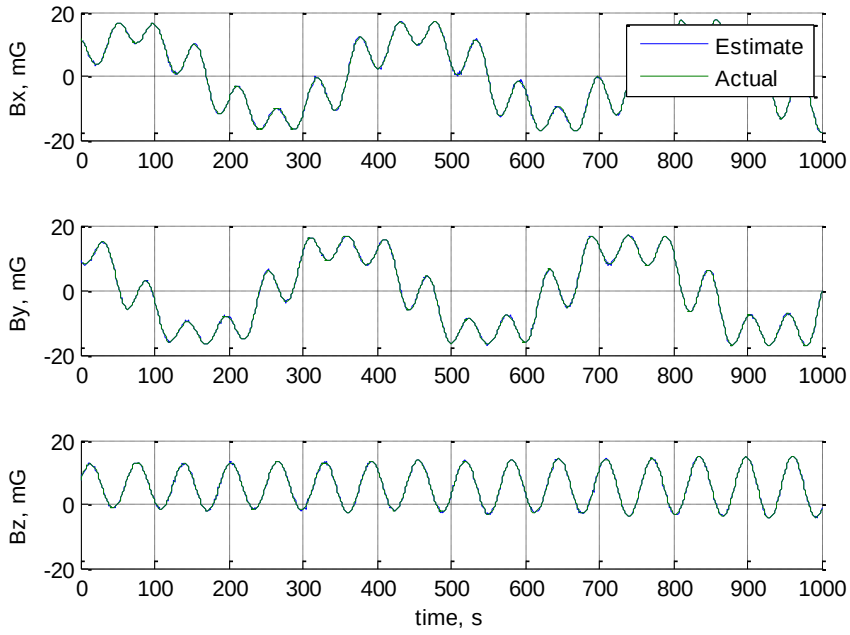

Figure 6.17. Magnetic Field Vector Estimation for 10,000 km Altitude

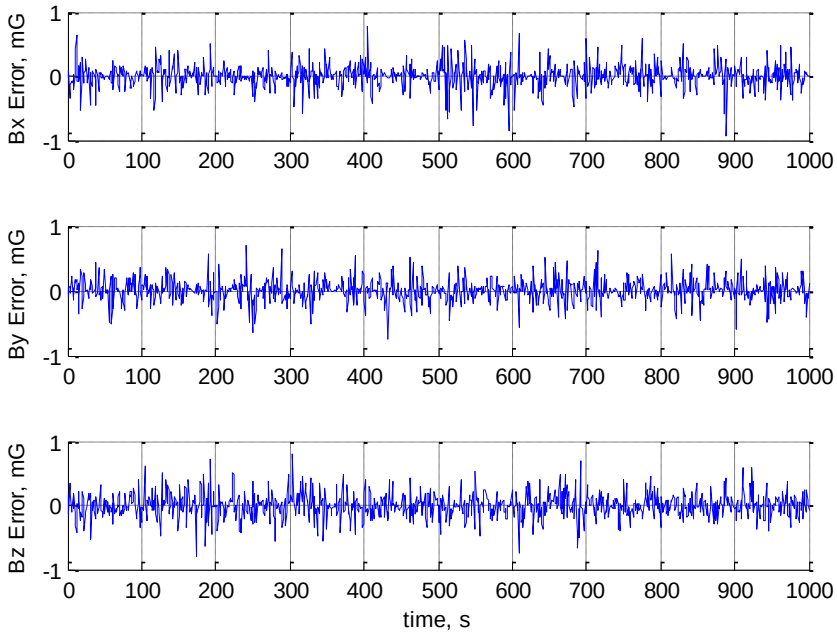

Figure 6.18. Magnetic Field Vector Estimation Error for 10,000 km Altitude

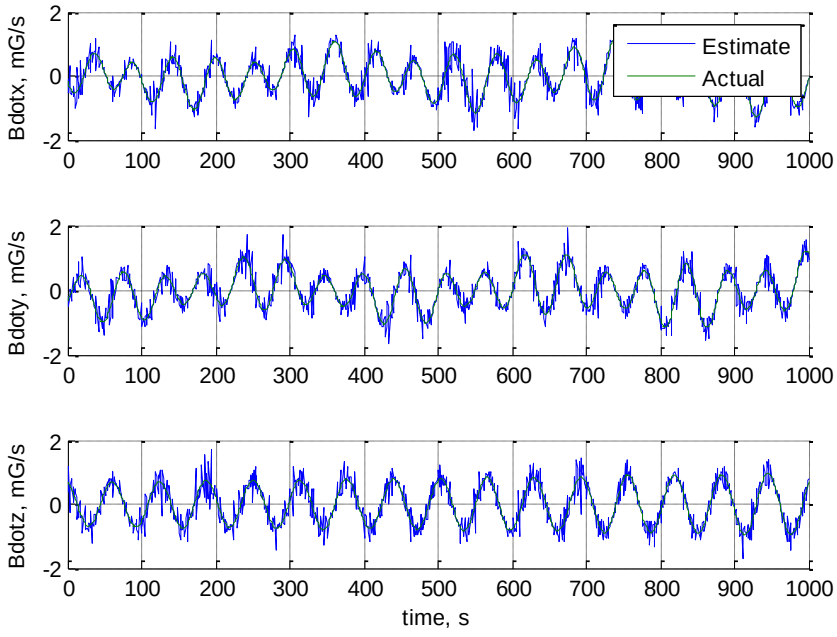

Figure 6.19. Magnetic Field Vector Derivative Estimation for 10,000 km Altitude

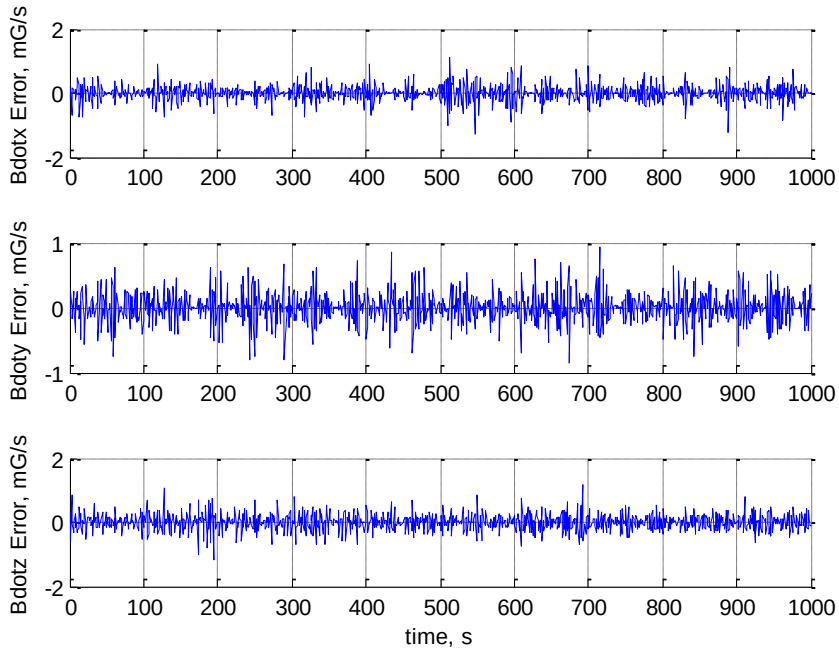

Figure 6.20. Magnetic Field Vector Derivative Estimation Error for 10,000 km Altitude

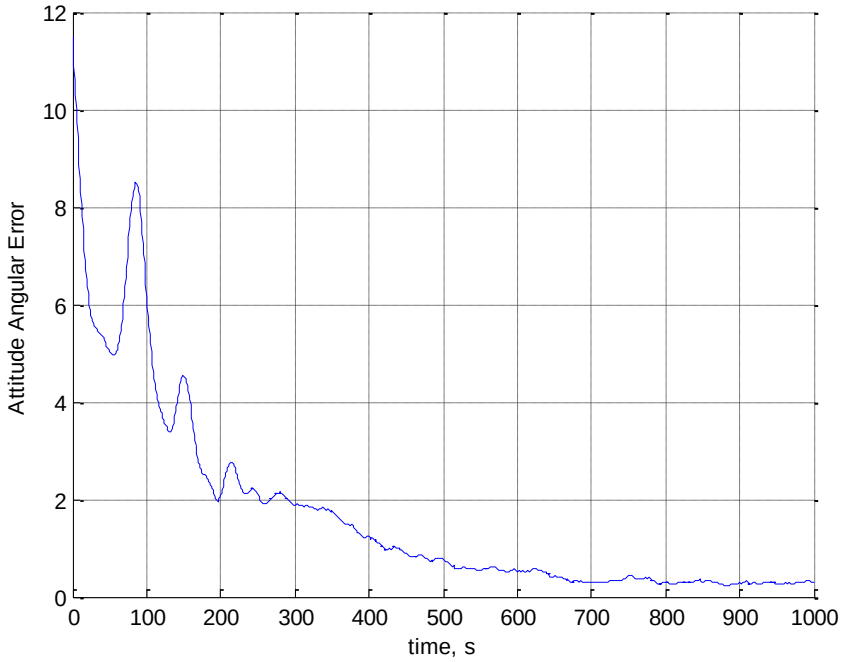

Figure 6.21. Angular Error in Spacecraft Attitude, in Degrees, for 10,000 km Altitude

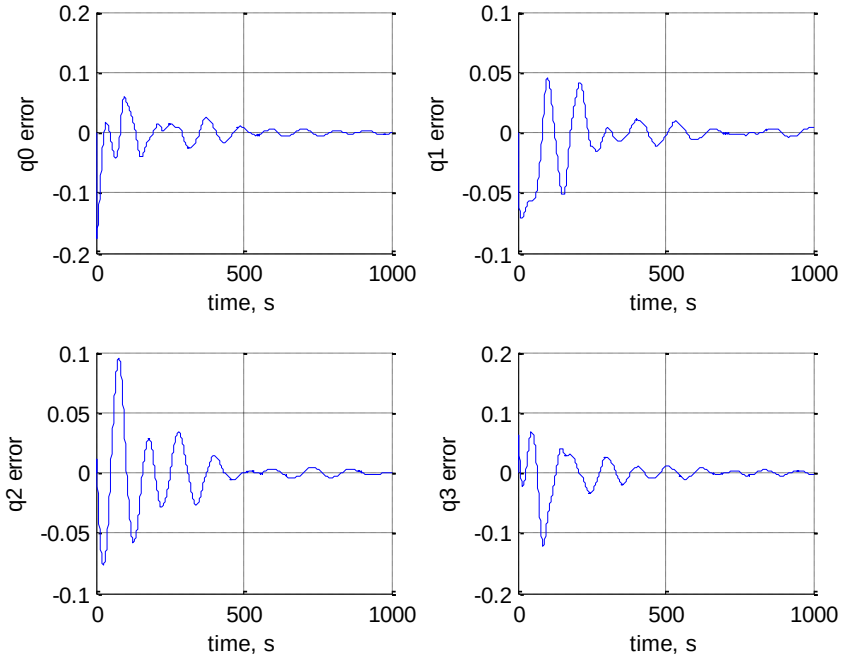

Figure 6.22. Attitude Quaternion Estimation Error for 10,000 km Altitude

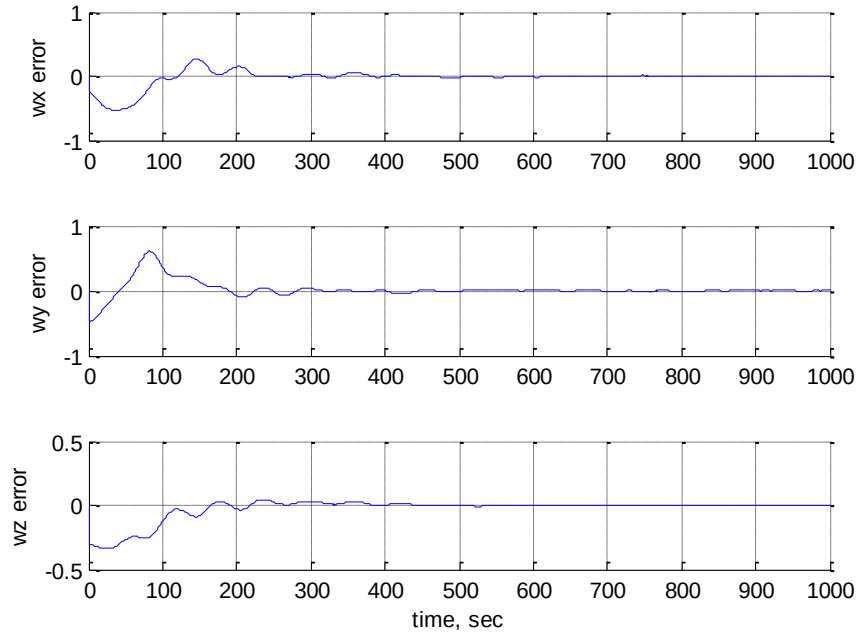

Figure 6.23. Angular Velocity Estimation Error in Degrees/Second for 10,000 km Altitude

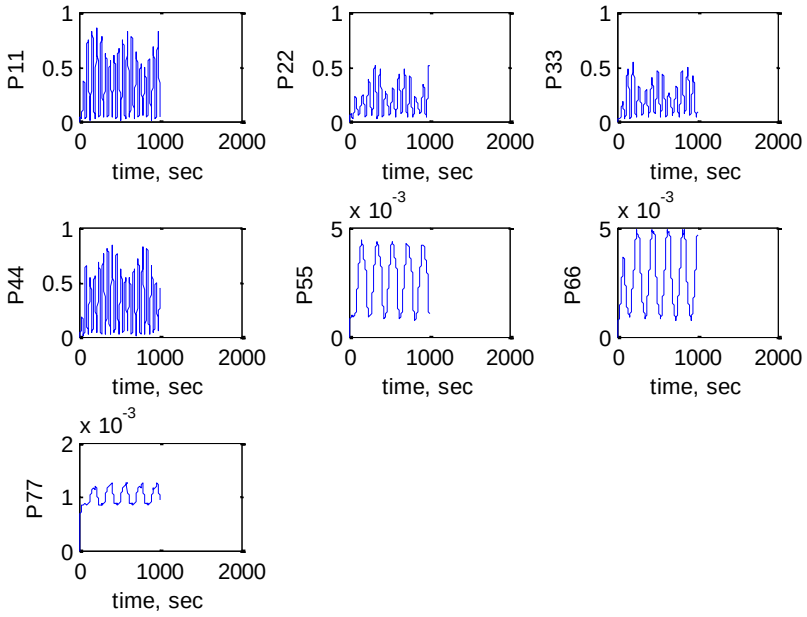

Figure 6.24. *A Posteriori* Error Covariance Estimation for 10,000 km Altitude

The results of the 10,000 km simulation show that the accuracy increase of the pre-filter continues as the altitude is increased. The attitude angular error reflects the increased pseudo-measurement accuracy for this case. The error decreases faster from the initial offset and is lower than the lower altitude simulations. This confirms that the algorithm accuracy does indeed improve for higher altitudes. The algorithm should eventually break down when there is no longer a magnetic field to measure. There is an explanation for the improvement with altitude. The Billingsley magnetometer data sheet declares one degree accuracy in the direction of the magnetic field, so the attitude code adds three degrees (three sigma) of normally distributed noise to the pointing direction of the "true" magnetic field vector without changing its magnitude. Officially, the filter uses only the vector elements for the attitude calculation. Adding three degree noise at a higher altitude, when the magnetic field vector magnitude is lower, changes the magnetic field vector elements less than adding three degrees at a lower altitude where the magnetic field vector magnitude is higher. Essentially the higher altitude case has higher

accuracy measurements of the magnetic field components. In reality, this would probably not be the case, but there is no data from Billingsley on the sensor performance for varying altitudes.

6.2.2. Inclination. Inclination change is the orbit parameter that most drastically affects the variance of the value of the magnetic field vector during orbit. The local magnetic field changes significantly as the position of the satellite moves over the poles. In contrast, the magnetic field at the equator is fairly constant as a spacecraft moves along an equatorial orbit. It is very important to test the effect of inclination on the attitude determination algorithm. This section shows the results of two more simulations: a polar orbit and an equatorial orbit.

The polar orbit is expected to perform better because the magnetic field vector is more dynamic, theoretically making the problem more observable. Figures 6.25-6.32 show the results of this simulation, with the altitude returned to the baseline value of 400 km.

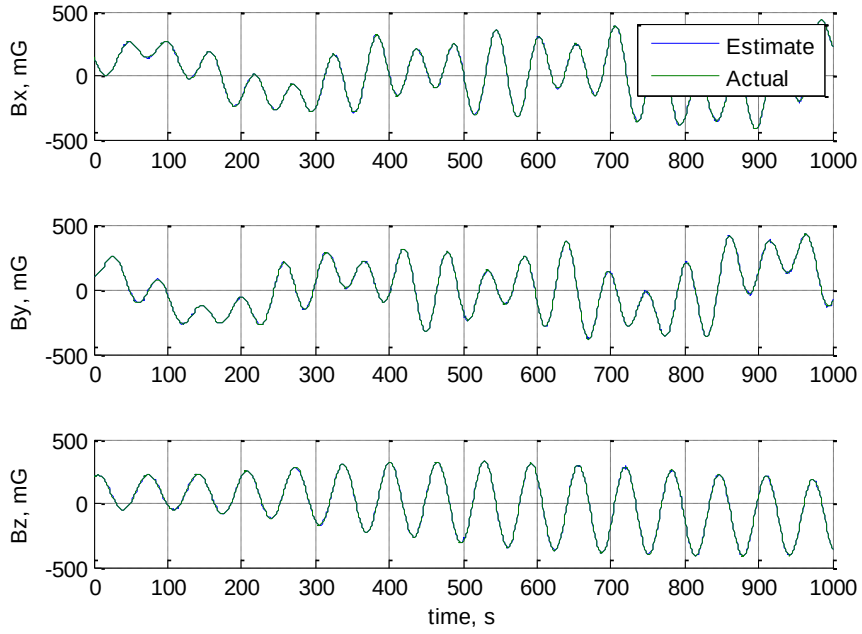

Figure 6.25. Magnetic Field Vector Estimation for Polar Orbit

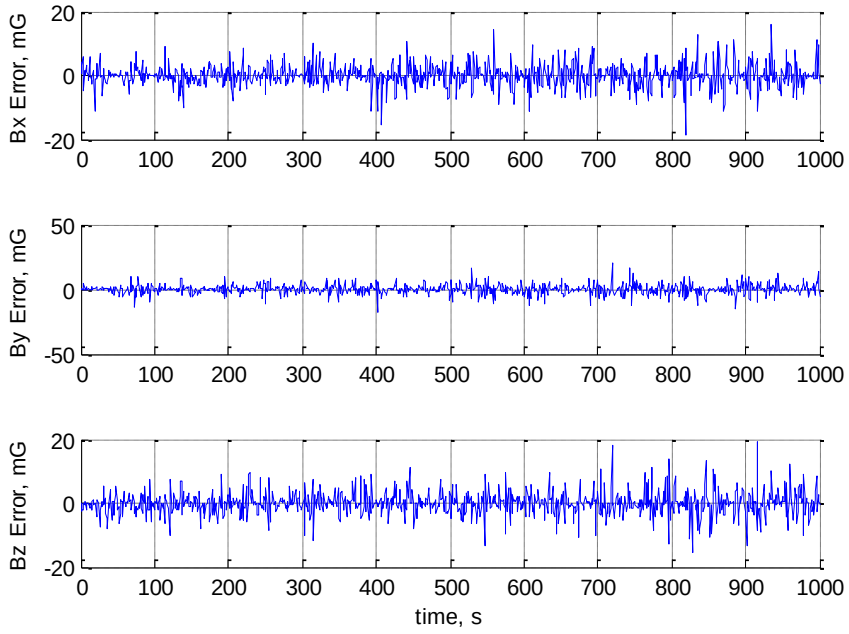

Figure 6.26. Magnetic Field Vector Estimation Error for Polar Orbit

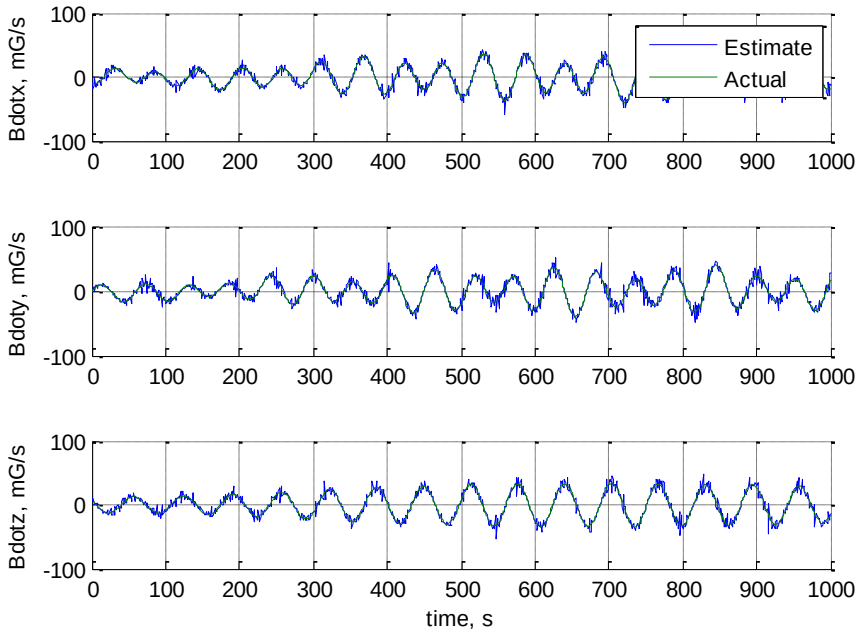

Figure 6.27. Magnetic Field Vector Derivative Estimation for Polar Orbit

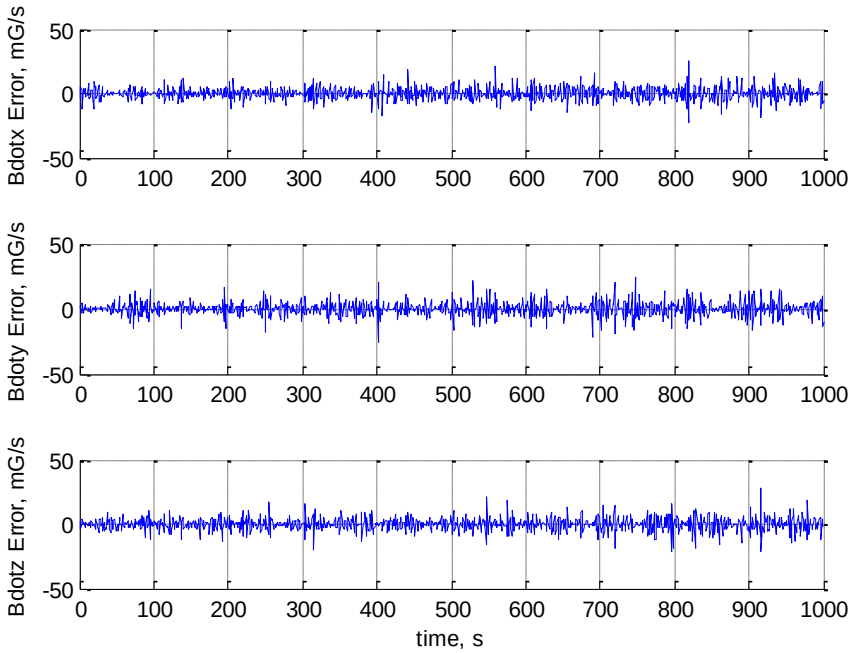

Figure 6.28. Magnetic Field Vector Derivative Estimation Error for Polar Orbit

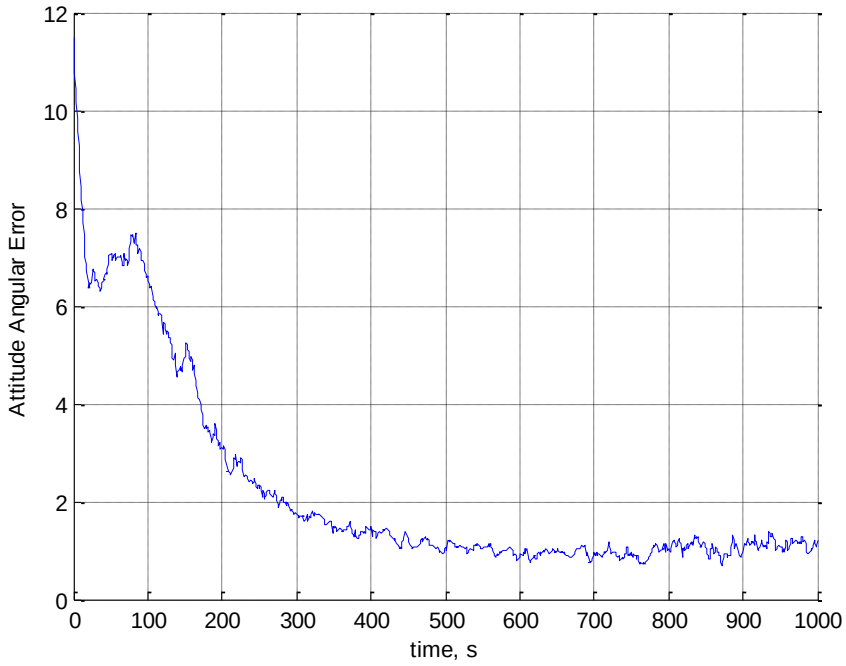

Figure 6.29. Angular Error in Spacecraft Attitude, in Degrees, for Polar Orbit

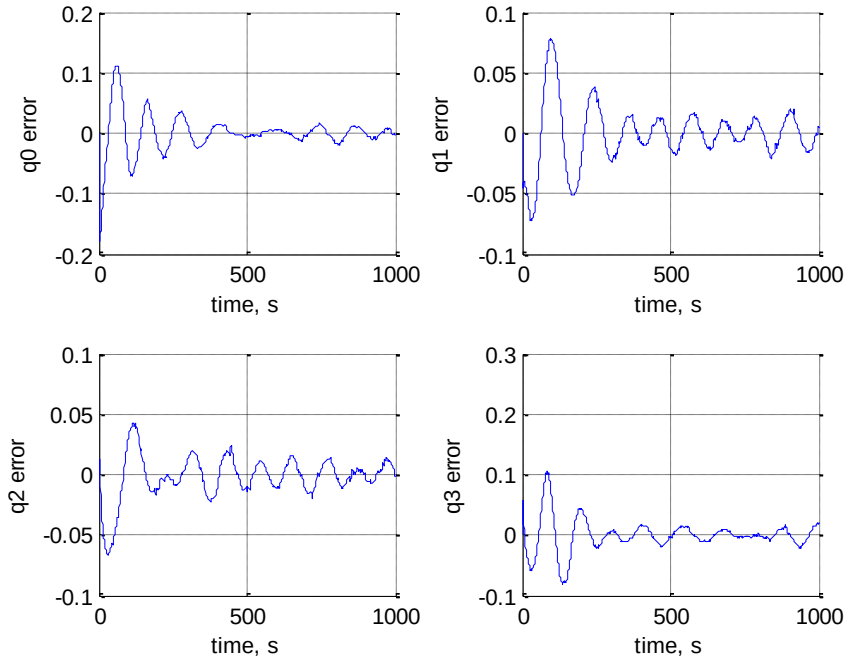

Figure 6.30. Attitude Quaternion Estimation Error for Polar Orbit

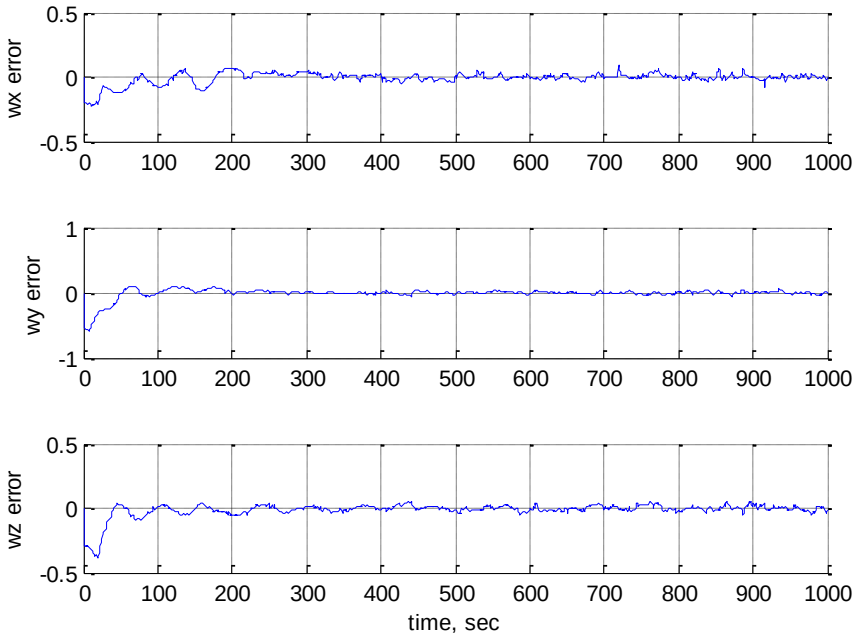

Figure 6.31. Angular Velocity Estimation Error in Degrees/Second for Polar Orbit

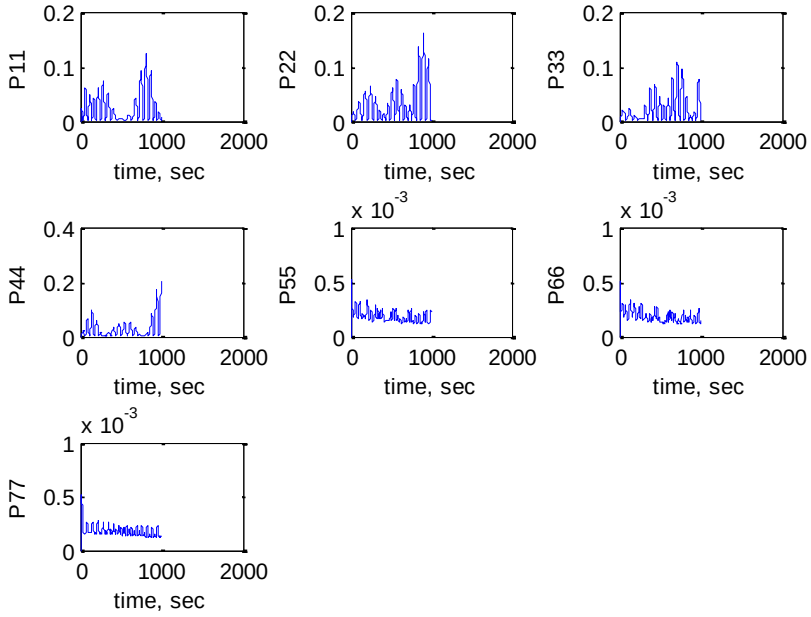

Figure 6.32. *A Posteriori* Error Covariance Estimation for Polar Orbit

The results for a polar orbit at 3000 km altitude are very similar to the results of the forty degree inclination baseline case. There is little difference in convergence time or steady state error.

Figures 6.33-6.40 show the baseline simulation with the inclination lowered such that the orbit is now an equatorial orbit. This is one of cases of concern for testing the limits of the new algorithm, because the magnetic field does not change as rapidly in an equatorial orbit. The spacecraft attitude rotation should be helpful to the estimation; however, if the spacecraft happens to be rotating about an axis nearly aligned with the magnetic field vector (which is more likely to occur in an equatorial orbit, but still unlikely) the problem is unobservable.

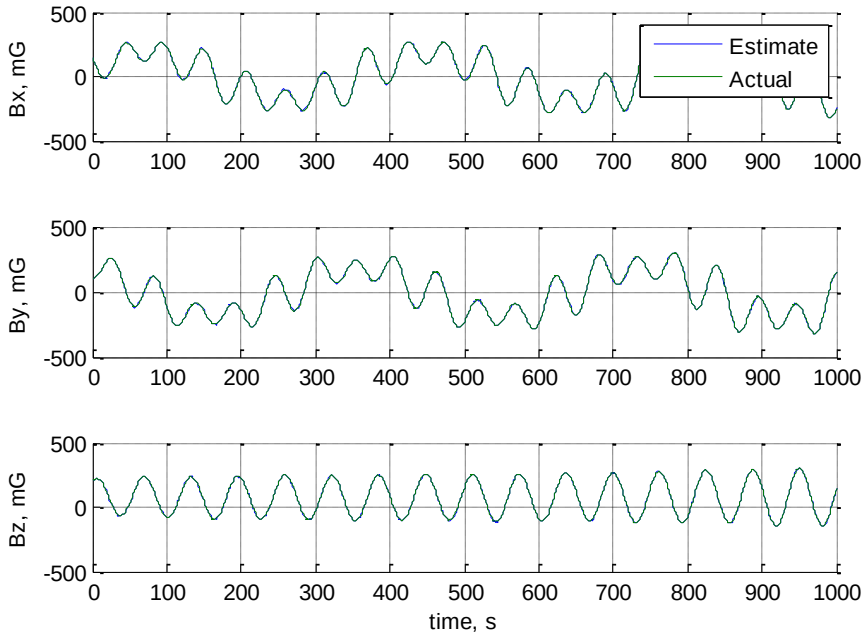

Figure 6.33. Magnetic Field Vector Estimation for Equatorial Orbit

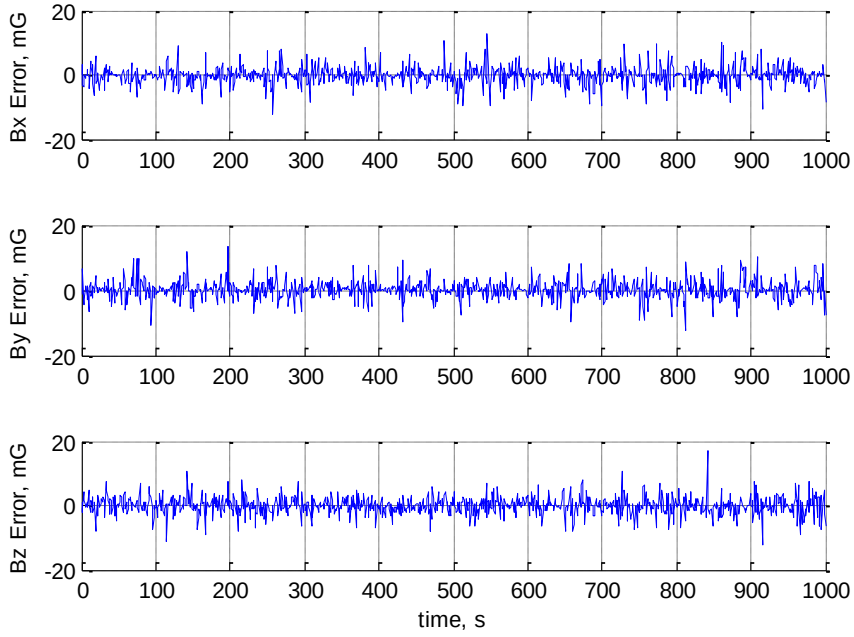

Figure 6.34. Magnetic Field Vector Estimation Error for Equatorial Orbit

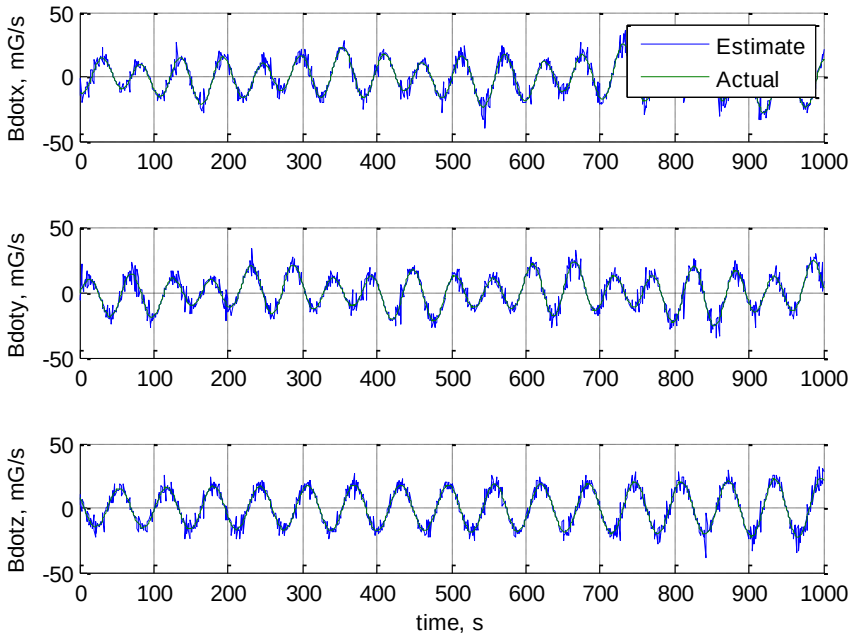

Figure 6.35. Magnetic Field Vector Derivative Estimation for Equatorial Orbit

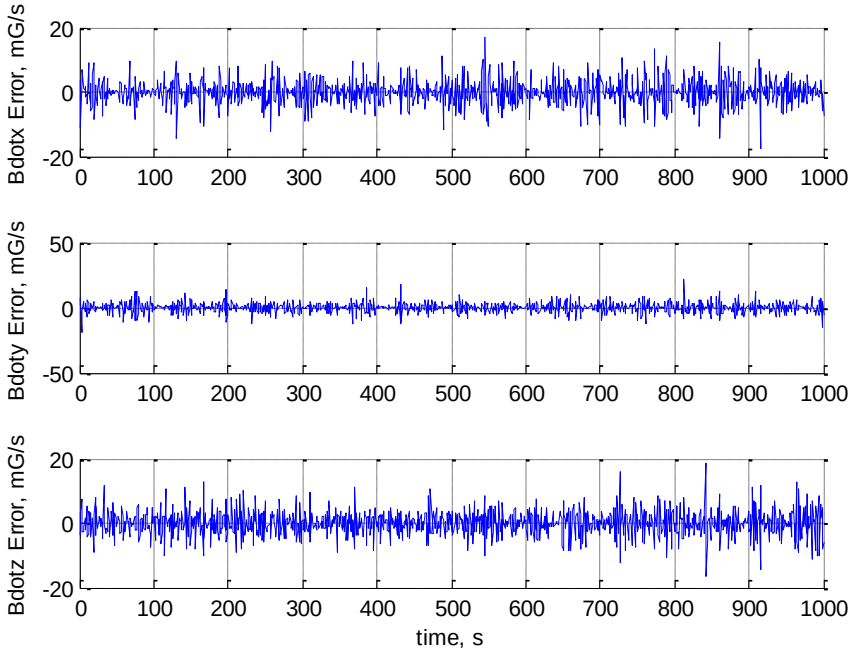

Figure 6.36. Magnetic Field Vector Derivative Estimation Error for Equatorial Orbit

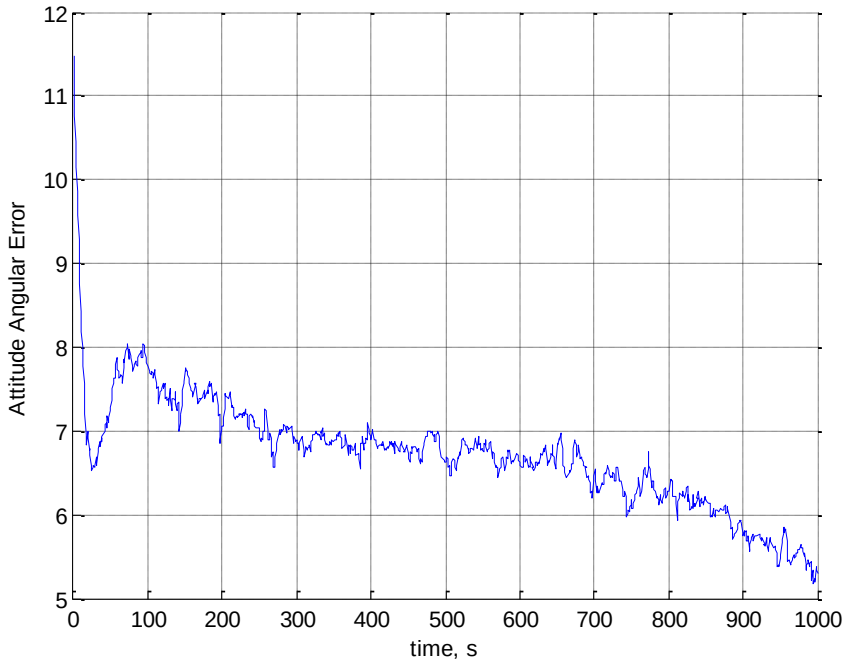

Figure 6.37. Angular Error in Spacecraft Attitude, in Degrees, for Equatorial Orbit

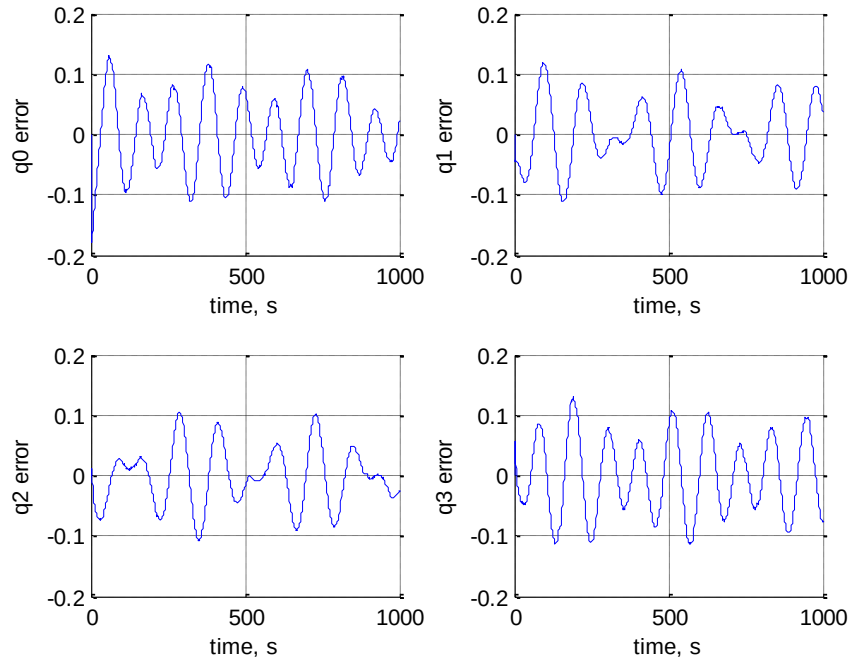

Figure 6.38. Attitude Quaternion Estimation Error for Equatorial Orbit

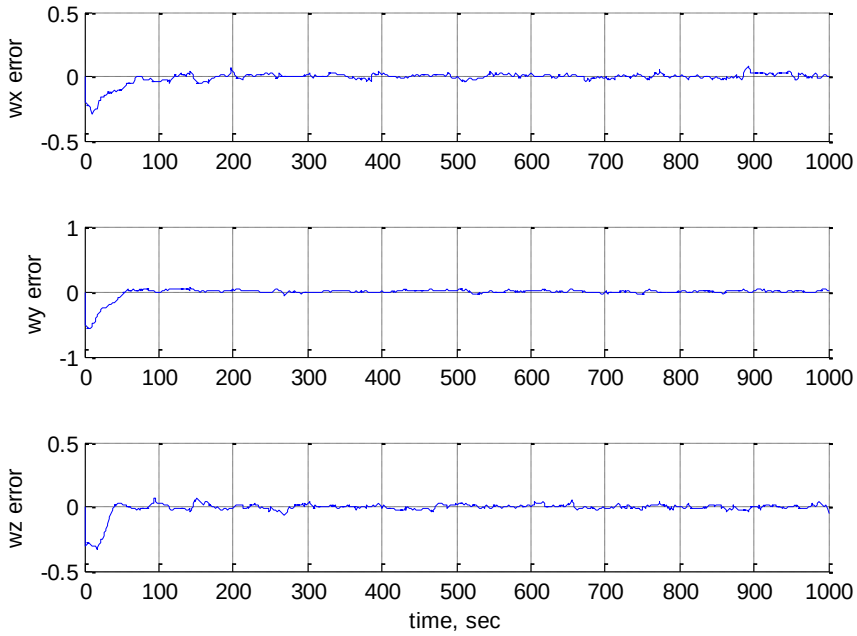

Figure 6.39. Angular Velocity Estimation Error in Degrees/Second for Equatorial Orbit

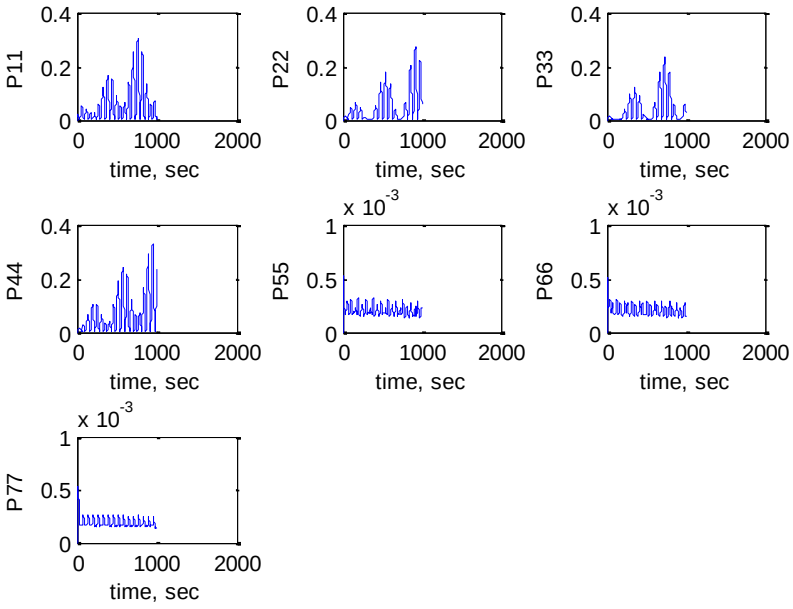

Figure 6.40. *A Posteriori* Error Covariance Estimation for Equatorial Orbit

The equatorial orbit inclination does have a significant effect on the estimation of the attitude. By examining the magnetic field derivative plot (Figure 6.35), it can be seen that the rate of change of the magnetic field vector is about half of the previous, polar orbit simulation. Even though the error plot shows that the magnetic field is estimated to roughly the same error level, the lower magnitude means that the amount of error will have more significant impact. The angular error is still decreasing at the end of the simulation, so an additional simulation was run to see if the steady state drops below five degrees estimation error. A simulation was run for 6000 seconds instead of 1000 to show the steady state error, as shown in Figure 6.41. The error eventually converges to around the same as all of the other simulations, taking approximately ten times longer to reach steady-state. The algorithm appears to be sufficiently robust to successfully converge to the proper attitude when faced with the observability challenges from equatorial orbits (given a longer period of time). The algorithm appears to require a longer time history of the magnetic field data in order to converge to an estimate.

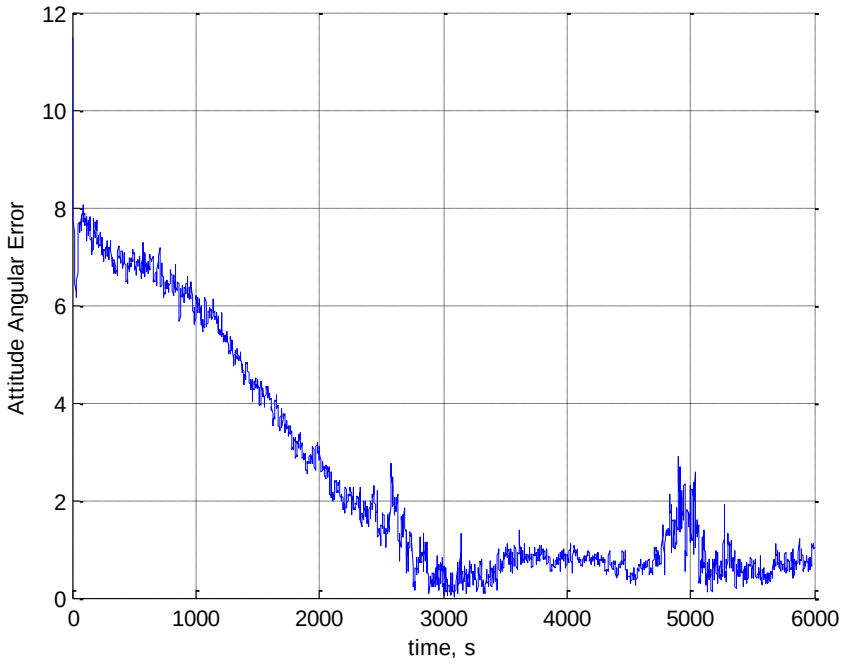

Figure 6.41. Angular Error in Spacecraft Attitude, in Degrees, for Equatorial Orbit at 6000 s

6.2.3. Spacecraft Angular Velocity. The spacecraft angular velocity is a critical parameter in this algorithm. Because there is no measurement of the angular rates, and the measurements of the magnetic field and its derivative vary largely with angular velocity, there is the potential for difficulties with certain angular velocities. There are two expected issues with the angular velocity. It has been determined through previous simulations that a more rapid change in the magnetic field vector leads to better accuracy. It can thus be assumed that as the spacecraft rotates faster the attitude determination accuracy will increase. A low rotation rate lowers the amount that the magnetic field vector changes between each measurement and should lower the observability.

The second issue is with high angular velocity. The higher the angular velocity, the faster filter response time required. Tuning the filter earlier, the response time of the filter was purposefully slowed minimize over corrections. This could pose a concern, and a case with angular velocity much higher than anticipated for the M-SAT mission is included in this study.

The simulation results shown in Figures 6.42-6.49 reflect a decrease in the angular velocity to values that have been determined by trial-and-error to be at the lower limit at which the algorithm can successfully converge. The attitude estimate diverges for zero angular velocity. This failure could be avoided by inducing a spin about an axis that is unimportant for the mission success criteria. It is also possible that further tuning of the Kalman filters could allow for the solution to be found in this case. It was found that by varying the weights, the performance in the zero angular velocity case could be improved; however, the performance in cases with nonzero angular velocity was then decreased. The attitude filter estimate has a bias in the zero angular velocity case that causes the algorithm to "believe" the spacecraft is rotating slowly. In this thesis study, the low spacecraft angular velocity case has the initial value

$$\omega = \begin{bmatrix} 0.02 \\ 0.05 \\ 0.1 \end{bmatrix} \text{deg/ sec} \tag{63}$$

The MR SAT spacecraft nominal attitude requires a rotation of 360 degrees per orbit, which leads to an angular velocity of approximately 0.06 degrees per second. The algorithm at this time will not converge to a proper estimate unless there is about a tenth of a degree per second or more along one axis. For the method presented here to work, a slight spin will need to be induced. The results for the low angular velocity case show that the attitude error drops to less than one degree but requires more time to reach steady state.

Figure 6.42 shows that the magnetic field vector does not oscillate as in the other simulations, because most of the variance in the magnetic field vector is due to the spinning of the spacecraft and the angular velocity is greatly reduced for this simulation.

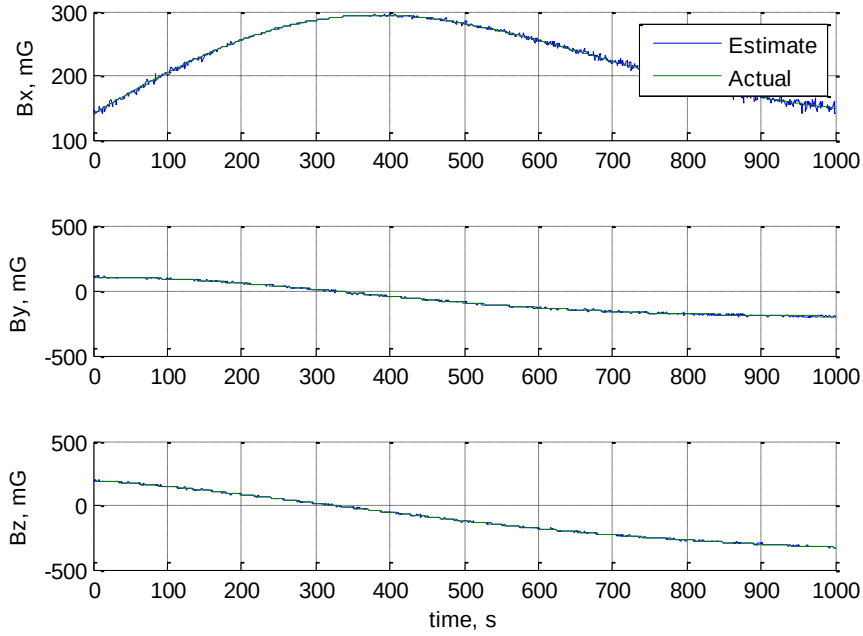

Figure 6.42. Magnetic Field Vector Estimation for Low Angular Velocity

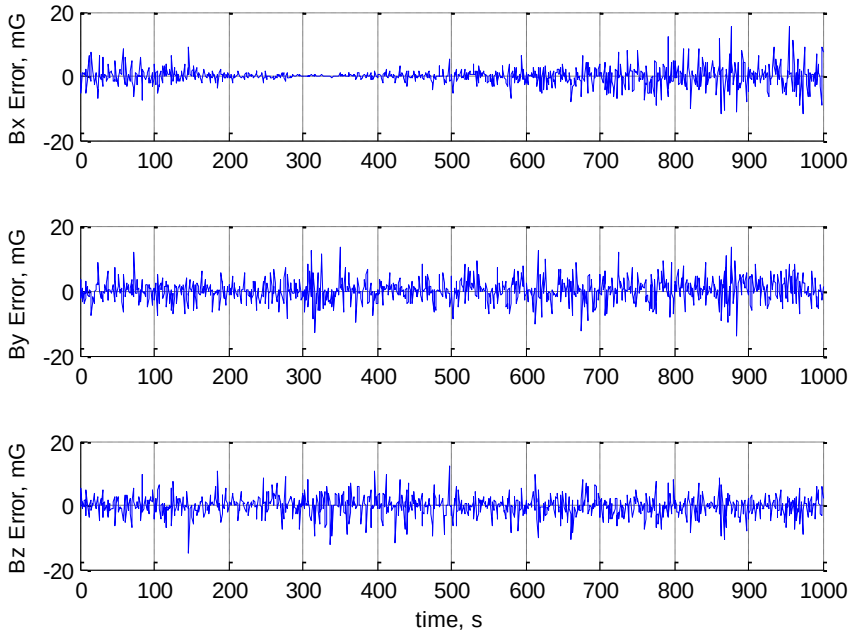

Figure 6.43. Magnetic Field Vector Estimation Error for Low Angular Velocity

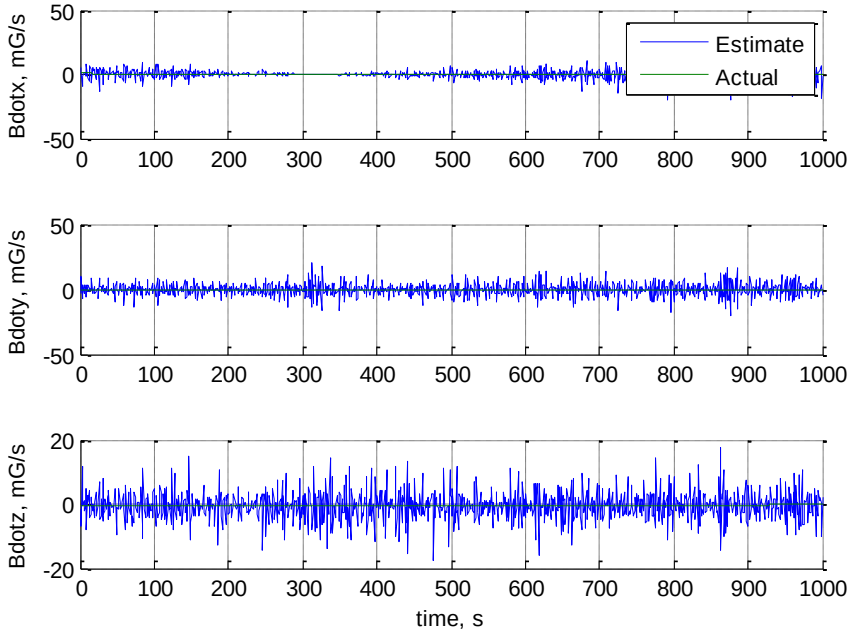

Figure 6.44. Magnetic Field Vector Derivative Estimation for Low Angular Velocity

Figure 6.45 shows that the error in the estimation of the magnetic field derivative is of the same order of magnitude as those in previous simulations. It would be easier to rationalize if the error in the magnetic field estimate were increased. With a reasonable estimate of the magnetic field and derivative the filter should be able to find an accurate estimate for the attitude, but yet the algorithm fails. This leads to the assumption that the problem is in the attitude filter itself. The problem may be as simple as tuning the filter, but the evidence appears to show that the pre-filter is not at fault.

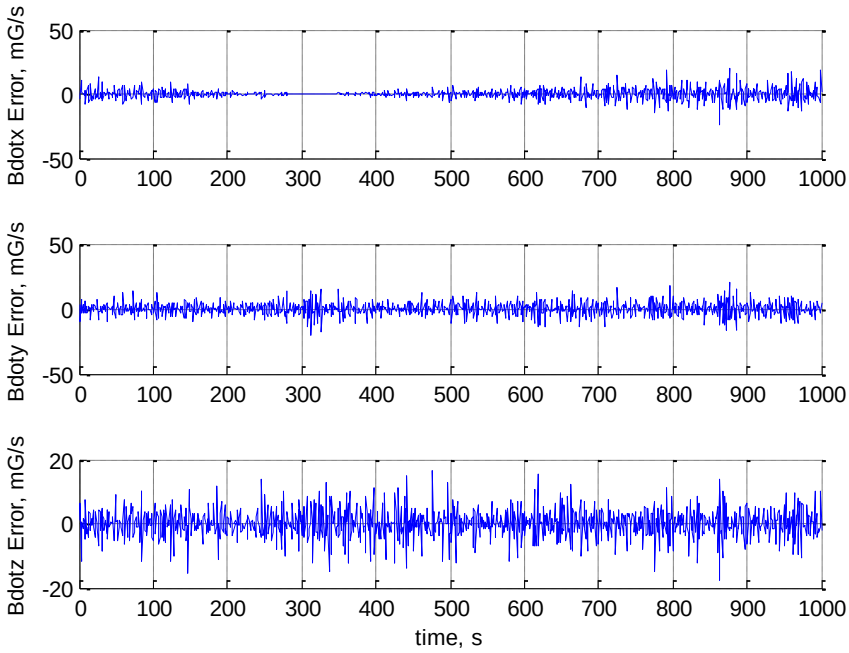

Figure 6.45. Magnetic Field Vector Derivative Estimation Error for Low Angular Velocity

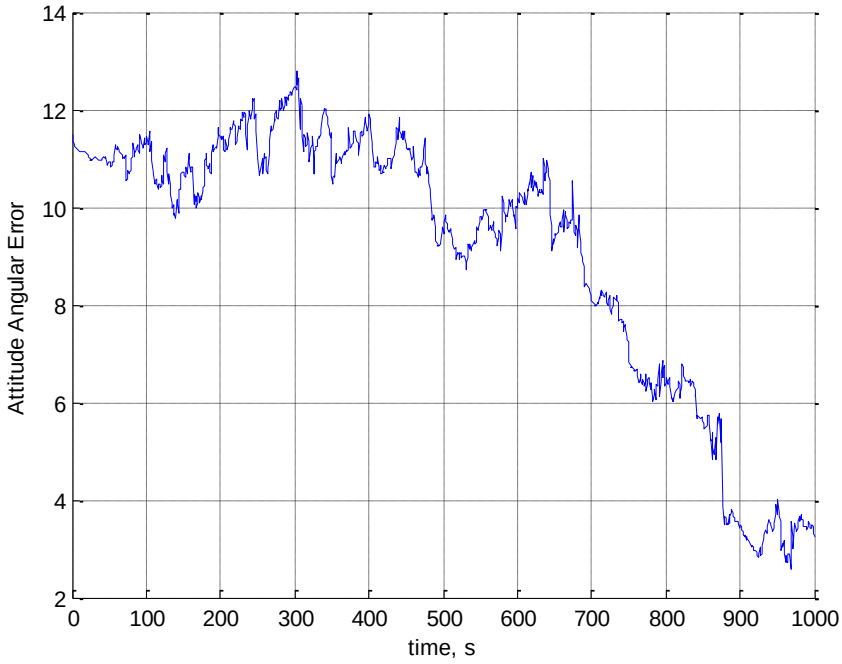

Figure 6.46. Angular Error in Spacecraft Attitude, in Degrees, for Low Angular Velocity

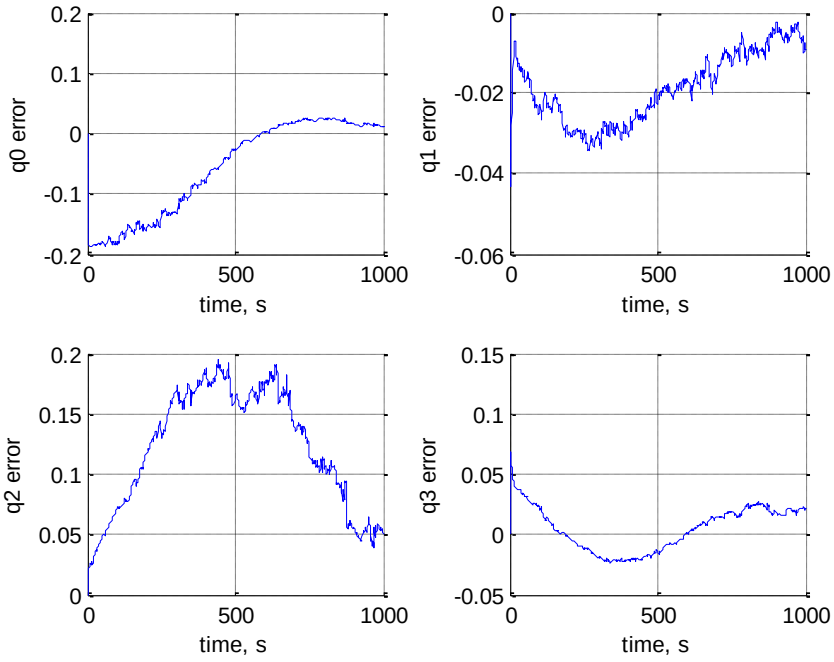

Figure 6.47. Attitude Quaternion Estimation Error for Low Angular Velocity

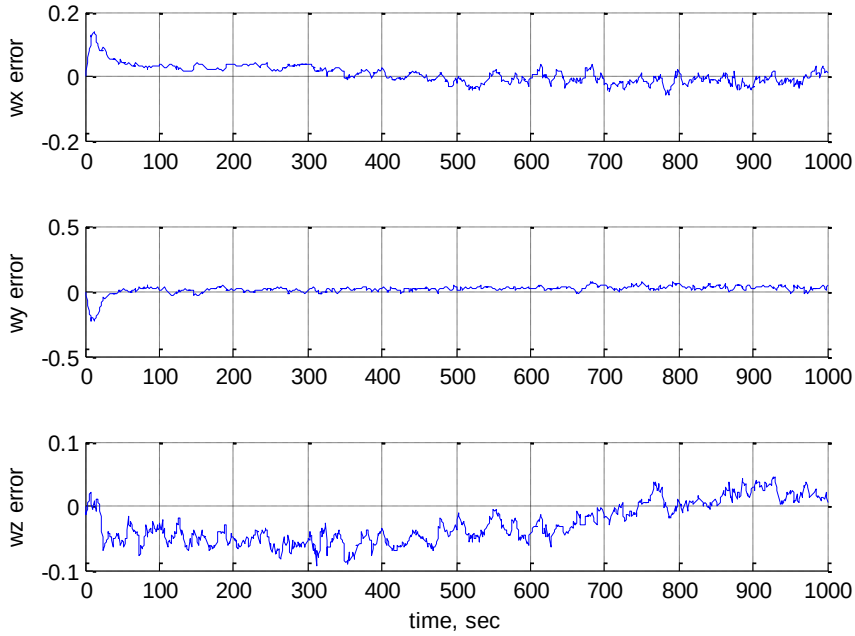

Figure 6.48. Angular Velocity Estimation Error in Degrees/Second for Low Angular Velocity

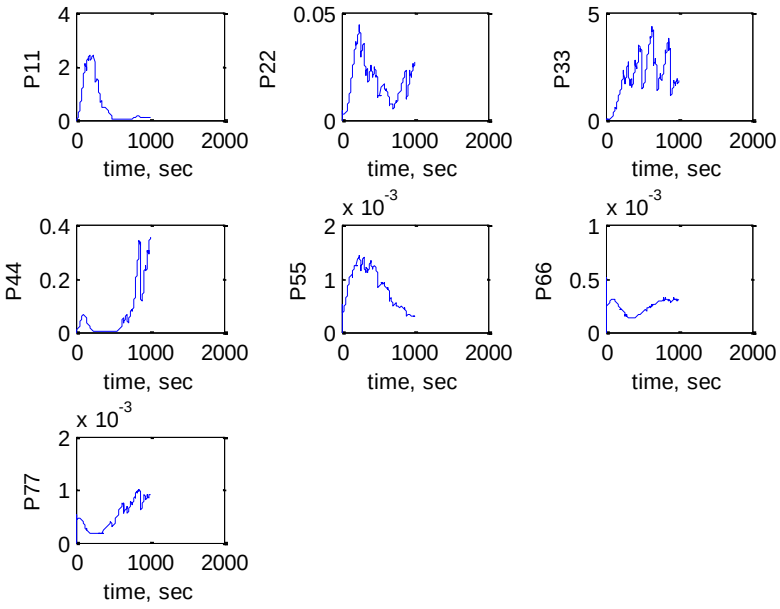

Figure 6.49. *A Posteriori* Error Covariance Estimation for Low Angular Velocity

The simulation showed that orbits with low angular velocity are more difficult to solve using magnetometer-only determination. The convergence time of the algorithm was much higher in the zero angular velocity case than for the nonzero cases. It is important to note the other differences in this simulation compared to the others presented. The quaternion and angular velocity estimation errors show a bias, or a lack of convergence. The errors in previous simulations quickly converge and oscillate slightly around zero. The covariance diagonal elements also behave differently than the other simulations. The diagonal elements vary more slowly, and do not show the bounded behavior seen earlier.

The simulation results shown in Figures 6.50-6.57 are for the case where the MR SAT spacecraft rotates at 20 degrees per second along each axis. The results show an improvement over the baseline case. The maximum tip-off angular velocity expected to be experienced by MR SAT is five degrees per second (even after a factor of safety), so this case should effectively test the viability of using the algorithm in this situation.

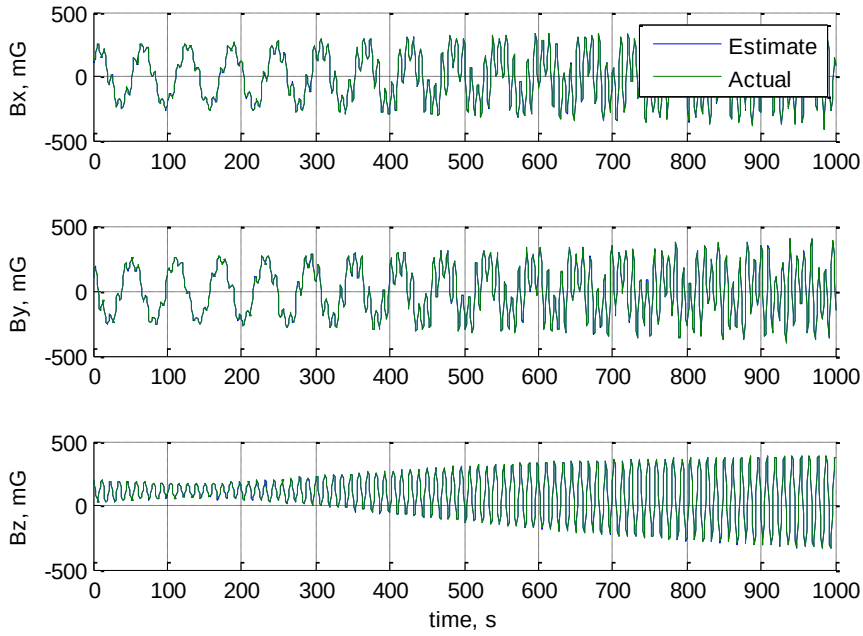

Figure 6.50. Magnetic Field Vector Estimation for 20 Degrees/Second Angular Velocity

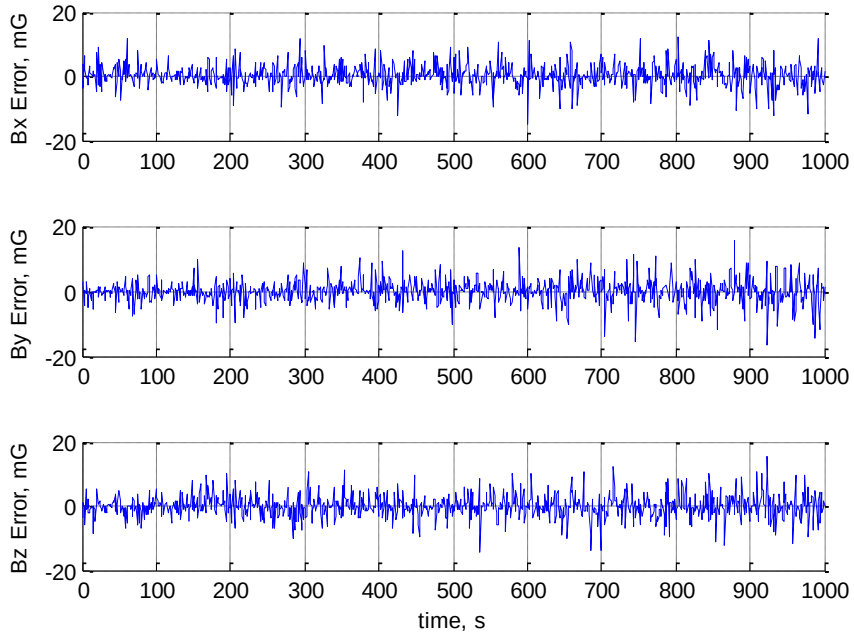

Figure 6.51. Magnetic Field Vector Estimation Error for 20 Degrees/Second Angular Velocity

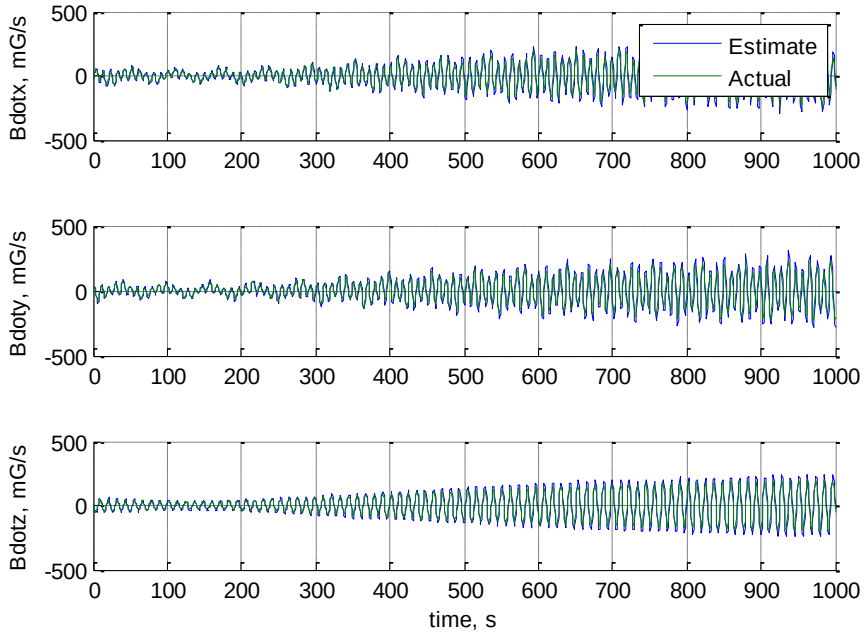

Figure 6.52. Magnetic Field Vector Derivative Estimation for 20 Degrees/Second Angular Velocity

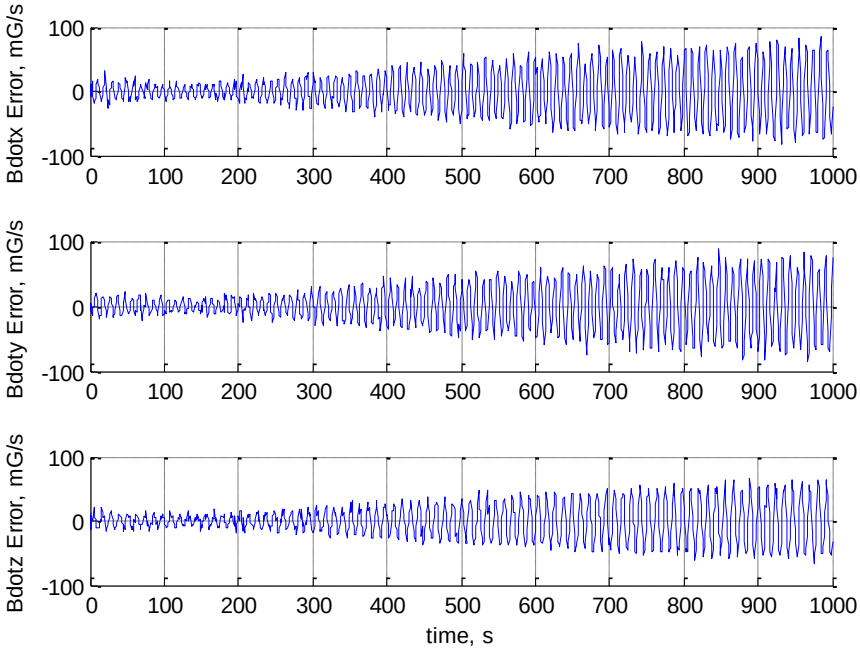

Figure 6.53. Magnetic Field Vector Derivative Estimation Error for 20 Degrees/Second Angular Velocity

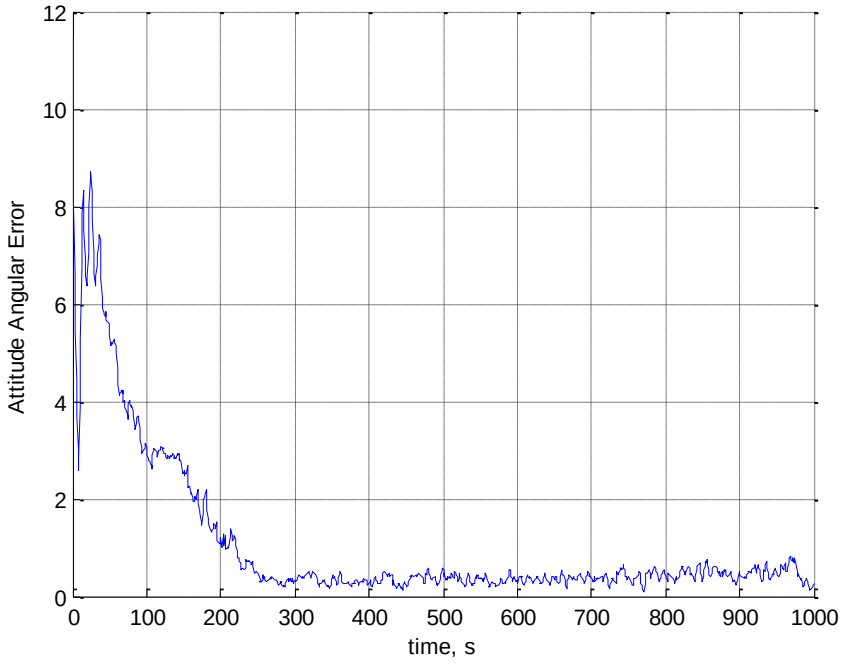

Figure 6.54. Angular Error in Spacecraft Attitude, in Degrees, for 20 Degrees/Second Angular Velocity

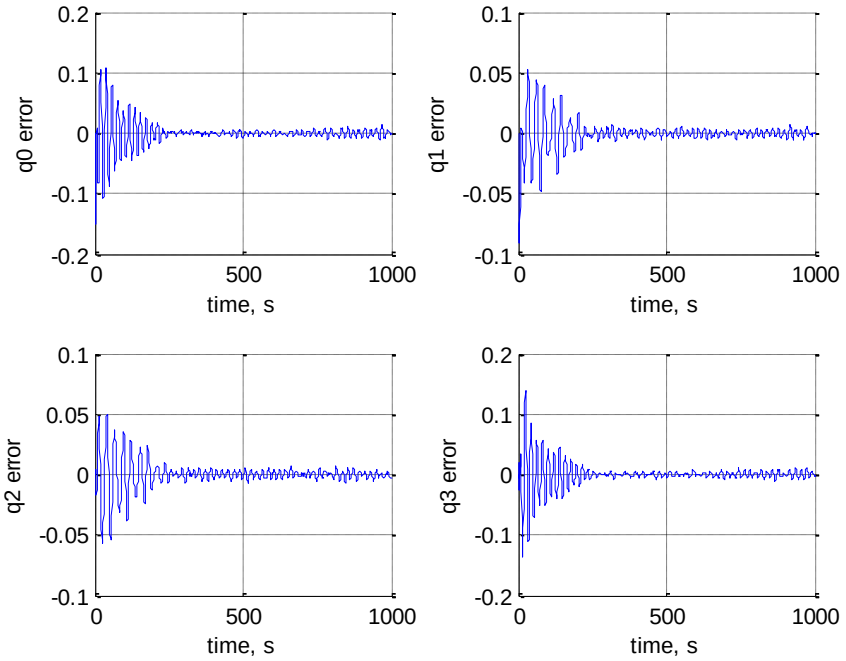

Figure 6.55. Attitude Quaternion Estimation Error for 20 Degrees/Second Angular Velocity

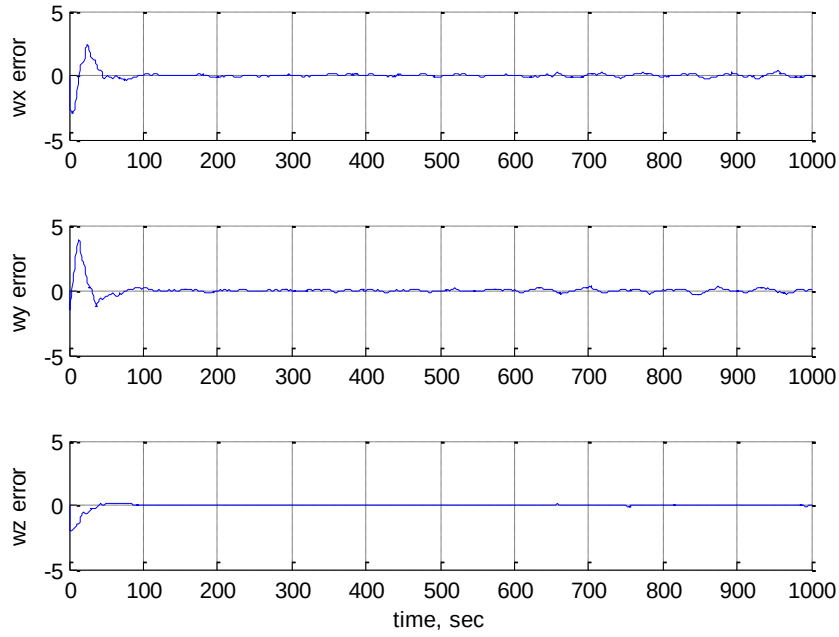

Figure 6.56. Angular Velocity Estimation Error in Degrees/Second for 20 Degrees/Second Angular Velocity

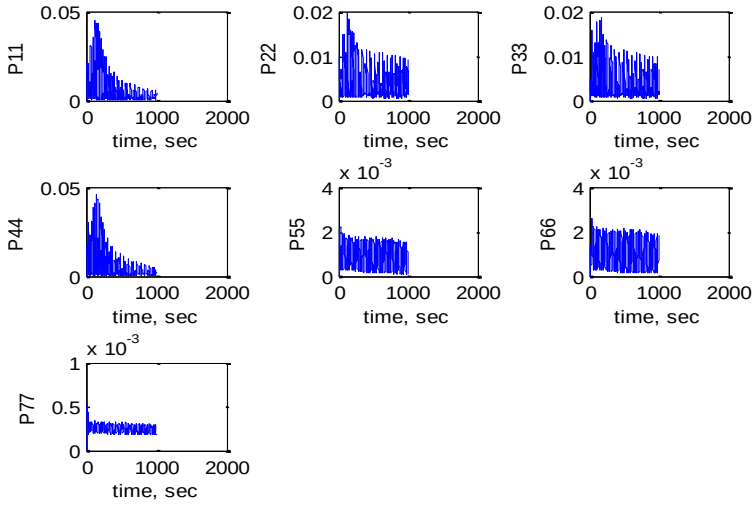

Figure 6.57. *A Posteriori* Error Covariance Estimation for 20 Degrees/Second Angular Velocity

The simulation with twenty degrees per second angular velocity along each axis shows that the results improve with increasing angular velocity. This can be explained by considering the dynamics of the problem. As the magnetic field vector changes more rapidly, the derivative vector magnitude increases, and will be easier to estimate. The angular velocity is thus important to consider when using this algorithm. Spacecraft that do not rotate may encounter difficulty in obtaining an accurate attitude estimate, especially near an equatorial orbit.

6.2.4. Error in GPS Measurements. The last parameter to be examined for the parametric analysis is error in the GPS measurement. The magnetometer-only algorithm relies on the position of the satellite being known so that the model can calculate the magnetic field vector and its derivative to use in the calculation of the estimated magnetic field in the body frame. The attitude determination filter performance could be degraded by inaccuracies in the spacecraft position estimation. In this study, a simulation was conducted in which half a kilometer of normally distributed, zero mean noise was added to the spacecraft position and the simulation converged to a solution without any apparent difficulties. The results for the simulation are shown in Figures 6.58-6.65.

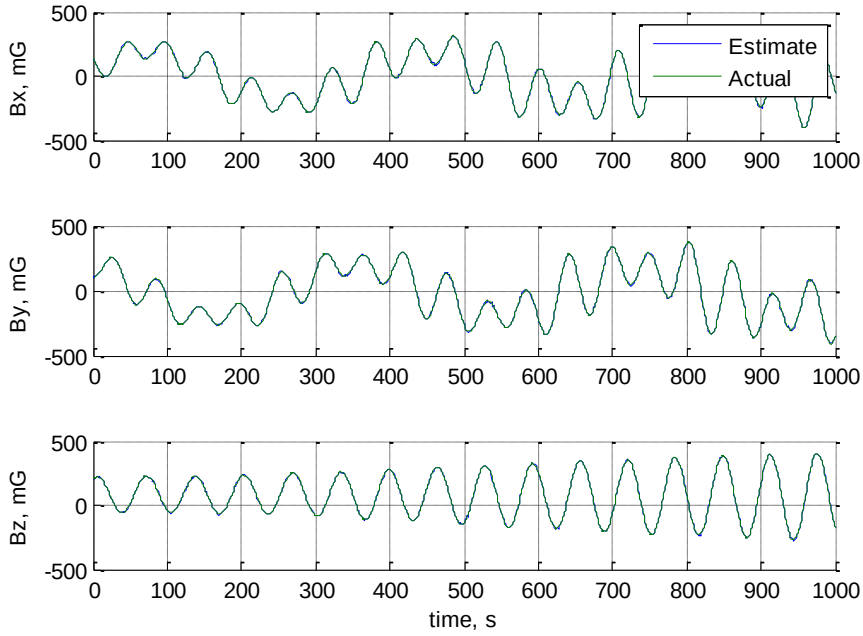

Figure 6.58. Magnetic Field Vector Estimation for 0.5 km Position Error

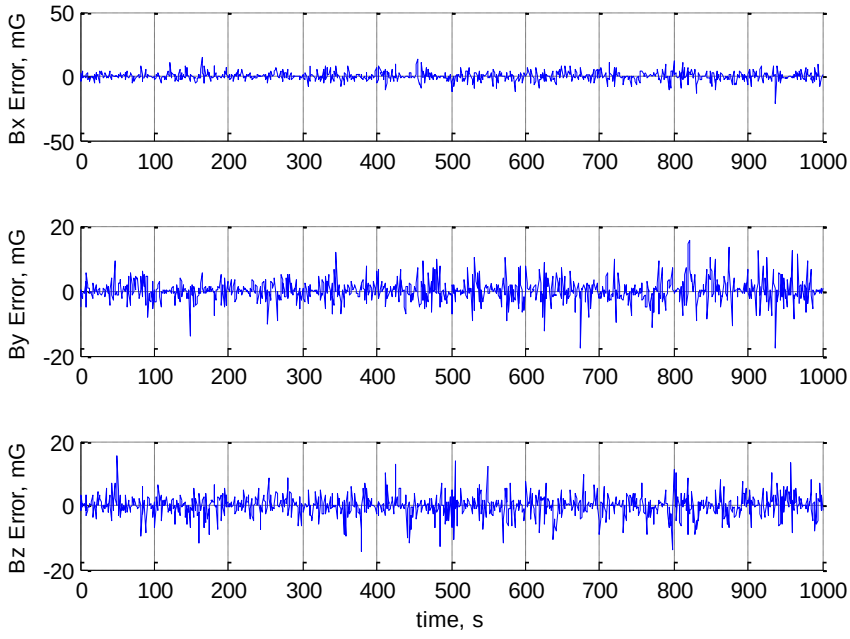

Figure 6.59. Magnetic Field Vector Estimation Error for 0.5 km Position Error

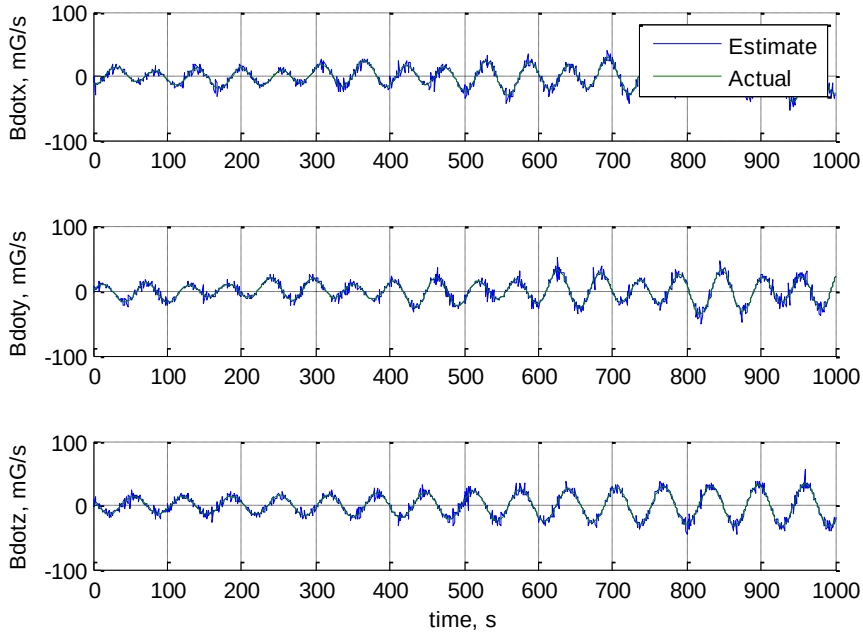

Figure 6.60. Magnetic Field Vector Derivative Estimation for 0.5 km Position Error

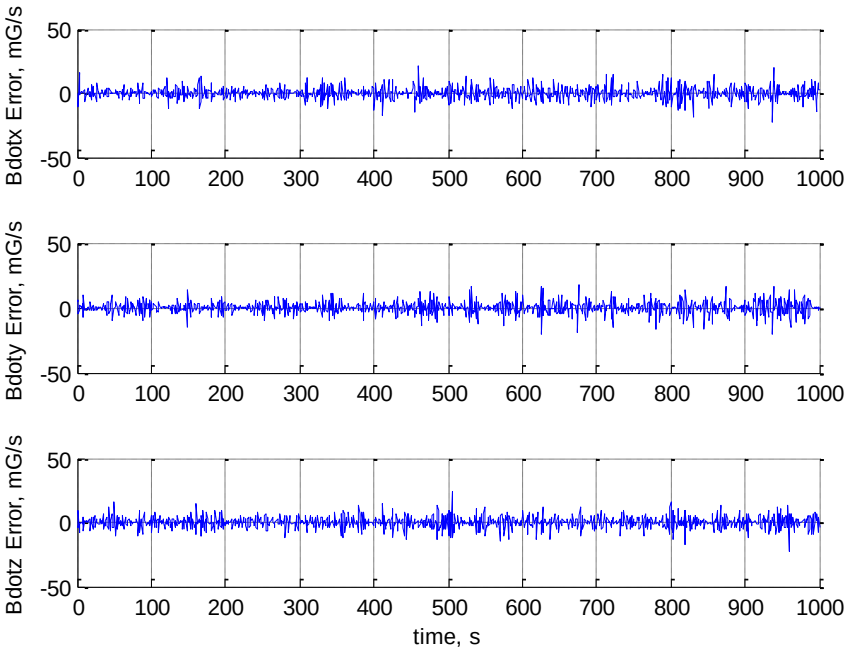

Figure 6.61. Magnetic Field Vector Derivative Estimation Error for 0.5 km Position Error

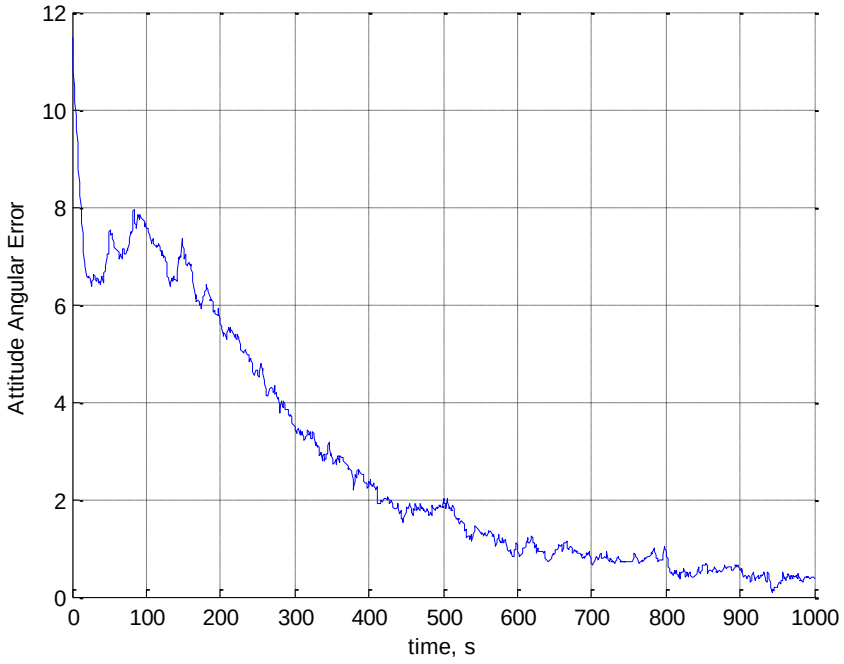

Figure 6.62. Angular Error in Spacecraft Attitude, in Degrees, for 0.5 km Position Error

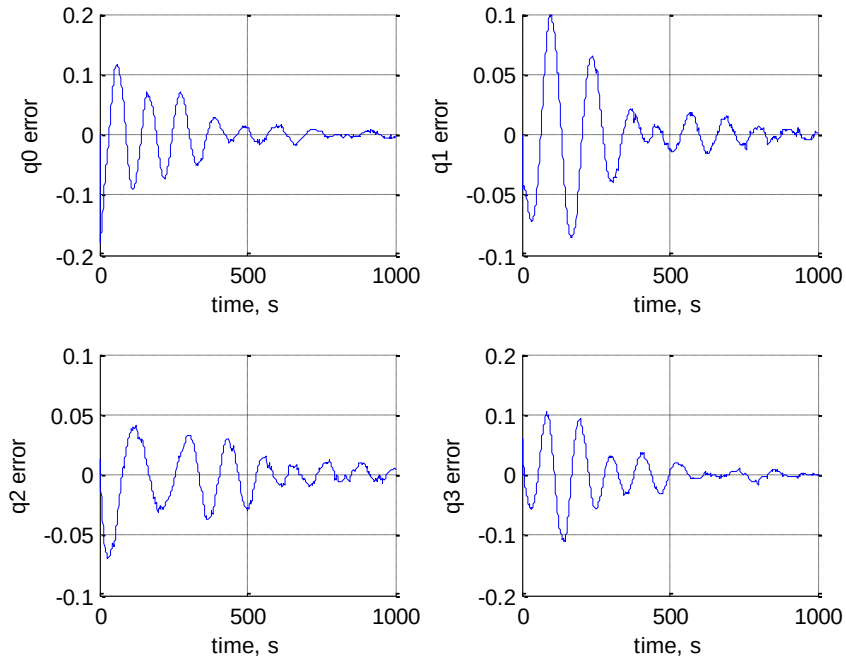

Figure 6.63. Attitude Quaternion Estimation Error for 0.5 km Position Error

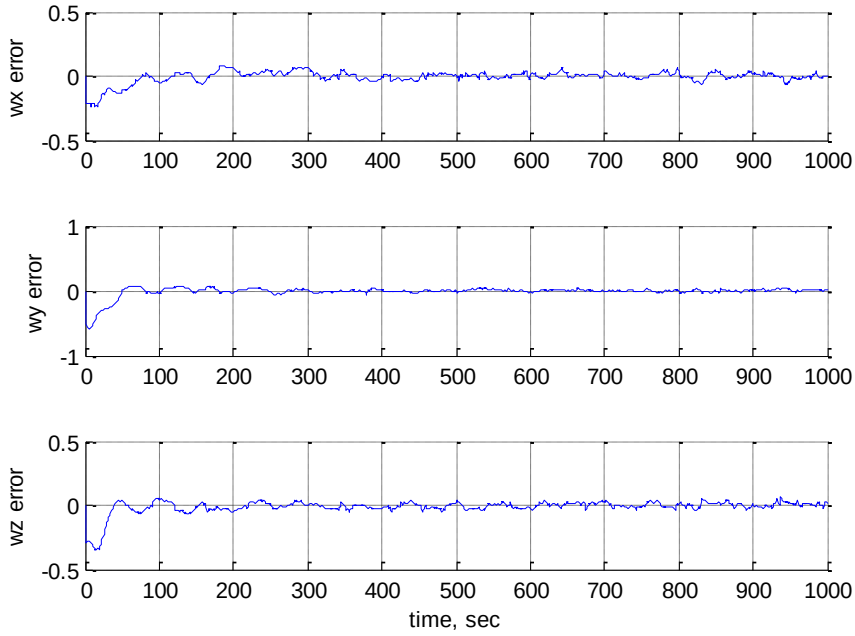

Figure 6.64. Angular Velocity Estimation Error in Degrees/Second for 0.5 km Position Error

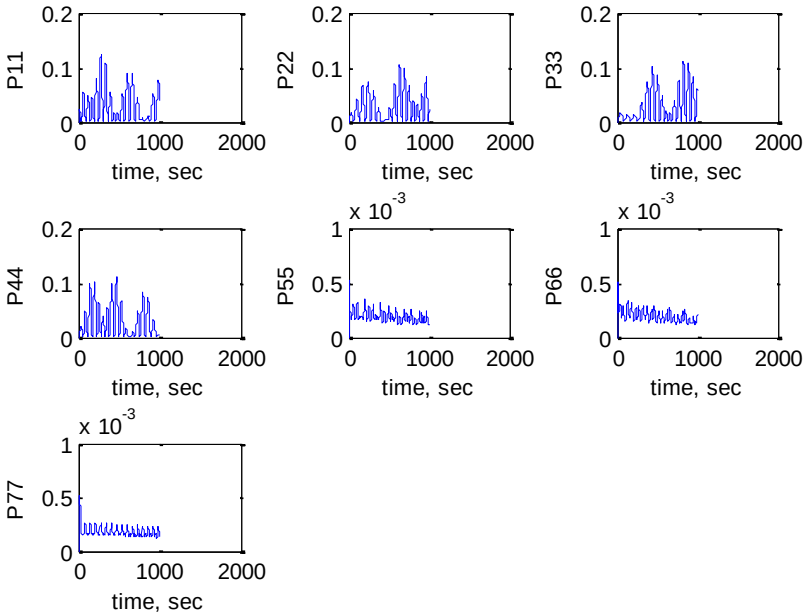

Figure 6.65. *A Posteriori* Error Covariance Estimation for 0.5 km Position Error

The half kilometer of position error added to the simulation shows that the relatively small change in the magnetic field is not enough to significantly affect the attitude determination algorithm. The spinning of the spacecraft would cause a much larger change in the magnetic field vector than the position of the spacecraft. Extremely accurate position information is not vital for the attitude algorithm to provide a suitable attitude estimate.

7. CONCLUSIONS

7.1. COMPLETED WORK.

This thesis describes the development of an attitude determination algorithm that can rely solely on magnetometer measurements and achieve accuracies of less than one degree. The algorithm was tested through a rigorous parametric study, and conclusions were drawn about the performance of the attitude determination system. The algorithm can be used for low-cost satellites where only a single sensor can be procured, or as a contingency to a more accurate system that may experience a system failure or gap in measurements. The software has been tuned to run efficiently, though there are some improvements suggested in the Future Work section.

The method developed is effective when the angular velocity along at least one axis is higher than one tenth of a degree per second. Unfortunately, this is higher than the ideal, normal operating conditions for MR SAT. A solution to the problem could be to induce a slight rotation about a non-essential axis. The problem seems to be caused by an observability issue with the EKF filter formulation when the angular velocity is zero. However, future modifications or tuning may alleviate the problem. From the simulations conducted, it was observed that increasing the initial covariance diagonals slowed or stopped the divergence of the algorithm. Raising the covariance diagonals, however, causes divergence in cases with nonzero angular velocity. The results presented in this thesis study are meant to show how robust the algorithm is to varying conditions, as well as find its flaws.

It is important to note that this system was developed for the MR SAT spacecraft and although the system is portable to other spacecraft, the system seems to fail for any fully symmetric satellite. The algorithm has some complications that may need to be resolved with additional tuning if the spacecraft has zero angular velocity as well. And lastly, the algorithm has occasional convergence difficulties if the spacecraft is in an equatorial orbit. The tuning of the two nested Kalman filters was a very important factor in ensuring convergence of the algorithm to a suitable attitude solution. One issue noticed was when the initial covariance matrix is too large. The correction at the beginning of the simulation causes the estimates to diverge if the initial covariance matrix

is too large. Also, if the weights on the pseudomeasurements are too low, the system will perform less accurately. Determining the weights on the pseudomeasurements was a difficult task because there are no sensor data to determine the noise covariance. The first attempt was to use the error covariance of the pre-filter as the measurement noise covariance of the attitude filter, but the values were too low for the filter to succeed.

7.2. FUTURE WORK.

There are a few aspects that can be completed in order to improve the algorithm, either in accuracy or in computational efficiency. The first item that should be addressed is that the derivative of the magnetic field should be able to be analytically determined. A program was written to solve this problem, but it was never fully debugged. The alternative was to use finite differencing on the magnetic field model to find the derivative. Although this has proven to be effective, the analytical solution would be much more computationally efficient.

A second improvement to would be to add attitude perturbations and control to the system. There should be no difficulties with the algorithm when encountering a changing angular velocity (the asymmetries cause this effect anyway). The algorithm is improved in situations where the magnetic field body frame measurement is more dynamic, so adding an actual attitude model to the system dynamics should improve the results. Such a model would include solar radiation pressure effects, drag, and gravity gradient effects. These can easily be modeled and added to the attitude model that the filter uses to predict the future attitude.

Magnetometer calibration is also a concern for this type of attitude system. The spacecraft will produce residual magnetic fields from electronic components. Also, some missions (including MR SAT) have magnetic torque coils or rods. These attitude control devices cause control torques by creating a magnetic field that reacts with Earth's magnetic field. The magnetic field vector created by the torque coils will interfere with the measurement from the magnetometer. There are a couple of approaches to mitigate these effects. The first method would be to determine the Earth's magnetic field vector from the measurement by using the known magnetic field vector generated by the coils. This would require calibration of the magnetometer inside the completed satellite with

the coils activated. Using the known values before the coil is activated, and the measurements after they are activated, will allow for the disturbance to be accounted for and removed. The same process can be used for the residual magnetic field created by the electronic components. The amount of interference may also depend on the operating mode of the spacecraft. Another solution is to add states to the pre-filter to calculate and remove the interference. This is only necessary if the filter is unable to filter out the residual magnetic field when it filters the measurement, but only full-scale, fully integrated testing will determine what is necessary.

BIBLIOGRAPHY

[1] Lu, G.G. Lu "Development of a GPS Multi-Antenna System for Attitude Determination," *UCGE Reports*, No. 20073, Ph.D. Dissertation, 1995.

[2] Gebre-Egziabher, D. D. Gebre-Egziabher, Elkaim, G.H., Powell, J. D., and Parkinson, B. W."A Gyro-Free Quaternion Based Attitude Determination System for Implementation Using Low Cost Sensors," *Proceedings of the IEEE Position Location and Navigation Symposium*, San Diego, CA, 2000.

[3] Crassidis, J. L. and Markley, F. L. "A Minimum Model Error Approach for Attitude Estimation," *Journal of Guidance, Control and Dynamics*, Vol. 20, No. 6, November-December 1997.

[4] Santoni, F. and Bolotti, F. "Attitude Determination of Small Spinning Spacecraft Using Three Axis Magnetometer and Solar Panels Data," *Proceedings of the IEEE Aerospace Conference*, 2002.

[5] Ma, G. and Jiang, X. "Unscented Kalman Filter for Spacecraft Attitude Estimation and Calibration using Magnetometer Measurements," *Proceedings of the Fourth International Conference on Machine Learning and Cybernetics*, Guangzhou, China, August 2005.

[6] Bar-Itzhack, I. Y. and Oshman, Y. "Attitude Determination from Vector Observations," *IEEE Transactions on Aerospace and Electric Systems*, Vol. AES-21, No. 1, January 1985.

[7] Lizarralde, F. and Wen, J. "Attitude Control without Angular Velocity Measurements: A Passivity Approach," *Proceedings of the Conference on Robotics and Automation*, Osaka, Japan, 1995.

[8] Wang, P. K. C. "Synchronized Formation Rotation and Attitude Control of Multiple Free-Flying Spacecraft," *AIAA Journal of Guidance and Control*, August, 1998.

[9] Markley, F. L. "Attitude Determination using Vector Observations and the Singular Value Decomposition," *The Journal of the Astronautical Sciences*, Vol. 38, No. 3, pp. 245-258, July-September 1988.

[10] Crassidis, J. L. and Lai, K."Real-Time Attitude-Independent Three-Axis Magnetometer Calibration," *AIAA Journal of Guidance, Control and Dynamics*, Vol. 28, No. 1, 2005, pp. 115-120.

[11] Crassidis, J. L. and Lightsey, E. G. “Attitude Determination Using Combined GPS and Three-Axis Magnetometer Data,” *Space Technology,* Vol. 22, No. 4, 2001, pp. 147 – 156.

[12] Shuster, M. D. and Oh, S. D. “Three-Axis Attitude Determination from Vector Observations,” *AIAA Journal of Guidance and Control,* Vol. 4, No. 1, 1980.

[13] Liebe, C. C. “Star Trackers for Attitude Determination,” *IEEE Aerospace and Electronic Systems Magazine*, June 1995.

[14] M. S., Natanson, J. Challa, Deutschmann, D., and Baker, F. “Magnetometer-Only Attitude and Rate Estimation for Gyroless Spacecraft,” Determination for a Gyroless Spacecraft," *Proceedings of the Third International Symposium on Space Mission Operations and Ground Data Systems*, NASA Conference Publication 3281, NASA-GSFC, Greenbelt, MD, November 1994

[15] Humphreys, T. “Attitude Determination for Small Satellites with Modest Pointing Constraints,” *Proceedings of the Sixteenth Annual AIAA/USU Conference on Small Satellites,* Logan, Utah, 2002.

[16] Shuster, M. D.“Kalman Filtering of Spacecraft Attitude and the QUEST Model,” *The Journal of the Astronautical Sciences,* Vol. 38, No. 3, 1990, pp. 377-393.

[17] Shuster, M. D. “A Survey of Attitude Representations,” *The Journal of the Astronautical Sciences,* Vol. 41, No. 4, 1993, pp. 439-517.

[18] Van Dyke, M. C., Schwartz, J. L., and Hall, C. D. “Unscented Kalman Filtering for Spacecraft Attitude State and Parameter Estimation,” *The Journal of the Astronautical Sciences,* Vol. 41, No. 4, 1993, pp. 439-517.

[19] Psiaki, M. and Martel, F. “Three-Axis Attitude Determination Via Kalman Filtering of Magnetometer Data,” *Journal of Guidance, Control and Dynamics,* Vol. 13, No. 3, 1990.

[20] Wahba, G. “A Least Squares Estimate of Satellite Attitude,” *SIAM Review*, Vol. 7, No. 3, 1965, pp. 409-409.

[21] Wertz, J. R. *Spacecraft Attitude Determination and Control,* Reidel Publishing Company, 1980.

[22] Shuster, M. “The Quest for Better Attitudes,” *The Journal of the Astronautical Sciences*, Vol. 54, Nos. 3 & 4, December 2006.

[23] Keat, J. “Analysis of Least Squares Attitude Determination Routine DOAOP,” Computer Sciences Corporation, CSC/TM-77/6034, February, 1977.

[24] Davenport, P. B. Attitude Determination and Sensor Alignment via Weighted Least Squares Affine Transformations," *NASA X-514-71-312,* August 1971.

[25] Simon, D., *Optimal State Estimation*, Wiley-Interscience, Hoboken, New Jersey, 2006.

[26] Kuipers, J. B., *Quaternions and Rotation Sequences*, Princeton University Press, Princeton, New Jersey, 1999.

[27] Sidi, M., *Spacecraft Dynamics & Control*, Cambridge University Press, New York, New York, 1997.

[28] Hughes, P. C., *Spacecraft Attitude Dynamics*, Dover Publications, Mineola New York, 2004.

[29] "World Magnetic Model," National Geospatial-Intelligence Agency, <http://www.ngdc.noaa.gov/geomag/WMM/DoDWMM.shtml>

VITA

Jason David Searcy was born on January 5, 1984, in Louisville, KY. He graduated from Shelby County High School in May of 2002. From August 2002 through May 2006, he attended the Missouri University of Science and Technology, formerly known as the University of Missouri-Rolla, to obtain a Bachelor's of Science degree in Aerospace Engineering.

Jason started graduate school in August of 2006 and began work toward a Master's Degree in Aerospace Engineering. In August of 2007 he was awarded first place in the Frank J. Redd Scholarship Competition for co-authoring a paper on the attitude determination and control system for the MR SAT spacecraft. The same year, he was awarded a Student Excellence award from the Academy of Aerospace and Mechanical Engineers at Missouri University of Science and Technology. Jason will receive his Master of Science degree in Aerospace Engineering in May 2011 from the Missouri University of Science and Technology.